To the Graduate Council:

I am submitting herewith a thesis written by Derong Tu entitled "Evaluation of Calendered Activated Carbon Nonwovens for Gas Adsorption". I have examined the final copy of this thesis for form and content and recommend that it be accepted in partial fulfillment of the requirements for the degree of Master of Science, with a major in Textile and Apparel.

Maureen Dever, Major Professor

We have read this thesis
and recommend its acceptance:

Accepted for the Council:

Associate Vice Chancellor
and Dean of The Graduate School

STATEMENT OF PERMISSION TO USE

In presenting this thesis in partial fulfillment of the requirements for a Master's degree at The University of Tennessee, Knoxville, I agree that the Library shall make it available to borrowers under rules of the Library. Brief quotations from this thesis are allowable without special permission, provided that accurate acknowledgement of the source is made.

Permission for extensive quotation from or reproduction of this thesis may be granted by my major professor, or in her absence, by the Head of Interlibrary Services when, in the opinion of either, the proposed use of the material is for scholarly purposes. Any copying or use of the material in this thesis for financial gain shall not be allowed without my written permission.

Signature _____

Date July 29, 1994

EVALUATION OF CALENDERED ACTIVATED CARBON NONWOVENS FOR GAS ADSORPTION

A Thesis

Presented for the

Master of Science

Degree

The University of Tennessee, Knoxville

Derong Tu

August 1994

DEDICATION

This thesis is dedicated to my parents

Mr. Shouzhu Tu

and

Ms. Guier Huang

who have inspired me to pursue my education.

ACKNOWLEDGEMENTS

I would like to thank my major professor, Dr. Maureen Dever, for her guidance, patience and help. I would also like to thank other committee members, Dr. Wayne T. Davis, Professor and Coordinator of the Environmental Engineering Program and Dr. Nancy Fair, Head of the Department of Textiles, Retailing and Interior Design for their advice and assistance. I would also like to express my sincere appreciation to Mr. John Schneider, Statistical Consultant at the Agriculture Experiment Station, for his help in making the experimental design and conducting the data analysis, and assistance with the data interpretation.

Finally, I would like to thank all the other people at Department of Textiles, Retailing and Interior Design and Textiles and Nonwovens Development Center who helped me along the way.

ABSTRACT

Nuclear, biological and chemical (NBC) military protective clothing was found to heat stress to military personnel when worn in the desert climate in the Persian War. Research was begun by Dever, Davis, and Hood [1] in September 1990 to develop a safe but comfortable NBC protective material. Three levels (i.e., 40, 80 and 120 g/m^2) of standard and high surface area (HSA) activated carbon on meltblown-spunbond nonwovens before and after thermal point bonding (i.e., calendering) were evaluated. The non-calendered HSA activated carbon (i.e., 80 and 120 g/m^2) nonwovens had better gas adsorption properties than did the Army issue protective clothing [2]. Calendering, required to impart sufficient sample strength, created pinholes allowing the chemical warfare gas simulant to pass directly through the samples and melted polymer coated the activated carbon reducing the available carbon adsorption area.

The study described herein evaluates the effect of a central core (i.e., 1, 2 and 3 oz/yd^2 cotton and 1.8 and 2.6 oz/yd^2 polypropylene) containing 120 g/m^2 HSA activated carbon meltblown-spunbond nonwovens. Additional thickness of the core and the non-thermalplastic cotton was expected to eliminate the calendered pinholes. The optimal nonwoven was determined to be the 1.8 oz/yd^2 PP core calendered at 6 m/min, 250 pli nip pressure, 80°C top calender roll temperature, and a 110°C

bottom calender roll temperature. The gas adsorption behavior was mathematically modeled. Calculated and experimentally measured adsorption capacities compared favorably, i.e., R^2 = 0.9845. The film coefficient (K) values which predict the shape of the adsorption wave were determined.

Future research will focus on alternative methods of bonding and development of porous polymer supports as an alternative to the activated carbon.

TABLE OF CONTENTS

LIST OF TABLES

LIST OF FIGURES

CHAPTER 1

INTRODUCTION

1.1 The U.S. Army Chemical Protective Apparel

U.S. Army personnel are provided with a Battle Dress Overgarment (BDO) [3] which is worn over the uniform when personnel are exposed to chemical weapons. The BDO consists of an outer shell fabric and an inner liner. The shell fabric is a 50/50 nylon/cotton twill weave fabric which is coated with a water repellent finish, Quarpel®. It weighs 0.2374 kg/m^2. The inner liner is poly(urethane) foam impregnated with a slurry of latex containing 70 - 120 g/m^2 of activated carbon powder. The poly(urethane) foam also has a 0.0678 kg/m^2 (2 oz/yd^2) nylon tricot knit flame bonded to one side. The liner is 0.0023 m (0.09 inches or 90 mils) thick. The measured air permeability of the BDO liner was 50 cfm/ft^2. The liner must satisfy the standards specified in the U. S. Army standard MIL-C-43858B(GL). This includes a fabric weight of 0.2543-0.3391 kg/m^2, a thickness of 0.178 - 0.305 cm (0.00178 - 0.00305 m), a minimum air permeability of 40 cfm/ft^2 at 0.5 inches of water pressure drop across the fabric, a minimum bursting strength of 516.75 kPa, and a minimum carbon-tetrachloride adsorption of 1.8 mg/cm^2.

During the Desert Storm Operations in the Persian Gulf the BDO was found to cause heat stress to soldiers. The heat

stress was thought to be due to the liner being too thick, too heavy, and not sufficiently air permeable. The U.S. Army issued a call for research to address the problems encountered with the BDO liner in the desert climate. A study was conducted at the University of Tennessee, Knoxville, from 1990 to 1993 in an attempt to address that need. The research focused on the development of a lighter weight, thinner, and more air permeable liner composed of spraying activated carbon powder into a melt blown (MB) nonwoven.

1.2 Previous Research on the Development of a High Air Permeable Activated Carbon BDO Liner

Three levels of the activated carbon loadings (i.e., 40, 80 and 120 g/m^2), two types of activated carbon powder (i.e., a standard (STD) commercially available carbon manufactured by Fisher Scientific, Pittsburgh, PA, and a high surface area (HSA) activated carbon manufactured by Kansai Coke and Chemicals Company, Limited, 5 Misono-cho, Amagaski City, Japan 660) were evaluated. Laboratory testing revealed that the 33 g/m^2 polyethylene (PE) meltblown (MB) nonwoven webs with an average fiber diameter of 7.53 μm, thickness of 0.00004 m, and air permeability of 492 cfm/ft^2 were capable of retaining approximately 40 g/m^2 of HSA carbon. Higher carbon loadings were obtained by layering the HSA activated carbon-MB. The layers of activated carbon-MB nonwovens were sandwiched

between two layers of PE MB to prevent slough off of the HSA activated carbon. The activated carbon loaded melt blown laminates were tested for trichloroethylene (TCE) adsorption capacity before and after being subjected to thermal calendering. The tests were done at the laboratory room temperature, relative humidity and atmospheric pressure. The TCE gas concentration used throughout the study was 1700 ppmv. The TCE gas flow was one liter per minute (i.e., the carrier gas velocity was 0.00206 m/s). Breakthrough was defined as the occurrence when the outlet TCE gas concentration reached 1% (i.e., 17 ppmv) of its inlet concentration (i.e., 1700 ppmv).

Results of this study showed that in terms of the breakthrough times and adsorption capacities, the non-calendered laminates did better than the BDO liner did. [3]. The experimental laminates with 80 g/m^2 HSA activated carbon loading adsorbed 77 - 206% and 34 - 54 % more TCE than the BDO liner did at the point of breakthrough and total capacity, respectively. The experimental laminates failed to meet the bursting strength specified in MIL-C-43858B(GL). In an attempt to increase the bursting strength, the laminates were sandwiched between two layers of polypropylene (PP) spunbond (SB) nonwoven (0.022 kg/m^2) and thermally point bonded. The SB provided strength without reducing the air permeability.

Results showed that calendering decreased the breakthrough times and adsorption capacities by 40 - 60%. The air permeability of the calendered samples decreased by 50 -

75% [4]. The calendered laminates also had lower air permeabilities and higher pressure drops. Figure 1.1 shows pinholes (about 520 μm in diameter) and excessive melting in the calendered samples. It is likely that the melted polymer partially encapsulated the carbon reducing the amount of available carbon for adsorbing the TCE gas.

The pinholes in the calendered samples allowed the TCE gas to pass directly through the laminates without being adsorbed by the activated carbon. This phenomenon is referred to as "bleed through".

1.3 Theoretical Adsorption Model

A theoretical model written in BASIC language has been developed by Davis [5] to predict the behavior of the adsorbate and adsorbent. The theoretical model can be used to predict the breakthrough time for the TCE adsorption by the HSA activated carbon-meltblown laminates. The theoretical model consists of seven primary equations which are described in detail in Chapter 3.

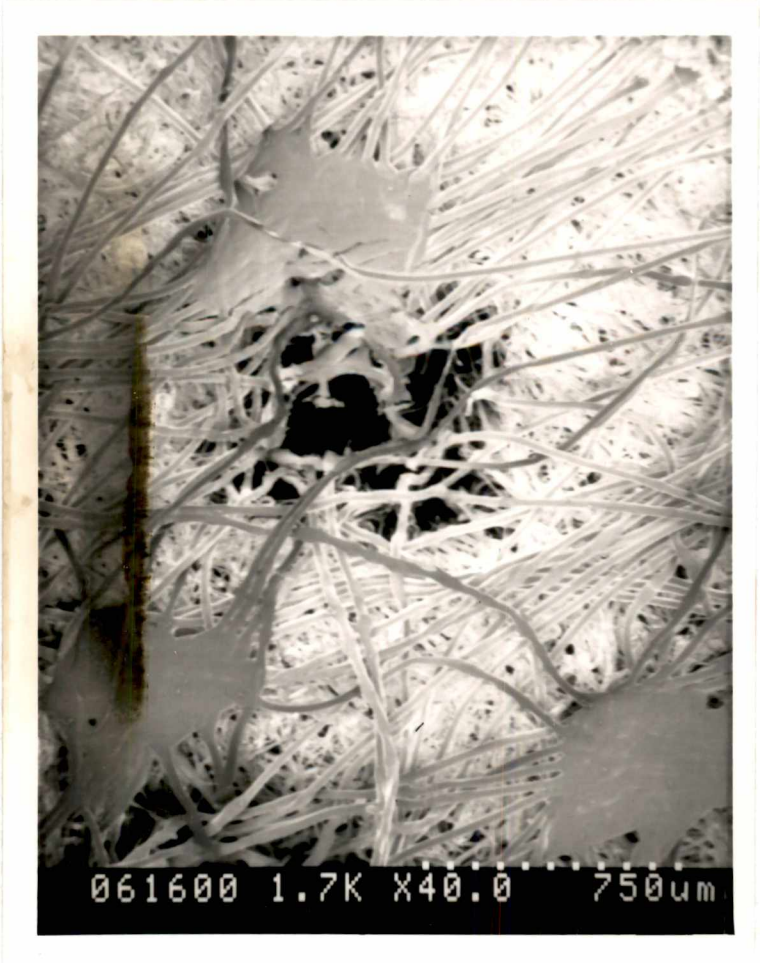

Figure 1.1 SEM photo showing pinholes and excessive melting resulting from the thermal calendering of laminates.

1.4 The Proposed Study

The findings from the previous study by Dever, Davis and Hood [1] and the gas adsorption theory [6] were used to redesign the structure of the laminates. The purpose of the proposed study was to minimize the detrimental effects resulting from calendering. The next series of laminates consisted of cotton and PP fiber cores. A non-thermalplastic cotton fiber core was selected because cotton does not melt. A PP core was used because PP has a high melting point than the PE used in the initial study. A polymer with a higher melting point was needed to eliminate the creation of pinholes and excessive melting in the laminates following calendering. The study evaluated four levels (i.e., 0, 1, 2, and 3 oz/yd^2) of carded cotton fiber web cores and two levels (i.e., 1.8 and 2.6 oz/yd^2) of carded PP fiber web cores. All samples contained 120 g/m^2 of HSA activated carbon. The TCE adsorption testing was done at room temperature and humidity using the 1700 ppmv inlet concentration of TCE gas. The gas flow rate was set at one liter per minute (i.e., the carrier gas velocity was 0.00206 m/s). The objectives of this study were to:

1) predict the breakthrough time of the TCE gas for the laminates using the adsorption theory described by Wark and Warner,

2) compare the predicted breakthrough times and adsorption capacities with the measured values,

3) determine a proper model for the breakthrough times and adsorption capacities for the TCE gas adsorption by the laminates,

4) eliminate the pin holes that occur following thermal calendering, and

5) reduce the loss in the TCE gas breakthrough times and adsorption capacities following thermal calendering.

A matrix of the fiber cores and calendering conditions resulted in almost 500 possible combinations. It is not practical and necessary to test all combinations, because a properly selected subset of all combinations could be used to predict the outcome.

A customized fractional factorial experimental design (CFFED) was generated using the E4 software [7]. The raw data were analyzed using the General Linear Model (GLM). The optimum calendering conditions were determined for the present study for the TCE adsorption performance by the HSA activated carbon impregnated fiber core nonwoven laminates.

CHAPTER 2

LITERATURE REVIEW

Due to its national defense nature, limited amount of literature is available on the chemical warfare protective clothing which utilizes activated carbon as an adsorbent to guard against the chemical agents. Listed below is the review of the literature the author has collected.

2.1 Chinese Army's Chemical Protective Suit

The Chinese Army (People's Liberation Army) is equipped with the air permeable chemical warfare protective suit called M82 [8]. The lining of M82 is a cotton flannel treated with flurochemicals and an active charcoal-polyacrylate emulsion. Active charcoal works as adsorbent to protect against the gaseous chemical agents, and fluorochemicals play the role of oil repellent. Utilizing cotton flannel as the base cloth provides the fabric desirable mechanical strength and comfort. The weight and construction of the cotton flannel is unknown from the literature. Also, no information is available on the active charcoal used in the emulsion.

The procedure for finishing cotton flannel consists of padding, drying, curing and washing. The procedure for finishing the charcoal-containing cotton flannel include spraying flame retardants on one surface of cotton flannel,

drying, spraying fluorochemicals on the same surface of cotton flannel, drying, curing, spraying polyacrylate emulsion with flame retardants and active charcoal on the other surface of cotton flannel, drying and curing.

2.2 French Army's S3P Garment for Nuclear/Biological/Chemical Protection

The French troops are furnished with S3P garment [9] for nuclear, biological and chemical protection. The S3P garment is intended for aggressive climatic conditions to provide the wearer with sufficient comfort as well as maximum protection. The garment operates roughly like a gasmask cartridge. It is composed of three layers. The outer layer is a highly air permeable woven fabric coated with a resin to produce an anti-bead effect so as to deter the penetration of toxic liquid droplets. A polyamide taffeta made from 82 dtex high tenacity filament with waterproof finish has been used as the outer layer. Kermel has been used as the outer layer as well. The intermediate layer is a viscose nonwoven material produced by the dry-laid system. The function of this layer is to disperse the chemical toxic droplets should they penetrate the outer layer fabric so as to reduce the toxic chemical potential per square unit and to obstruct aerosols. The inner layer works like a gas filter in a gasmask cartridge. It is made of a polyurethane foam of a very regular thickness, with calibrated

holes. The foam is impregnated with activated carbon, which, if necessary will adsorb the hazardous toxic chemicals. This structure is bonded on its internal surface to a polyamide net to obtain the extra strength. Colored in NATO green the complete garment weighs 1.7 kg. The garment is breathable. So it is very comfortable to wear. Since the outer layer has an antibead finish, it keeps the toxic liquids from sticking to the fabric. If the toxic material consists of aerosols in part, they may penetrate the fabric, but are stopped and scattered by the middle layer of nonwoven structure. Therefore, no toxic agents in liquid or aerosol form can ever reach the carbon impregnated inner layer. Toxic vapors emitted by aerosols, or droplets could pass through the nonwoven structure (the intermediate layer). However, they would be adsorbed by the activated carbon impregnated on the inner layer. The NBC protective garment should be worn over the battle dress so it will protect the soldiers against toxic substances under aggressive circumstances. In addition to the garment, the protective gloves and socks are also available for extended protection. The structure of the protective gloves is based on the same principle. The outer layer is a leather glove. Undergloves are made of polyurethane foam impregnated with activated carbon particles bonded with polyamide fabric (outer fabric) and cotton jersey knitted fabric (inner fabric) that is in direct contact with the skin of the wearer. The protective socks are similar to gloves but

without the outer leather layer. The S3P NBC protection garment has been extensively tested. The results show that it maintains protective properties for a long time. There is no change in its physical and protective properties after three weeks. Due to the three-layer structure this garment is rather expensive. This garment is not re-usable. When the carbon particles are saturated by toxic chemicals the garment no longer provides protection.

2.3 Clothing for Chemical and Biological Protection

A lightweight porous fabric has been developed by Richard D. Langton of Charcoal Cloth Ltd, Ferndown, the United Kingdom [10]. It provides good protection against chemical and biological agents for extended periods of time. The fabric (US patent 5 112 666) is abrasion resistant and flame retardant as well. It also has excellent aging properties and can be laundered. The material is a three-layer composite consisting of an outer layer, an intermediate layer and an inner layer. This structure allows perspiration to escape from the body and filtered air to pass through to the wearer. A proposed fabric is a 2x1 twill with a nylon warp and modacrylic weft. The fabric weight should be about 118 g/m^2. Other suitable materials are aramid woven or nonwoven fabrics that are resistant to fire and chemicals. The outer fabric should be oil repellent. And it is treated with a silicone water-

repellent and a flame-retardant additive. It could also be made infrared reflective, if necessary. Normally it will be showerproof, but not necessarily waterproof. The intermediate layer is made from activated carbon, so it adsorbs poisonous vapors but permits air and water vapor to pass through it. It also has a gas-permeable surface coating or particulate hydrophobic material which makes the activated carbon waterproof. Modified polytetrafluoroethylene (PTFE) could be used for this purpose. The activated charcoal cloth (ACC) is an activated carbon adsorbent available in the form of woven, nonwoven or knitted cloth of 100% pure activated charcoal. It can be used in the same way as a conventional textile and may be laminated to other fabrics. It is reported that in humid or wet conditions ACC offers better performance than other forms of activated charcoal. The inner layer of this composite is a lining providing increased tear strength, tensile strength and abrasion resistance as well as making the garment more comfortable to wear. It is important that the extensibility of this layer matches that of the charcoal fabric to prevent the charcoal material from breaking. The weight of the structure should be around 350 g/m^2 and it should allow outward passage of perspiration at a rate of 2500 - 5000 g/m^2 per 24 hour period at 100% relative humidity differential at 37°C. This structure provides good chemical protection for at least six hours in a mustard liquid test. Protection may be effective after at least 30 days continuous wear and in sealed packaging

the material will have a storage life of up to 25 years in normal conditions.

2.4 NBC Suit for U.K. Army

The UK service personnel are issued a protective garment named "the NBC suit" [11] to guard against chemical agents. The NBC suit is worn just on top of the normal battle uniform, thereby minimizing the time required to adopt defensive measures when the hazard of chemical attack occurs. Because it is an addition to the normal battle dress, restrictions are set on the thermal insulation and air permeability of the NBC suit if excessive heat must be avoided. The air permeable NBC suit consists of two layers. The outer fabric layer, termed the "wicking layer" is a twill woven modacrylic and nylon material. Although it has a silicone water repellant finish, organic liquids of surface tension less than 50 mN/m can disperse on the surface to form a thin layer. The inner layer consists of a nonwoven material of about 1 mm in thickness. It has a coating of powdered charcoal bonded with acrylic latex to the underside. Formally termed "Cloth, Bonded, Multi-Fibre, Anti-Gas", it is usually called "NBC suit material".

The sequences of the protection that occur when a liquid drop of a chemical warfare agent contaminates the NBC suit are:

1) Impaction on the surface.
2) Dispersion of the drop on the wicking layer to a relatively larger surface area.
3) Evaporation of the drop, both into the surrounding atmosphere and toward the inner layer of nonwoven fabric.
4) Transfer of vapor through the air gap between the outer layer and the inner layer. In still air this transport is done by diffusion, but dynamic wind pressure may force vapor laden air through the fabrics.
5) Adsorption of vapor by the inner layer of powdered charcoal.
6) Any agent that has not been adsorbed may then pass through to the normal battle uniform, and eventually get to the skin of the wearer.

Because the nonwoven fabric treated with a fluorocarbon finish is non-wettable, no liquid can penetrate to the inner charcoal layer. Only vapor emanating from the liquid may reach it. If the chemical warfare agent consists of vapor other than liquid droplets then steps 1), 2) and 3) are skipped.

A study was conducted by Jones [11] in the late 1980's on the adsorption of isopropylmethylphosphonofluoridate (GB) vapor by a protective material (i.e., the NBC suit material) consisting of powdered activated carbon bonded to a fabric substrate.

The fabric substrate used in the preparation of experimental NBC suit was made by Bondina Ltd., of Halifax, West Yorkshire, England. It was a nonwoven construction with a felt of nylon and viscose rayon fibers bonded together by a chloroprene binder. A layer of cotton reinforcing scrim was bonded to one side of the fabric while a perfluorocarbon oil and water repellant finish was applied to the other side of the fabric. The fabric was made of 85 nylon/15 viscose rayon blended yarns. The ratio of the fiber to chloroprene binder was 62:38. The cotton scrim accounted for a further 11% of the total weight of approximately 145 g/m^2.

The composite NBC suit materials were made on the CDE (Chemical Defense Establishment) pilot plant. Different combinations of charcoal and binder were used.

The apparatus used at CDE for the production of the experimental NBC suit material consisted of a traversing spray gun blowing the charcoal and latex slurry onto the fabric substrate, with a drive device to propel the fabric underneath the spray gun and through a drying oven. The spray gun was positioned on a gantry that crossed at 28 cycles per minute at right angles to the direction of the movement of the fabric. A "fish tail" spray was produced, directed downward with the gun nozzle 80 mm above the surface of the cloth. The charcoal and latex slurry was fed to the spray gun through flexible tubing by a peristaltic pump. Compressed air at 1.5 kg/cm^2 was employed for the spray generation. The fabric sample of 0.45

m x 1 m in size, was secured by tenterhooks to a frame that engaged on a worm gear to drive the sample under the spray gun and through the 1.8 m long drying oven at a speed of up to 5.5 meter per minute.

In the making of NBC suit material an aqueous dispersion of charcoal and latex was first prepared. Then the dispersion was sprayed onto the surface of the nonwoven fabric, followed by oven drying. The first step in the preparation of the dispersion was to add the charcoal to water, followed by high speed stirring for ten minutes to achieve wetting-out. A 2% solution of Methyl cellulose was also added as a dispersant, and stirring went on for another twenty minutes before the latex was added in, then followed by yet another twenty minutes stirring. The purpose of doing so was to accomplish a stable double dispersion of charcoal and latex particles. The total solid content of the mixture was 20%. The ratio of charcoal to latex was 4:1. Methyl cellulose accounted for 0.75% of the charcoal by weight. The moisture content of the charcoal must be checked to ensure a correct "dry weight" of charcoal in the mixture.

A mathematical model of dynamic vapor adsorption by the latex bonded activated carbon particles was developed by Jones and Watts [12]. The model accurately reproduced the experimentally observed results. The model divided the adsorbent bed into two different kinetic regions. The major region had an adsorption rate that was dependent exclusively

upon the mass transfer of the vapor. The remaining "slow" region exhibited that adsorption kinetics were consistent with a slow surface deposition or displacement reaction as the rate determining step. However, the results were not consistent with the permeation through the latex binder being a rate determining step. The mathematical model was successful in predicting the performance of multi-layer assemblies from the results observed on single layers.

CHAPTER 3

THEORETICAL ADSORPTION MODEL

3.1 Adsorption: Physical versus Chemical

Adsorption is a separation process based upon the ability of a solid (i.e., adsorbent) to remove a gas (i.e., adsorbate) preferentially from a flow stream. Adsorption can be subdivided into physical adsorption or chemisorption. In physical adsorption, weak van der Waals intermolecular attractive forces hold the adsorbate on the surface of the adsorbent. Physical adsorption is exothermic liberating heat typically on the order of the enthalphy of the condensation of the adsorbate vapor e.g., 2 to 20 kJ/g-mole [6]. An advantage of physical adsorption is the ability to remove the adsorbate (i.e., regeneration of the adsorbent) by reducing the pressure or raising the temperature.

Chemisorption results from a chemical interaction between the adsorbate and the adsorbing. The bonding forces associated with this type of adsorption tend to be much stronger than those found in physical adsorption. A chemical affinity between the adsorbate and adsorbent is required. Chemisorption is generally irreversible.

3.2 Adsorbent

Adsorbents are characterized by their surface area and pore volume and pore diameter. The surface area describes the amount of area per specific unit of volume or weight. For a typical activated carbon, the micropores comprise most of the internal surface and may account for 90% of the apparent surface area [13]. The adsorbate-adsorbent system is optimized when the pore diameter of the adsorbent is slightly larger than the molecular diameter of the adsorbate gas. Activated carbon has an affinity for high molecular weight, polar hydrocarbons [6].

3.3 Theoretical Equations

Development of a theoretical model for an activated carbon impregnated fabric requires knowledge of the adsorbent-adsorbate system. The activated carbon bed thickness, bulk density (i.e., weight), and the adsorbate concentration, temperature, pressure, and velocity must be known. The quantity of adsorbate retained by the adsorbent over time is determined experimentally. The data are graphed on a log-log scale and a least squared linear fit is determined. The gas phase equilibrium constants α and β are determined from the y-intercept and slope of the line, respectively. The velocity rate of the adsorption wave moving through the fabric (V_{ad}),

the film coefficient constant (K) which describes the shape of the adsorption wave, the mass transfer coefficient (d_{mp}), and the time (T_b) the adsorbate diffuses through the adsorbent can be predicted.

The adsorbent-adsorbate isotherm is Freundlich when the data (i.e., adsorbate concentration downstream of the sample with respect to time) plotted on a log-log scale results in a straight line. It must be assumed the adsorbate and adsorbent are at equilibrium at the trailing edge of the mass transfer zone (Figure -). The mass flow rate of the carrier gas must be approximately equal to the mass flow rate of the carrier gas containing the pollutant. The derivation of the breakthrough time (T_b) equation assumes that the mass transfer zone is fully established at the start of the test (i.e., time = zero).

The development of the adsorption wave velocity equation is based on the mass balance between the inlet and outlet of the adsorbate gas concentrations.

Equation 3-1 describes the mass balance for the adsorbate-adsorbent system.

$$\frac{m_g C_1}{\rho_g} = m_{ad} X_1 = \rho_{ad} A V_{ad} X_{sat} \qquad (3\text{-}1)$$

where:

m_g = the mass flow rate of the gas phase entering,

m_{ad} = the mass flow rate of the gas phase leaving,

ρ_g = the gas phase density,

ρ_{ad} = the apparent density of the granular adsorbent bed,

A = the cross-sectional area of the bed,

V_{ad} = the velocity of the adsorption wave,

C_1 = the gas phase concentration of the pollutant (expressed as mass of pollutant/mass of adsorbent),

X_1 = the trailing edge of the adsorption zone, and

X_{sat} = the solid phase concentration (expressed as mass of pollutant/mass of adsorbent).

Equation 3-2 is the Freundlich equation, which is a good approximation for the behavior of an organic compound adsorbed onto an activated carbon bed. The equation is based on the equilibrium concentration for both the gas and solid phase.

$$C_e = \alpha X^{\beta}_{sat} \qquad (3\text{-}2)$$

where:

C_e = gas phase equilibrium concentration (ppmv or kg/m^3),

α = experimental constant (ppmv or kg/m^3),

β = experimental constant (unitless), and

X_{sat} = equilibrium mass adsorbed (g/g).

Assuming the trailing edge of the adsorption wave is at equilibrium, it is logical to consider position 1 in the theoretical adsorption wave (Figure 3.1) to be $C_e = C_0 = C_1$ and $X_1 = X_{sat}$.

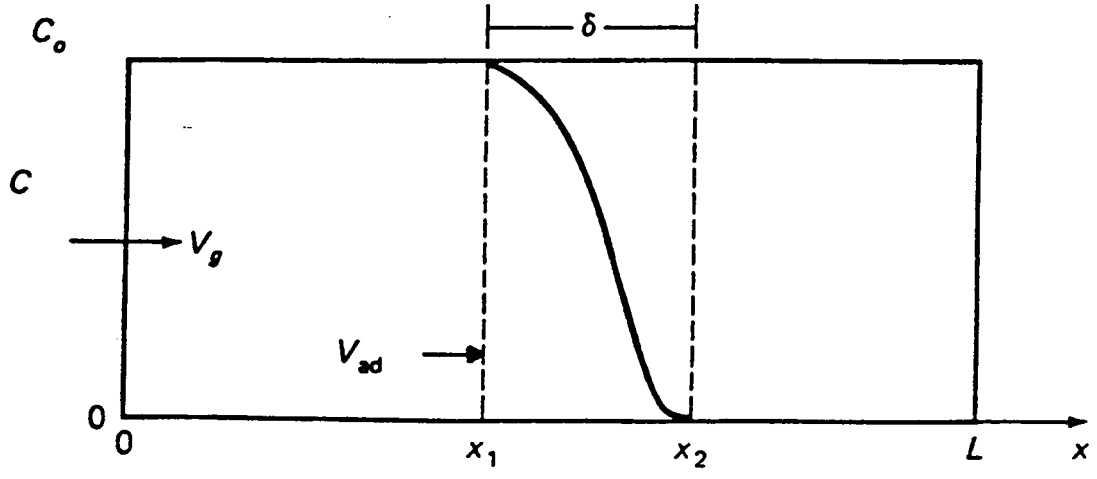

Figure 3.1 Theoretical Adsorption Wave

Equation 3-3 results from combining Equations 3-1 and 3-2 and solving for the adsorption wave velocity V_{ad}.

$$V_{ad} = \frac{V_g}{\rho_{ad}} (\alpha)^{\frac{1}{\beta}} (C_0)^{\frac{\beta-1}{\beta}} \qquad (3\text{-}3)$$

where:

C_o = the inlet pollutant gas concentration (ppmv or kg/m^3),

V_g = the superficial velocity of the carrier gas.

The adsorption wave velocity is described by the movement of the adsorbate through the adsorbent. Equations 3-4 and 3-5 express the mass transfer zone width and breakthrough time for a given adsorbent bed thickness. Equation 3-4 described the differential rate of mass transfer of the adsorbate gas on the adsorbent solid phase (dm_p).

$$dm_p = \frac{m_g}{\rho_g} dC \qquad (3\text{-}4)$$

Equation 3-5 is another expression of dm_p. In that equation the mass transfer rate is defined in terms of the volume of the adsorption bed, the mass flow rate, adsorbate concentration, and a film transfer coefficient K.

$$dm_p = KA(C - C_e)\,dx \qquad (3\text{-}5)$$

where K is a film resistance coefficient, which is defined by Jonas et. al [14] and Davis [5]. Combining Equations 3-4 and 3-5 and integrating between x_1 and x_2 results in an equation that describes the position (x) and width of the mass transfer zone, δ, which is equal to $x_2 - x_1$.

Equation 3-6 describes the position (x) in the adsorption zone based on the concentration limits. In the case of the model for the present study, the limits selected on the system are from 1% to 99% of the inlet concentration. These limits can be changed by replacing the 0.99 values in Equation 3-6 with the desired percentage of the inlet concentration value. The distance, x_1, from the start of the adsorbent bed to the trailing edge of the adsorption zone, usually is defined as the location where the pollutant gas concentration is 99% of its inlet concentration (i.e., $C = 0.99\ C_0$). x is any position in the adsorption zone where the pollutant gas has a concentration of C ranging between $0.99\ C_0$ and $0.01\ C_0$.

$$x = x_1 + \frac{m_a}{KA\rho_g}\left[ln0.99\frac{C_0}{C} + \frac{1}{\beta-1}\ln\frac{1-\left(\frac{C}{C_0}\right)^{\beta-1}}{1-(0.99)^{\beta-1}}\right] \qquad (3\text{-}6)$$

Equations 3-1 through 3-6 provide a dynamic description of adsorption. The breakthrough time, a critical factor in designing protective clothing, is defined by Equation 3-7. Equation 3-7 is a function of Equations 3-3 and 3-6.

$$T_b = \frac{L-\delta}{V_{ad}} \qquad (3\text{-}7)$$

where:

L = the thickness of the adsorbent bed (i.e., thickness of the activated carbon impregnated fabric).

A theoretical computer model based on the equations described herein has been developed by Davis [5] to predict breakthrough times. Predicted and experimentally measured breakthrough times were compared to determine a certain distribution pattern of the film resistance coefficient (K) for the thin activated carbon impregnated nonwoven protective fabric.

3.4 Development of Adsorption Isotherms

A series of adsorption tests were conducted to total capacity on the activated carbon-MB-SB impregnated nonwovens before and after subjecting them to thermal point bonding (i.e., calendering). The adsorption isotherms to total

capacity before calendering (sample PP18-8) were determined using 167 ppmv and 1666 ppmv TCE. The adsorption isotherms to total capacity before calendering (samples PP26-7 and PP26-8) were obtained using 1646 ppmv TCE. Total TCE gas adsorbed, determined gravimetrically, was 1.3547 (g TCE/g activated carbon). Figure 3.2 shows the breakthrough curves for the adsorption isotherms obtained from the noncalendered samples.

The adsorption isotherms for the calendered sample PP26-3 was obtained using 180 and 1700 ppmv TCE. Another adsorption isotherm was also determined on sample PP26-4 using 1700 ppmv TCE. Figure 3.3 shows the breakthrough curves for the calendered samples.

Breakthrough times (the time when 1% of the inlet challenge gas concentration diffuses through the fabric) and equilibrium times (the time when 100% of the inlet challenge gas concentration diffuses through the fabric) of the adsorption isotherms tests for the non-calendered and calendered laminates are listed in Table 3.1 and 3.3, respectively. Adsorption capacities at break and equilibrium are shown in Table 3.2 and 3.4, respectively.

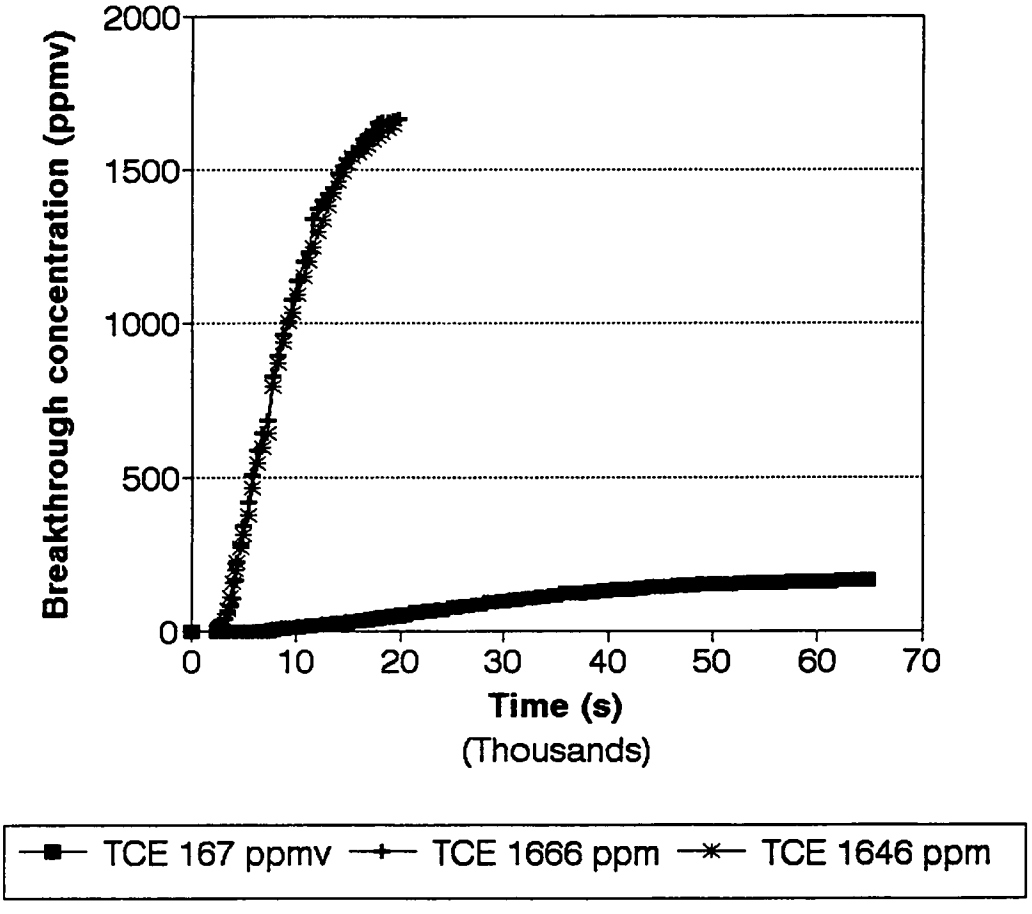

Figure 3.2 Breakthrough curves for adsorption isotherm tests for the non-calendered laminates.

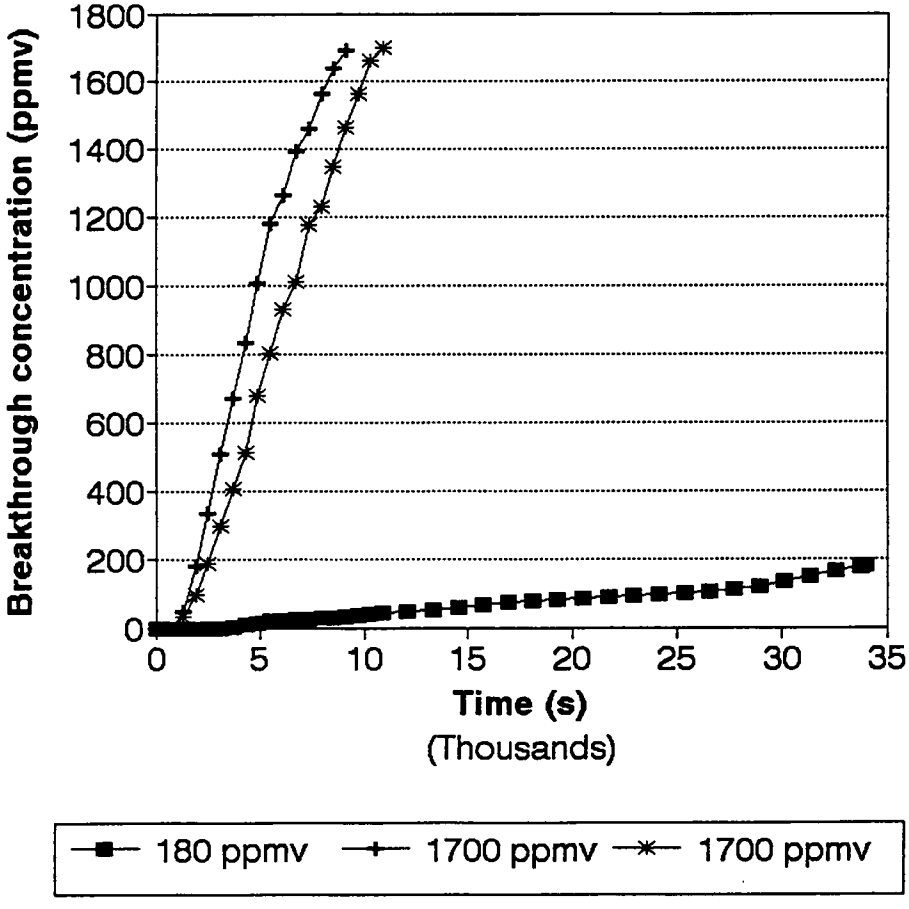

Figure 3.3 Breakthrough curves for adsorption isotherm tests for the calendered laminates.

Table 3.1 Breakthrough Times of the Adsorption Isotherm Tests for Non-calendered Laminates.

SAMPLE NUMBER	TCE CONCENTRATION (PPMV)	BREAKTHROUGH TIME AT BREAK (S)	TOTAL BREAKTHROUGH TIME (S)
PP18-8	167	7080	64800
PP26-7	1646	2952	19320
PP18-8	1666	2952	19800

Table 3.2 Adsorption Capacities of the Adsorption Isotherm Tests for Non-calendered Laminates.

SAMPLE NUMBER	TCE CONCENTRATION (PPMV)	ADSORPTION CAPACITY AT BREAK (G/G)	TOTAL ADSORPTION CAPACITY (G/G)	
			GRAVI *	MIRAN *
PP18-8	167	0.1104	0.5658	0.4329
PP26-7	1646	0.4533	1.3927	1.3171
PP18-8	1666	0.4588	1.5149	1.3068

* GRAVI = gravimetrically measured
* MIRAN = spreadsheet calculated

Table 3.3 Breakthrough Times of the Adsorption Isotherm Tests for Calendered Laminates.

SAMPLE NUMBER	TCE CONCENTRATION (PPMV)	BREAKTHROUGH TIME AT BREAK (S)	TOTAL BREAKTHROUGH TIME (S)
PP26-3	180	3576	33960
PP26-3	1700	1080	9240
PP26-4	1700	1128	10560

Table 3.4 Adsorption Capacities of the Adsorption Isotherm Tests for Calendered Laminates.

SAMPLE NUMBER	TCE CONCENTRATION (PPMV)	ADSORPTION CAPACITY AT BREAK (G/G)	TOTAL ADSORPTION CAPACITY (G/G)	
			GRAVI *	MIRAN *
PP26-3	180	0.05958	0.3788	0.3422
PP26-3	1700	0.1712	0.8501	0.7213
PP26-4	1700	0.1787	1.005	0.9321

* GRAVI = gravimetrically measured
* MIRAN = spreadsheet calculated

The two columns in Tables 3.2 and 3.4 list total TCE gas adsorption capacity determined gravimetrically and by measuring the adsorbate gas concentration using the Miran 1A IR. The Miran 1A IR detector values were put into a spreadsheet which integrated the amount of TCE gas detected downstream of the sample at 24 s intervals. A linear regression revealed that there was good agreement as well as correlation (R^2 = 0.9845) between the "gravimetrically measured" and "spreadsheet calculated" adsorption capacity values (Figure 3.4). The "gravimetrically measured" total TCE adsorption capacities were used to generate adsorption isotherms.

Figures 3.5 and 3.6 show the adsorption isotherms for breakthrough and total capacity for the non-calendered and calendered laminates, respectively.

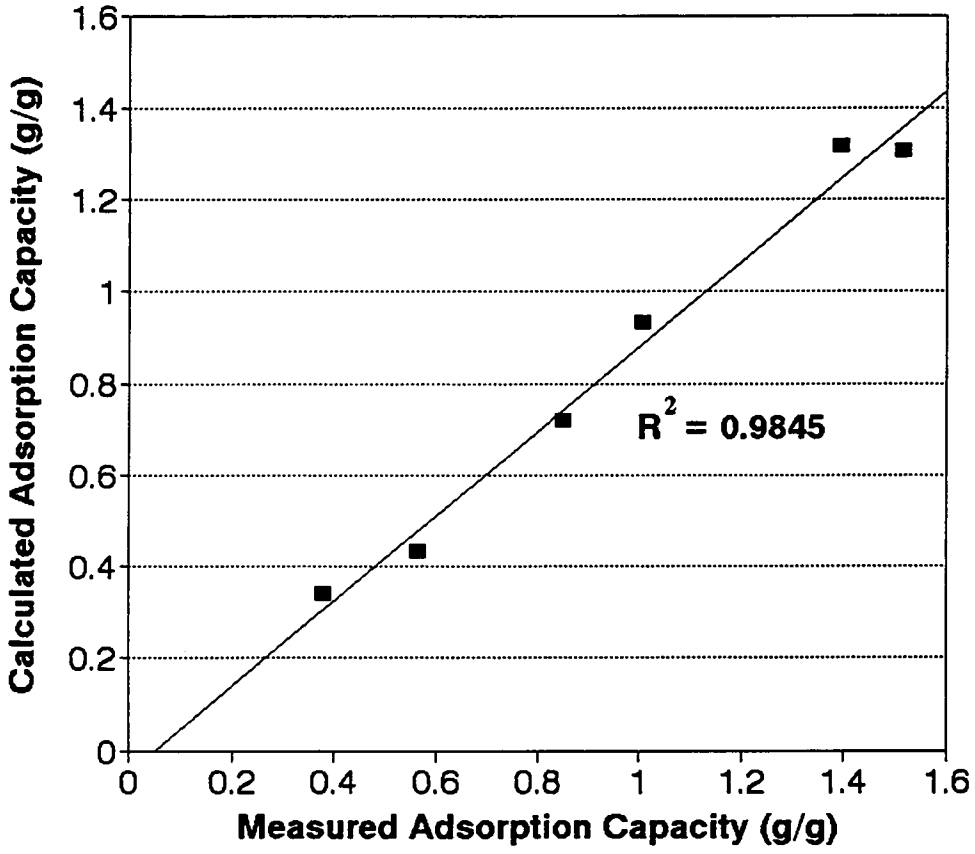

Figure 3.4 Least square fit of "gravimetrically measured" and "spreadsheet calculated" adsorption capacities for the adsorption isotherm tests.

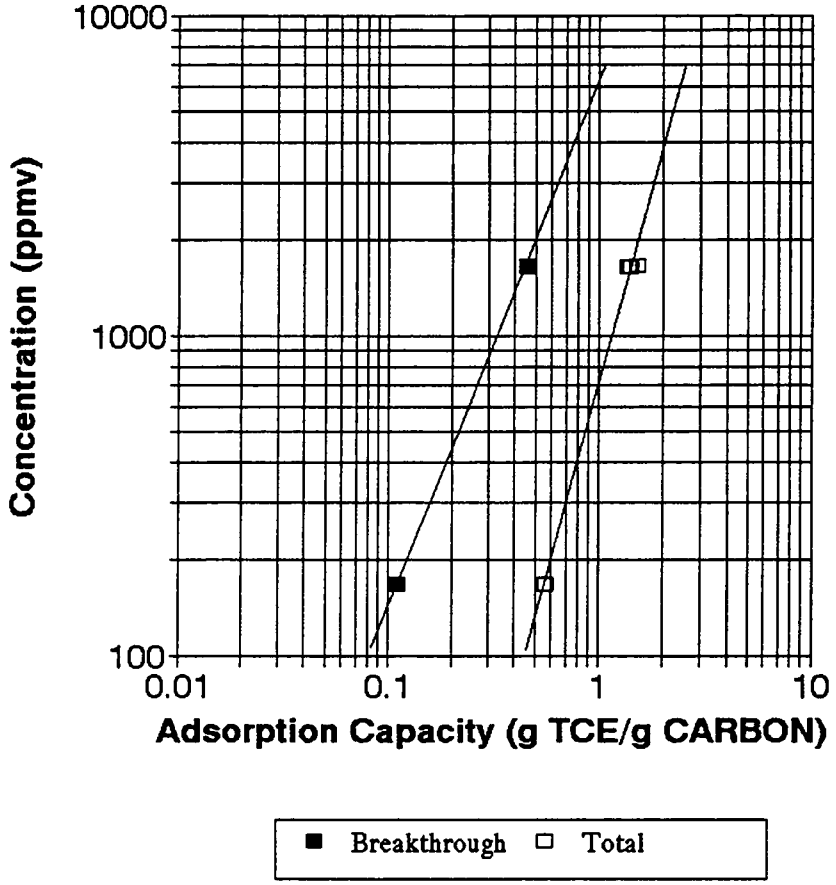

Figure 3.5 Adsorption isotherms for the non-calendered laminates.

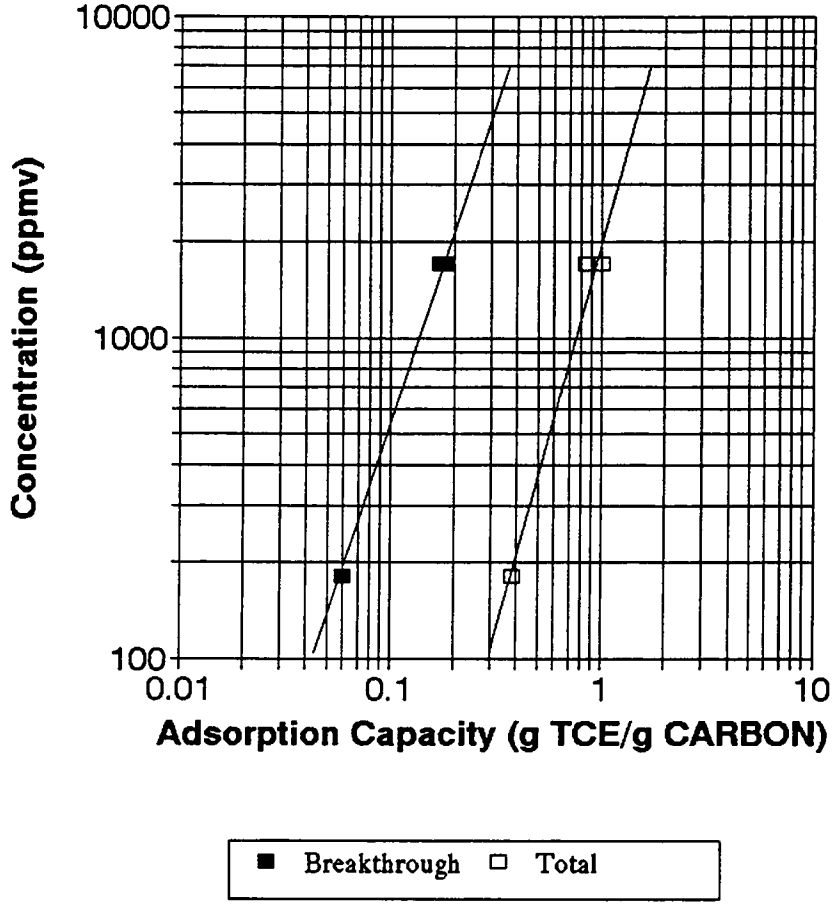

Figure 3.6 Adsorption isotherms for the calendered laminates.

Total adsorption capacity for the non-calendered laminates were from 0.57 g TCE/g activated carbon for the 167 ppmv TCE gas concentration to 1.39 g TCE/g activated carbon for the 1646 ppmv TCE gas concentration, and 1.51 g TCE/g activated carbon for the 1666 ppmv TCE gas concentration. Breakthrough adsorption (1% penetration of the inlet TCE gas concentration) was 0.11 g TCE/g activated carbon for the 167 ppmv TCE gas concentration, 0.45 g TCE/g activated carbon for the 1646 ppmv TCE gas concentration, and 0.46 g TCE/g activated carbon for the 1666 ppmv TCE gas concentration.

Total adsorption capacity for the calendered laminates was 0.38 g TCE/g activated carbon for the 180 ppmv TCE gas concentration and 1.00 g TCE/g activated carbon for the 1700 ppmv TCE gas concentration. The 1% TCE gas adsorption capacity was 0.06 g TCE/g carbon) for the 180 ppmv TCE gas concentration and 0.18 g TCE/g carbon for the 1700 ppmv TCE gas concentration. Figures 3.5 and 3.6 show the data are straight lines when plotted on log-log scale (i.e., Freundlich type described by Equation 3-2).

The linear regression equation for the Freundlich isotherm (Figure 3.5) is as follows:

$$C_e = (692.7)X^{2.47},\ R^2 = 0.9952,$$

where:

C_e = TCE gas concentration at equilibrium (ppmv) or

$$C_e = (0.00377)X^{2.47},$$

where:

C_e = TCE gas concentration at equilibrium (kg/m^3).

The linear regression equation for the 1% breakthrough capacity is as follows:

$$C_{breakthrough} = (5895.7)X^{1.62},\ R^2 = 0.9999,$$

where:

$C_{breakthrough}$ = TCE gas concentration at breakthrough (ppmv)

or

$$C_{breakthrough} = (0.0321)X^{1.62},$$

where:

$C_{breakthrough}$ = TCE gas concentration at breakthrough (kg/m^3).

The linear regression equation for the Freundlich isotherm (Figure 3.6) is as follows:

$$C_e = (2022.6)X^{2.45},\ R^2 = 0.9871,$$

where:

C_e = TCE gas concentration at equilibrium (ppmv) or

$$C_e = (0.011)X^{2.45},$$

where:

C_e = TCE gas concentration at equilibrium (kg/m^3).

The linear regression equation for the 1% breakthrough capacity is as follows:

$$C_{breakthrough} = (64107.7)X^{2.08},\ R^2 = 0.9994,$$

where:

$C_{breakthrough}$ = TCE gas concentration at breakthrough (ppmv)

or

$$C_{breakthrough} = (0.349)X^{2.08},$$

where:

$C_{breakthrough}$ = TCE gas concentration at breakthrough (kg/m^3).

3.5 Prediction of Breakthrough Times

The profiles of the theoretical adsorption wave can be generated by limiting the value C in Equation 3-6 from 0.01 to 0.99. By converting the distance to an equivalent time point, a group of predicted breakthrough curves of the outlet gas concentration versus time can be established by varying the film resistance coefficient (K). The computer program (Appendix E) developed by Davis [5] predicts the breakthrough time. The time to reach total TCE gas adsorption capacity and shape of the adsorption wave inside the fabric were also predicted. To account for assuming the adsorption wave is fully established at the beginning of the adsorbent bed, the predicted breakthrough curve is shifted so the integration of the total area above the predicted breakthrough curve results in the same total adsorption capacity predicted by the equation. This modification would be negligible in thick adsorption beds where the adsorption wave width is much smaller than the total adsorbent bed thickness. The K value is important when describing the mass transfer of the adsorbate through chemical protective clothing where the activated carbon adsorbent bed is relatively short.

Initial efforts were made to statistically determine the value of the film resistance coefficient (K) which provided the highest correlation between the predicted 1% breakthrough times and the measured values. However, the results showed no single K value could be found to accurately represent all samples. This indicates that unlike the thick adsorption bed systems where an empirical equation is used to estimate the K value, the large variation in the narrow or thin nonwoven laminates resulted in large variations in the K values. Efforts were then made to look for a K value for each sample which provided the predicted breakthrough time closest to the measured values. The K values for laminates before and after calendering are listed in Tables 3.5 and 3.6. The K values were 1.9 to 4.6 for the non-calendered samples, and 5.2 to 10.0 for the calendered samples.

It is now clear that the activated carbon bed inside the calendered samples is severely deformed as a result of calendering under high pressure and temperature. The characteristics describing the adsorption isotherms for non-calendered and calendered samples are listed in Table 3.7.

Table 3.5 K Value for Non-calendered Laminates.

SAMPLE NUMBER	MEASURED BREAKTHROUGH TIME (s)	K (s^{-1})	PREDICTED BREAKTHROUGH TIME (s)
0-1	2304	4.1	2327
0-2	2184	4.5	2185
0-3	2088	3.7	2002
0-4	1872	4.1	1804
0-5	2232	4.6	2253
0-6	2208	4.1	2278
1-1	2136	3.4	2089
1-2	2616	3.3	2541
1-3	2040	2.9	2088
1-4	1920	2.7	2032
1-5	2016	3.1	2080
1-6	2448	2.9	2437
2-1	2664	2.3	2779
2-2	2016	2.5	1927
2-3	2016	2.4	2036
2-4	2112	2.3	2126
2-5	1992	2.2	2126
2-6	1896	2.4	2005
3-1	2136	1.9	2094
3-2	1776	2.2	1687
3-3	2376	2.2	2467
3-4	3000	2.3	3040
3-5	2832	2.2	2797
3-6	1944	1.9	2118
PP18-1	2592	3.2	2608
PP18-2	2424	3.4	2494
PP18-3	2712	3.5	2738
PP18-4	2808	3.8	2786

SAMPLE NUMBER	MEASURED BREAKTHROUGH TIME (s)	K (s^{-1})	PREDICTED BREAKTHROUGH TIME (s)
PP18-5	2472	3.0	2494
PP18-6	2280	3.1	2215
PP26-1	2784	3.7	2848
PP26-2	2136	3.4	2045
PP26-3	2208	3.3	2154
PP26-4	2808	3.7	2848
PP26-5	2232	3.6	2158
PP26-6	2472	3.3	2504

Table 3.6 K Value for Calendered Laminates.

SAMPLE NUMBER	MEASURED BREAKTHROUGH TIME (s)	K (s^{-1})	PREDICTED BREAKTHROUGH TIME (s)
0-1	1272	9.2	1258
0-2	1008	9.6	995
0-3	1008	8.7	1033
0-4	888	8.6	893
0-5	1176	9.4	1198
0-6	1176	9.3	1189
1-1	936	6.7	920
1-2	1224	6.7	1200
1-3	1008	6.0	1046
1-4	912	6.3	902
1-5	1008	5.3	1000
1-6	1344	5.9	1333
2-1	936	5.2	982
2-2	672	5.8	636
2-3	816	5.5	783
2-4	1056	5.7	1017
2-5	552	6.5	556
2-6	744	5.7	732
3-1	1152	7.8	1185
3-2	720	7.8	692
3-3	672	7.8	650
3-4	1104	8.1	1078
3-5	1032	7.6	1026
3-6	648	7.4	664
PP18-1	1800	8.1	1779

SAMPLE NUMBER	MEASURED BREAKTHROUGH TIME (s)	K (s^{-1})	PREDICTED BREAKTHROUGH TIME (s)
PP18-2	1440	8.1	1456
PP18-3	1200	7.1	1200
PP18-4	1560	8.7	1577
PP18-5	624	7.0	647
PP18-6	1128	8.9	1102
PP26-1	1320	9.8	1309
PP26-2	768	9.3	741
PP26-3	1128	9.3	1147
PP26-4	1440	9.7	1459
PP26-5	1152	9.1	1167
PP26-6	1488	10.0	1479

Table 3.7 Characteristics of Adsorption Isotherms for Non-calendered and Calendered Samples.

Characteristics	Non-calendered Samples	Calendered Samples
α (kg/m^3)	0.00377	0.0110
β (pure number)	2.47	2.45
K (s^{-1})	1.9 - 4.6	5.2 - 10.0

Comparing Figure 3.5 to Figure 3.6, it is obvious that the adsorption isotherms for calendered samples are shifted to the left for some distance. This shift back means that the adsorption capacity for calendered samples was reduced by a certain percent. This distance of the shift back reflects the α value difference between calendered and non-calendered samples. The total adsorption isotherms for non-calendered and calendered samples look like parallel to each other. This is because the slopes (i.e, the β values) of those two isotherms are very close to each other (i.e., 2.45 versus 2.47). The change in α and β indicate that the adsorption wave shape is different from that for non-calendered samples. Consequently, the breakthrough curves are changed as well. Compared with non-calendered samples, the breakthrough curves for calendered samples were shifted back to the left and had steeper curves (Figure 3.7). The shift back accounted for breakthrough time loss (over 50% on the average) and adsorption capacity (over 50% on the average). The steeper curves indicated that the TCE

gas permeated calendered samples at an accelerated rate. The different K value ranges for the calendered and non-calendered samples also explained the fact that the carbon bed was critically distorted by the thermal calendering. As a result of the carbon bed deformation, the shape of the adsorption wave was changed. So were the position and shape of the breakthrough curves for the calendered samples.

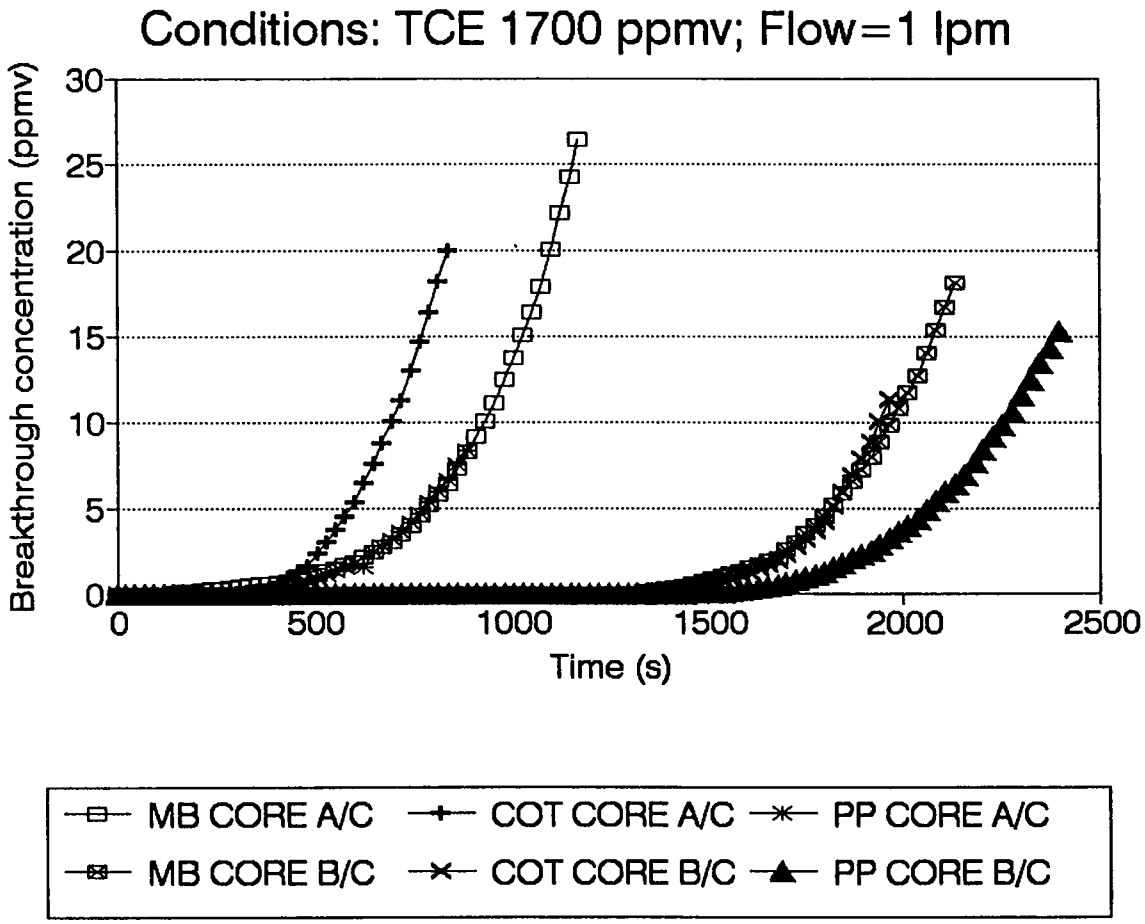

Figure 3.7 Average Breakthrough Curves for Non-calendered and Calendered Samples. (Abbreviation in legend: A/C = after calendering; B/C = before calendering, MB = melt blown, COT = cotton, PP = polypropylene).

CHAPTER 4

EXPERIMENTAL METHOD

4.1 Materials

4.1.1 Spunbond Nonwoven Fabric

A polypropylene (PP) spunbond nonwoven, made at the University of Tennessee, Textiles and Nonwovens Development Center (TANDEC), on the one meter Reicofil spunbonding processing pilot line facility was used throughout the study.

Spunbond material was chosen as the outer layer of the experimental laminates because it is strong, highly air permeable and light in weight. The processing parameters and the characterization of the spunbond nonwoven material are shown in Tables 4.1 and 4.2.

4.1.2 Melt Blown Nonwoven Fabric

Nylon (N), polyethylene (PE), polyester (PET), and polypropylene (PP) were the initial polymer candidates for the melt blown (MB) fabric. Trial tests indicated that activated carbon powder did not adhere to the melt blown web of nylon.

Table 4.1 Processing Parameters of One Meter Reicofil PP Spunbond Nonwoven Material.

Process Parameter	Parameter Setting
Polymer type	Exxon 9355, MFR 35
Extruder temperatures	
Extruder zone 1, °F	365
Extruder zone 2, °F	374
Extruder zone 3, °F	383
Extruder zone 4, °F	392
Extruder zone 5, °F	392
Die temperature, °F	410
Air Settings, suction blower, rpm	2500
Air Settings, cooling air blower, rpm	1270
Cabin pressure, P	100

Table 4.2 Characterization of the PP Spunbond Nonwoven Material.

Physical Property	Value
Melt temperature, °C	141
Average fiber diameter, μm	30.88 ± 0.31
Coefficient of Variation, %	25
Minimum, μm	0.8
Maximum, μm	1.8
Breaking strength (MD), mN/tex	16.8 ± 1.9
Breaking strength (CD), mN/tex	9.9 ± 0.3
Elongation (MD), %	108.6 ± 16.8
Elongation (CD), %	109.8 ± 10.2
Bursting strength, lb/in^2	21.25 ± 4.02
Frazier air permeability, cfm/ft^2	416.6
Fabric weight, g/m^2	31.28 ± 3.06
Thickness, mm	0.404

Melt blown webs of PET and PP retained activated carbon but not as well as PE webs did. Therefore, PE was selected as the polymer for MB material. The MB used throughout the study was made on the 6-inch wide line at the University of Tennessee, Knoxville, Textile Processing Laboratory. The processing parameters and characterization of the PE meltblown nonwoven material are shown in Tables 4.3 and 4.4.

Table 4.3 Processing Parameters of the PE Melt Blown Nonwoven Material.

Processing Parameter	Parameter Value
Nozzle hole diameter, mm	0.0145
Number of holes	501
Air Gap, mm	0.060
Polymer type	PD-3545G, 56329, 850 MFR
Extruder Temperature, °F	
Extruder Zone 1, °F	360
Extruder Zone 2, °F	400
Extruder Zone 3, °F	420
Extruder Zone 4, °F	440
Die 1-9, °F	510
Air Temperatures, °F	
Furnace 1, °F	400/403
Furnace 2, °F	450/454
Furnace 3, °F	600/622
Throughput, g/hole/minute	0.4

Table 4.4 Characterization of the PE Melt Blown Nonwoven Material.

Parameter	Value
Average fiber diameter, μm	7.53 ± 1.52
Coefficient of Variation, %	51
Minimum, μm	1.75
Maximum, μm	17
Breaking strength (MD), mN/tex	0.6 ± 0.0
Breaking strength (CD), mN/tex	0.6 ± 0.1
Elongation (MD), %	87.2 ± 1.6
Elongation (CD), %	116.7 ± 9.2
Bursting strength, lb/cm^2	2.16 ± 0.07
Frazier air permeability, cfm/ft^2	924
Fabric weight, g/m^2	27.16 + 0.22
Thickness, mm	0.379

4.1.3 Cotton Carded Core

Four levels of bleached carded cotton web (0, 1, 2, and 3 oz/yd^2) were used as the core of the laminates. In the case of 0 oz/yd^2 level of cotton webs, the core consisted of three layers of MB. Each MB layer was sprayed with approximately 40 g/m^2 of HSA carbon powder.

In the case of the 1 oz/yd^2 cotton core, one layer of the 1 oz/yd^2 cotton web was sprayed with 40 g/m^2 carbon and two separate layers of 1 oz/yd^2 MB web were loaded with 40 g/m^2 carbon. The 1 oz/yd^2 cotton core was sandwiched between the two carbon-loaded MB layers to constitute an integral core

with a total carbon loading of 120 g/m^2. The core was further sandwiched between two separate layers of 1 oz/yd^2 MB webs. The 1.0 oz/yd^2 carded cotton web is characterized in Table 4.5. In the case of the 2 oz/yd^2 cotton core, two separate layers of 1 oz/yd^2 cotton web and one layer of 1 oz/yd^2 MB were each sprayed with 40 g/m^2 of activated carbon. The carbon-loaded MB layer was sandwiched between 2 single carbon-loaded cotton webs to form an integral core with a total carbon loading of 120 g/m^2. A 1 oz/yd^2 MB web was put on the top and bottom of the laminate. In the case of 3 oz/yd^2 cotton core, three 1 oz/yd^2 cotton webs were each loaded with 40 g/m^2 carbon, and then sandwiched between separate layers of 1 oz/yd^2 MB.

Table 4.5 Characterization of 1.0 oz/yd^2 carded cotton web.

Characteristic	Value
Air permeability, cfm/ft^2	1,559
Web weight, g/m^2	25.67
Thickness, mm	0.397

4.1.4 Polypropylene Carded Core

Two weights of polypropylene (PP) carded webs were also used in this study. The PP carded webs were used to differentiate the significance of "laminate core fiber effects" between the non-thermoplastic cotton core and

thermoplastic PP on the gas adsorption properties of corresponding laminates before and after thermal calendering. The two PP carded web weights used throughout the study were 1.8 and 2.6 oz/yd^2. In the case of 1.8 oz/yd^2 PP core, one layer of 1.8 oz/yd^2 PP web was sprayed with 80 g/m^2 of the activated carbon and one layer of 1.0 oz/yd^2 MB web was sprayed with 40 g/m^2 of activated carbon. These two carbon-loaded layers were then sandwiched between two separate layers of 1.0 oz/yd^2 PE MB webs to form a laminate with a total activate carbon loading of 120 g/m^2. In the case of the 2.6 oz/yd^2 PP core, a single layer of 2.6 oz/yd^2 PP web was loaded with 120 g/m^2 carbon and sandwiched between two separate layers of 1.0 oz/yd^2 PE MB. The carded PP webs are characterized in Table 4.6.

Table 4.6 Characterization of 1.8 and 2.6 oz/yd^2 carded PP webs.

Characteristic	1.8 oz/yd^2 PP web	2.6 oz/yd^2 PP web
Air permeability, cfm/ft^2	507.5	386.4
Web weight, g/m^2	59.58 ± 2.32	81.17 ± 3.04
Thickness, mm	0.940	1.159

4.1.5 High Surface Area Activated Carbon

The high surface area (HSA) activated carbon - Anderson AX-21 used in this study was manufactured by the Kansai Coke

and Chemicals Company, Limited, 5 Misono-cho, Amagaski City, Japan 660. The HSA carbon has a pore volume of 1.62 cm^3/g and a surface area of 3,050 m^2/g.

4.2 Loading of High Surface Area Activated Carbon

The HSA activated carbon was sprayed onto the core using a fluidized bed spray apparatus. Each fabric layer was weighed gravimetrically before and after the application of the HSA activated carbon to determine the amount of carbon being loaded onto the sample.

4.3 Preparation of Laminates

The structures of the laminates are shown in Table 4.7.

Table 4.7 Diagram of the composition of the laminates.

Cotton Carded Core, oz/yd^2			PP Carded Core, oz/yd^2		Control, oz/yd^2
1	2	3	1.8	2.6	
MB MB-C COTTON-C MB-C MB	MB COTTON-C MB-C COTTON-C MB	MB COTTON-C COTTON-C COTTON-C MB	MB MB-C PP-C MB	MB PP-C MB	MB MB-C MB-C MB-C MB

PP = Polypropylene web.
C = HSA activated carbon.
MB = meltblown web.

The 8 X 8 in^2 laminates were made and then, cut into a six inch-diameter circle to fit into the challenge gas adsorption test apparatus. Because there was no substantial bonding between the layers around the perimeter of the laminates, the edge of every and each laminate was sewn by hand to prevent carbon powder from falling out during handling and testing. Characteristics of the non-calendered samples are shown in Table 4.8.

Table 4.8 Non-calendered Laminate Characteristics.

Sample Number	Core Type	Weight (g)	Thickness (mm)	Air Permeability (cfm/ft^2)
0-1	MB	5.8237	2.79	8.330
0-2	MB	5.5778	2.49	9.244
0-3	MB	5.7514	2.95	8.330
0-4	MB	4.9296	2.59	9.634
0-5	MB	5.2901	2.46	5.102
0-6	MB	5.5052	2.77	8.415
1-1	COTTON	5.1285	3.25	4.200
1-2	COTTON	6.3344	3.58	3.420
1-3	COTTON	4.3043	3.81	5.590
1-4	COTTON	6.4308	4.06	3.420
1-5	COTTON	6.1060	3.56	4.980
1-6	COTTON	6.3950	4.01	3.420
2-1	COTTON	5.5074	5.33	9.790
2-2	COTTON	4.8710	4.32	16.700
2-3	COTTON	4.9516	4.57	16.050
2-4	COTTON	5.1956	4.83	3.420
2-5	COTTON	5.2381	5.05	10.720
2-6	COTTON	4.9147	4.55	6.921
3-1	COTTON	4.4435	5.82	52.680
3-2	COTTON	4.5225	4.75	18.560
3-3	COTTON	5.4954	5.31	26.500
3-4	COTTON	5.3584	5.56	28.580
3-5	COTTON	4.8910	5.59	17.620
3-6	COTTON	5.0828	5.84	31.500
PP18-1	PP	4.3253	3.73	10.156
PP18-2	PP	5.2349	3.45	14.900
PP18-3	PP	4.7342	3.48	12.740
PP18-4	PP	4.2828	3.23	33.600

Sample Number	Core Type	Weight (g)	Thickness (mm)	Air Permeability (cfm/ft^2)
PP18-5	PP	4.7837	3.91	11.760
PP18-6	PP	4.3564	3.63	32.100
PP26-1	PP	4.1595	3.35	48.980
PP26-2	PP	4.2240	3.23	41.900
PP26-3	PP	4.3719	3.38	51.380
PP26-4	PP	4.0938	3.35	44.900
PP26-5	PP	4.2069	3.10	57.760
PP26-6	PP	4.7547	3.56	34.000

4.4 Trichloroethylene (TCE) Adsorption Test

4.4.1 Test Gas

Trichloroethylene (TCE) was used as the challenge gas throughout the study. A 1700 ppmv concentration of TCE in nitrogen was purchased from National Specialty Gases (Durham, NC). The concentration of the gas was certified by the vendor using a gas chromatograph.

4.4.2 Test Apparatus

The experimental set-up, as shown in Figure 4.1, used a modified Dawson cup filter holder. The challenge gas from a compressed gas tank was guided through a two stage regulator and a rotameter to the filter holder at a constant flow rate of one liter per minute. From the flowmeter, the gas passed through a T fitting with ball valves in each line, which made it possible for the operator to bypass the Dawson cup before or after the adsorption test and routing the gas directly to the gas detector to measure the inlet gas concentration. During the adsorption test, the gas was routed through the Dawson cup assembly where the adsorption occurred and then, to the gas detector to measure the outlet gas concentration. The departing gas was filtered through a thick activated carbon column so that any unadsorbed gas would be depleted.

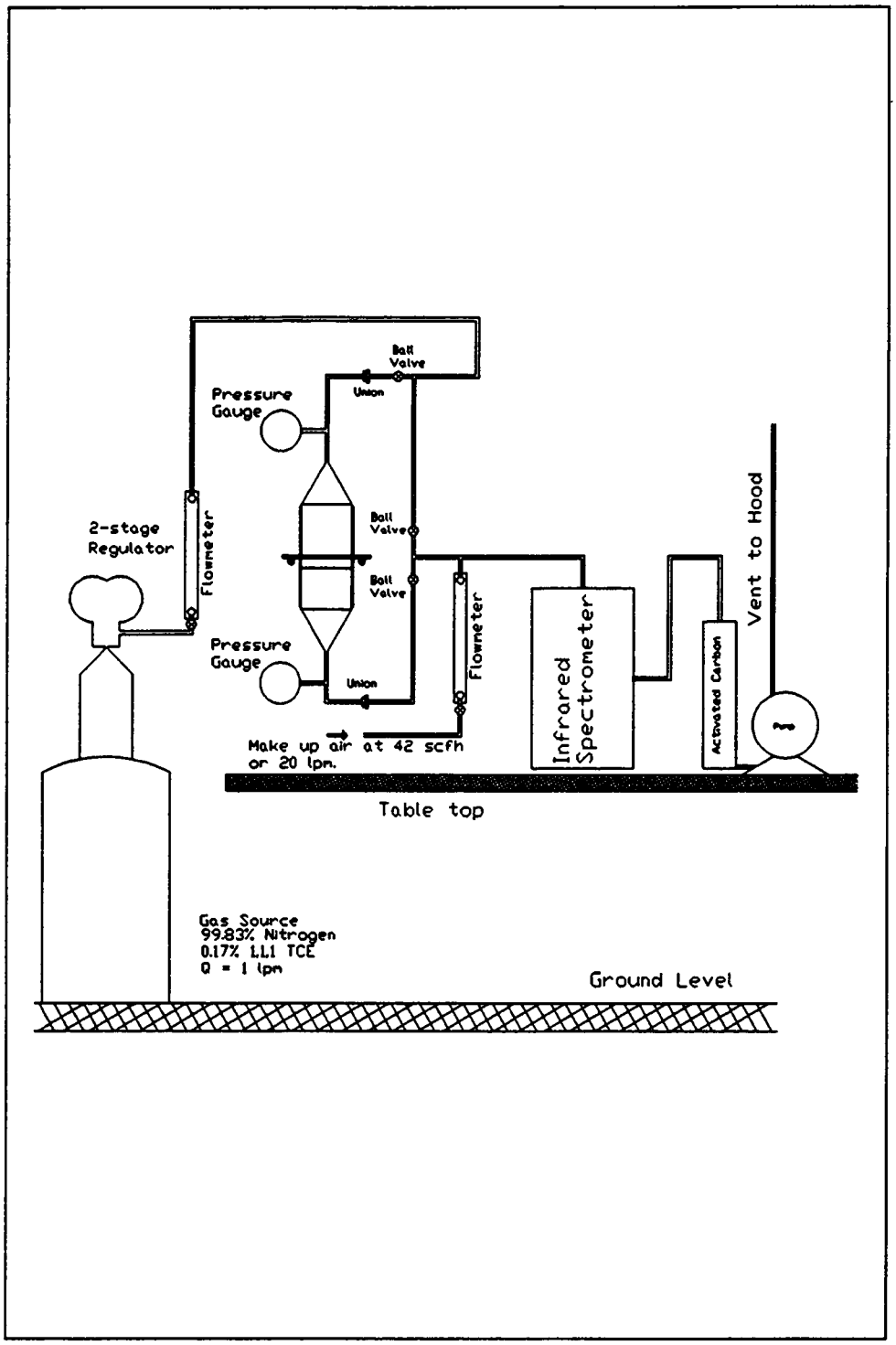

Figure 4.1 TCE adsorption test setup.

4.4.3 Test Gas Detector

A Foxboro Miran 1A infrared spectrometer was used to continuously measure the concentration of the challenge gas. The detector was calibrated every time before and after the gas adsorption test by routing the gas directly to the detector to ensure that the inlet gas concentration was constant. Miran 1A is a variable wavelength, variable pathlength spectrometer capable of measuring a host of gases which have infrared adsorption spectra. The output of the spectrometer is the dimensionless adsorption unit (AU), which can be converted to parts per million (ppm). A strip chart recorder connected to the Miran 1A output was used to continuously log the response of the spectrometer.

4.4.4 Testing Procedure

At least 24 hours before testing, samples were placed in a forced draft oven at 66°C to be regenerated to ensure that any gases that might have been adsorbed during and after the preparation of the laminates were desorbed.

Before testing, the Miran 1A was warmed up for ten minutes to ensure the apparatus reached equilibrium and was zeroed. The instrument was calibrated before each test by routing the gas directly to the detector. Nitrogen was then used to flush the system. The challenge gas was then routed

through the sample where the TCE gas adsorption by the HSA activated carbon loaded nonwoven laminate occurred. The breakthrough time was defined as the time that elapsed between the initial contact of the TCE with the laminate (zero time point) and the time at which the outlet concentration reached 1% of the inlet gas concentration (i.e., 1% x 1700 ppmv = 17 ppmv). The inlet gas concentration was also determined at the end of the test by switching the bypass valve to allow the gas to run directly to the Miran 1A detector. Samples were put back into the oven to be regenerated immediately after the test.

4.4.5 Data Analysis

The Miran 1A detects the gas concentration in a continuous manner, and its output is recorded on the strip chart recorder. The gas concentration at any time of the test can be read from the strip chart if an appropriate chart speed is selected. The chart speed was set at 2 cm/min throughout this study, and a 24 second time interval was used to read concentration values because of the normally long test time and flat slope of the adsorption wave. After the test, the average gas concentration value for each 24 second time interval was read from the chart, and then entered into a spreadsheet in Quattro Pro. A spreadsheet was used to do a simple mass balance to determine the amount of the TCE

adsorbed by the carbon loaded laminates at any given time of the test, and plot the breakthrough curve.

At the beginning and the end of test, the system was calibrated to make sure that TCE flow rate was constant. The highest point (equilibrium point) on the calibration curve was equal to the inlet TCE concentration, i.e., 1700 ppmv. The average value (in blocks) of the equilibrium points on the calibration curves at the beginning and end of a specific test was used as the conversion factor to calculate the outlet TCE concentration at any time point from the strip chart. All calibrations were done at 1.0 AU (a dimensonless absorption unit) of Miran 1A infrared spectrometer, while most of the tests were done at 0.1 AU, which is 10 times more sensitive than 1.0 AU. For example, if the average value of the equilibrium points on the calibration curves at 1.0 AU is 34 blocks, which is equivalent to 1700 ppm of inlet TCE concentration, then each block unit on the strip chart at 0.1 AU during the adsorption test is equivalent to 1700 ppmv/(34 blocks x 10) = 5.0 ppmv.

Since the chart speed was 2 cm/min, and the length of 10 blocks on the chart is equal to 2 cm, then each block length on the chart was equivalent to a time interval of 6 seconds. The time axis was divided into equally spaced intervals of 24 seconds, which spanned 4 blocks. The mid-point of each 24 s time interval was marked on the strip chart as the data point of that particular interval. And its value in blocks was read

and recorded. All the values in blocks were input into a spreadsheet to be converted to the outlet TCE concentration in ppmv. It was assumed that the outlet TCE concentration during the 24 s period is constant, so it is easy to calculate the amount of TCE in grams adsorbed by the laminate during the 24 s time interval. This calculation involves converting the TCE concentration adsorbed in ppmv (i.e., the difference between the inlet and outlet TCE concentration) to g/m^3, then multiplying by the flow rate (1 lpm) and the time (24 s). The amount of TCE adsorbed during each 24-second period was determined in this way. By using the spreadsheet, it is very easy to do a simple integration on any given time period to determine the amount of TCE adsorbed up to that time point. Because the carbon loading and effective adsorption area are known, the amount of adsorbing carbon on the laminate can be determined. To figure out the adsorption capacity in the unit of grams of TCE/grams of carbon, the TCE amount adsorbed should be divided by the adsorbing carbon amount.

It is fairly easy to plot breakthrough curves which consist of time in the x-axis, and the outlet TCE gas concentration in the y-axis.

4.5 Calendering of Laminates

Before the thermal calendering, each sample was sandwiched between two layers of 1.2 oz/yd^2 PP spunbond

nonwoven. The edges were hand sewn to the SB to prevent slipping of the layers during the calendering. The thirty-six before-calendered laminates were thermally calendered using a one-meter wide Kuester calender roll. The top calender roll had a 15% pattern surface area, and the bottom calender roll was a smooth roll. Thirty different thermal calendering conditions were tested using a customized fractional factorial experimental design.

4.6 Experimental Design

The parameters in the experimental design are shown in Table 4.9.

The total number of possible process parameter combinations is 486 which is the number required using a full factorial design. However, 486 parameters is impractical for this study. The E4 software, developed by Sanders and Schneider at the University of Tennessee, Knoxville, is able to generate a customized fractional factorial experimental design (Appendix B). Thirty-six combinations of the process parameters were selected using the software. The confidence level of the design was over 95%. The actual calendering run sheet is listed in Appendix C.

The experimental data were collected and then statistically analyzed using the General Linear Model procedures. Chapter 5 describes the results of the statistical

analysis.

Table 4.9 Parameters in the experimental design.

Process variables in this study	Level(s)	Description of the level(s)
Core	6	Cotton carded web: 1, 2, and 3 oz/yd^2 PP carded web: 1.8 and 2.6 oz/yd^2 Control: No carded nonwoven core.
Adsorbent	1	HSA activated carbon, 120 g/m^2
Adsorbate	1	Trichloroethylene (TCE), 1700 ppmv
Top calender roll temperature	3	110, 120, and 130°C
Bottom calender roll temperature	3	80, 90, and 100°C
Nip pressure	3	250, 300, and 350 pli*
Calender speed	3	4, 6, and 8 m/min
Total possible combinations	486	(6 x 1 x 1 x 3 x 3 x 3 x 3 = 486)

* pli = pounds per liner inch.

CHAPTER 5

RESULTS AND DISCUSSION

5.1 Scope of The Study

The purpose of this study was to reduce the detrimental effects of the thermal point bonding on the TCE adsorption properties of the HSA activated carbon impregnated nonwoven laminates. The detrimental effects of the calendering included pinholes, decreased breakthrough times and reduced adsorption capacities of the calendered laminates. Six laminate structures (core types) were evaluated in the study. The core types consisted of 1.8 and 2.6 oz/yd^2 PP webs and 0, 1, 2 and 3 oz/yd^2 cotton webs. The carbon type (i.e., HSA activated carbon) and loading (i.e., 120 g/m^2) were held constant. The carbon loaded core was sandwiched between two layers of 1 oz/yd^2 PE meltblown. The MB/core/MB was sandwiched between two layers of 1.2 oz/yd^2 PP spunbond. A customized fractional factorial experimental design was generated using the E4 software. The data were analyzed using the General Linear Model (GLM). The optimum thermal calendering conditions for the SB/MB/carbon/core/MB/SB laminates were determined for the present study.

5.2 Statistical Analysis of The Data

Before the E4 software program was developed, experimental designs had to be made in such a way that it was possible to conduct the analysis of variance using a rotary calculator [15]. This demanded the designs be orthogonal (i.e., the effect of each factor was completely independent of every other factor). Statisticians spent an enormous amount of time generating orthogonal experimental designs, and those orthogonal designs were published in tables. One disadvantage of orthogonal designs was that each factor could have only two or three levels. Another restraint was that the number of design points was a power of the number of levels of the factor. For example, if each factor had three levels, then the designs could only have 9, 27, or 81 design points (i.e., powers of 3). With the help of computers researchers can now analyze data using the GLM and the E4 software can be used to generate customized fractional factorial experimental designs, thereby eliminating the old constrains. The GLM does not require experimental designs be orthogonal. It is possible to use an experimental design even when the number of design points is limited. For example, it may be necessary to restrict the amount of the material used in testing due to the cost limitation. The more design points, the more reliable and accurate the results. In addition, the number of design points is not required to be a power of the number of the levels of

the factor. One factor can have five levels, anther factor can have three levels, while the third factor may have seven levels. The advantage of not requiring the same number of levels for every factor enables researchers to perform the statistical analysis even when the data are incomplete due to the accidental breakdown of the equipment. It is possible to tailor the experimental design to the researchers' questions, rather than the reversed. Researchers can now broaden the range of their investigations and simultaneously analyze several response variables. This leads to the "region of compromise", while consuming fewer resources and less time.

There were 486 possible combinations of the core fiber types with the thermal calendering in the study. It is not practical and not economical to test all possible combinations because a properly selected subset of the total combinations (i.e., a customized fractional factorial experimental design) could be tested to predicted all possible outcomes. The E4 fractional factorial experimental design is listed in Appendix B. The actual calendering run sheet listed in Appendix C. The CFFED consisted of 36 design points.

The data were analyzed using the GLM procedure. GLM, an extension of analysis of variance (i.e., ANOVA) is able evaluate the effects of several response variables simultaneously for both balanced and unbalanced data. Contrast statements were also used in the GLM procedure to compare the levels of each factor.

5.3 Effect of The Independent Variables

5.3.1 Before Calendering

The results for the breakthrough times and the adsorption capacities of the laminates before thermal calendering are listed in Appendix A. The class information for the statistical analysis is shown in Table 5.1.

Table 5.1 Class Information - Before Calendering.

Class Information: Before Calendering		
RESPONSES = Breakthrough Time (seconds) Adsorption Capacity (g TCE/g CARBON)		
CLASS	**LEVEL**	**VALUES**
CORE FIBER TYPE	2	COTTON, PP
CORE WEIGHT	6	COTTON: 0, 1, 2 and 3 oz/yd^2 PP: 1.8 and 2.6 oz/yd^2
Number of observations = 36		

The ANOVA of the breakthrough time for the before calendered samples is shown in Table 5.2.

The probability value of 0.0098 indicates the core fiber type has a statistically significant effect on the breakthrough time at the 0.01 probability level.

The ANOVA of the adsorption capacity is shown in Table 5.3.

Table 5.2 ANOVA of the Breakthrough Time Before Calendering.

Dependent Variable: Breakthrough Time (seconds)					
Source	DF	Sum of Squares	Mean Square	F Value	Pr > F
Model	5	904832.00	180966.40	2.01	0.1063
Error	30	2705664.00	90188.80		
Corrected Total	35	3610496.00			

R^2	C.V.	Root MSE	Breakthrough Time Mean
0.250612	13.06473	300.31450	2298.66667

Source	DF	Type III SS	Mean Square	F value	Pr > F
CORE FIBER	1	686792.00	686792.0	7.62	0.0098*
CORE_WT	4	218040.000	54510.00	0.60	0.6625

* Indicating factor is significant at 0.01 probability level.

Since its probability value is 0.0097, the core fiber type has a statistically significant effect on the adsorption capacity; but the core weight has no effect (p-value = 0.7015)

The adjusted (least squared) means of the breakthrough time and the adsorption capacity are reported in Appendix D.1 and D.2 respectively.

The effect of the core fiber type on the breakthrough time and the adsorption capacity are illustrated in Figures 5.1 and 5.2 respectively.

Table 5.3 ANOVA of the Adsorption Capacity Before Calendering.

Dependent Variable: Adsorption Capacity (gram/gram)					
Source	DF	Sum of Squares	Mean Square	F Value	Pr > F
Model	5	0.02185175	0.00437035	1.97	0.1128
Error	30	0.06669741	0.00222325		
Corrected Total	35				
R^2	C.V.	Root MSE	Adsorption Capacity Mean		
0.246775	13.00218	0.04715132	0.36264167		
Source	DF	Type III SS	Mean Square	F value	Pr > F
CORE FIBER	1	0.0169740	0.0169740	7.63	0.0097*
CORE_WT	4	0.0048777	0.0012194	0.55	0.7015

* Indicating factor is significant at 0.01 probability level.

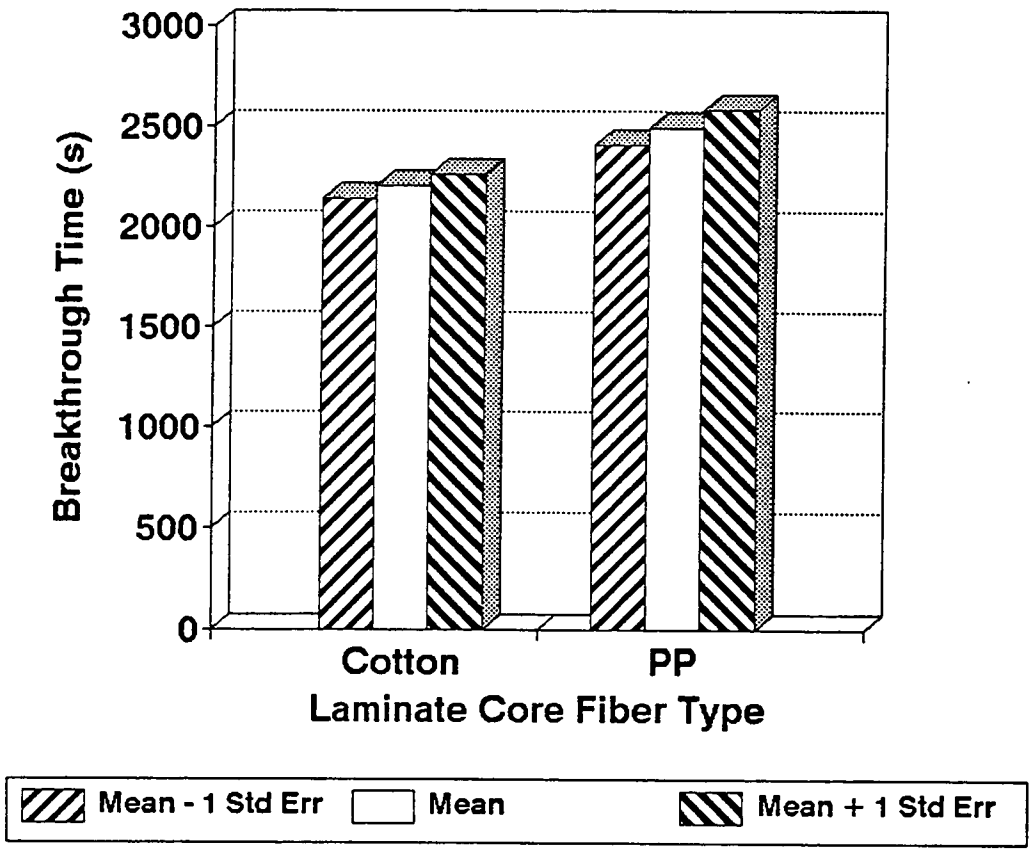

Figure 5.1 Effect of laminate core fiber type on breakthrough time for the non-calendered laminates.

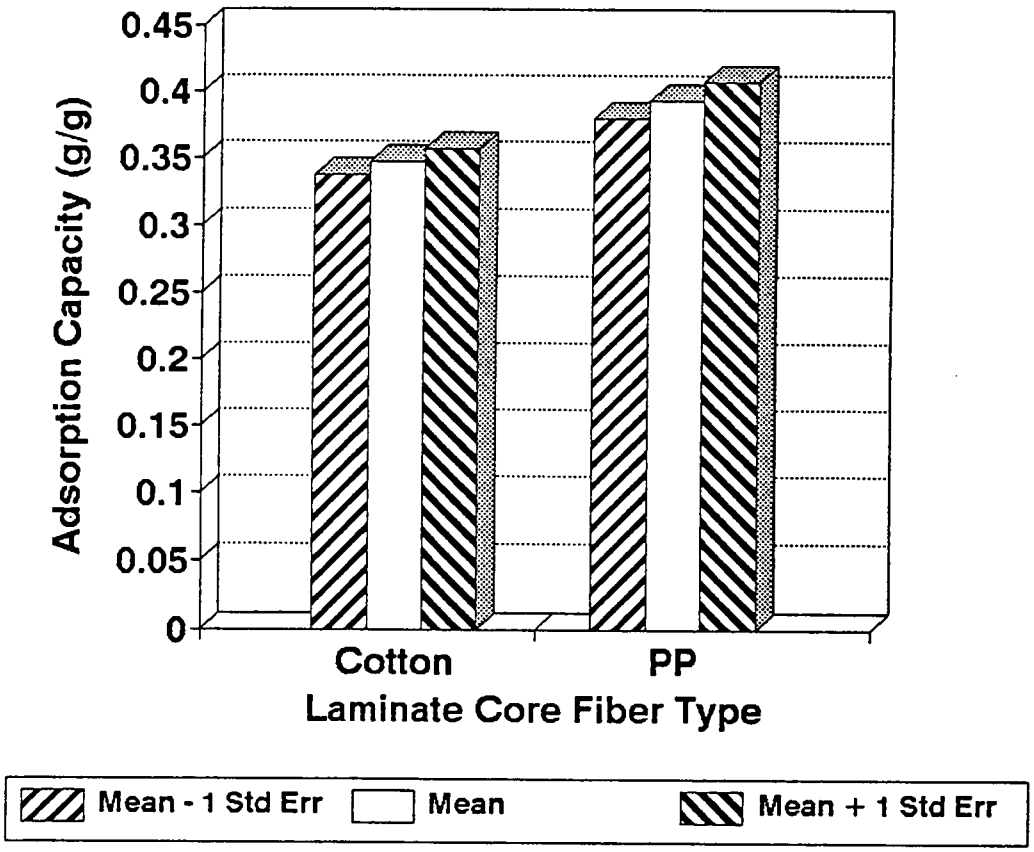

Figure 5.2 Effect of laminate core fiber type on adsorption capacity for the non-calendered laminates.

5.3.2 After Calendering

The measured values for the breakthrough time, the percent change in breakthrough time, the adsorption capacity and the percent change in adsorption capacity are listed in Appendix A. The percent change in breakthrough time and the percent change in adsorption capacity are defined by Equations 5-1 and 5-2 respectively.

$$\Delta T(\%) = \frac{T_{before} - T_{after}}{T_{before}} x100\% \qquad \textbf{(5-1)}$$

where: $\Delta T(\%)$ = percent change in breakthrough time,

T_{before} = breakthrough time before calendering, and

T_{after} = breakthrough time after calendering.

$$\Delta X(\%) = \frac{X_{before} - X_{after}}{X_{before}} x100\% \qquad \textbf{(5-2)}$$

where: $\Delta X(\%)$ = percent change in adsorption capacity,

X_{before} = adsorption capacity before calendering, and

X_{after} = adsorption capacity after calendering.

The class information for the statistical analysis for the laminates after calendering is shown in Table 5.4.

Table 5.4 Class Information After calendering.

Class Information: After Calendering		
RESPONSES = Breakthrough Time (seconds) Adsorption Capacity (gram/gram) Percent Change in Breakthrough Time (%) Percent Change in Adsorption Capacity (%)		
CLASS	**LEVEL**	**VALUES**
Speed	3	4, 6, 8 m/min
Pressure	3	250, 300, 350 pli*
Top_temp	3	110, 120, 130 °C
Bot_temp	3	80, 90, 100 °C
Core Fiber Type	2	Cotton, PP
Core_wt	6	Cotton: 0, 1, 2 and 3 oz/yd^2 PP : 1.8 and 2.6 oz/yd^2
Note: Factor 'core_wt' is nested in 'core fiber type'.		
Number of observations = 36		

* pli = pounds per linear inch

Abbreviations in Table 5.4:

Speed = calender speed

Pressure = calender nip pressure

Top_temp = top calender roll temperature

Bot_temp = bottom calender roll temperature

Core fiber = laminate core fiber type

core_wt = core weight

The ANOVA from the GLM procedures are shown in Tables 5.5 through 5.8 for the four responses variables breakthrough time, percent change in breakthrough time, adsorption capacity, and percent change in adsorption capacity respectively. The p-values of the model for these four responses are 0.0161, 0.0320, 0.0164 and 0.0396 respectively. Therefore, the model for all four responses is significant at the 0.05 probability level.

Table 5.5 ANOVA of the Breakthrough Time for Calendered Laminates.

Dependent Variable: Breakthrough Time (s)					
Source	**DF**	**Sum of Squares**	**Mean Square**	**F Value**	**Pr > F**
Model	21	2422025	115335	3.13	0.0161 *
Error	14	515319	36809		
Corrected Total	35	2937344			
R^2	**C.V.**	**Root MSE**		**Breakthrough Time Mean**	
0.824563	18.12237	191.85543		1058.66667	
Source	**DF**	**Type III SS**	**Mean Square**	**F value**	**Pr > F**
Speed	2	343043	171522	4.66	0.0281 *
Pressure	2	471453	235727	6.40	0.0106 *
Bot_Temp	2	45276	22638	0.62	0.5546
Top_Temp	2	27877	13939	0.38	0.6916
Core Fiber	1	553211	553211	15.03	0.0017 *
Core_wt (laminate)	4	374842	93710	2.55	0.0860
Speed x Laminate	2	410894	205447	5.58	0.0165 *
Pressure x Laminate	2	309603	154802	4.21	0.0371 *
Bot_Temp x Laminate	2	213049	106524	2.89	0.0887
Top_Temp x Laminate	2	13180	6590	0.18	0.8380

* Indicating factor is significant at the 0.05 probability level.

Table 5.6 ANOVA of the Percent Change in Breakthrough Time for Calendered Laminates.

Dependent Variable: Percent Change in Breakthrough Time (%)					
Source	DF	Sum of Squares	Mean Square	F Value	Pr > F
Model	21	0.272579	0.012980	2.66	0.0320 *
Error	14	0.068230	0.004864		
Corrected Total	35	0.340809			
R^2	C.V.	Root MSE		Percent Change in Breakthrough Time	
0.799801	12.89864	0.06981076		0.54122584	
Source	DF	Type III SS	Mean Square	F value	Pr > F
Speed	2	0.037989	0.018994	3.90	0.0451 *
Pressure	2	0.053043	0.026521	5.44	0.0178 *
Bot_Temp	2	0.005078	0.002539	0.52	0.6050
Top_Temp	2	0.003472	0.001736	0.36	0.7065
Core Fiber	1	0.023550	0.023550	4.83	0.0452 *
Core_wt (laminate)	4	0.082725	0.020681	4.24	0.0186 *
Speed x Laminate	2	0.026157	0.013079	2.68	0.1031
Pressure x Laminate	2	0.046016	0.023008	4.72	0.0271 *
Bot_Temp x Laminate	2	0.016098	0.008049	1.65	0.2270
Top_Temp x Laminate	2	0.002704	0.001352	0.28	0.7618

* Indicating factor is significant at the 0.05 probability level.

Table 5.7 ANOVA of the Adsorption Capacity for Calendered Laminates.

Dependent Variable: Adsorption Capacity (g TCE/g Carbon)					
Source	DF	Sum of Squares	Mean Square	F Value	Pr > F
Model	21	0.058030	0.002811	3.12	0.0164 *
Error	14	0.012610	0.000901		
Corrected Total	35	0.071640			
R^2	C.V.	Root MSE	Adsorption Capacity Mean		
0.823981	17.75447	0.03001197	0.16903889		
Source	DF	Type III SS	Mean Square	F value	Pr > F
Speed	2	0.008361	0.004181	4.64	0.0284 *
Pressure	2	0.011516	0.005758	6.39	0.0107 *
Bot_Temp	2	0.001096	0.000548	0.61	0.5581
Top_Temp	2	0.000681	0.000341	0.38	0.6919
Core Fiber	1	0.013467	0.013467	14.95	0.0017 *
Core_wt (laminate)	4	0.009112	0.002278	2.53	0.0875
Speed x Laminate	2	0.009994	0.004997	5.55	0.0168 *
Pressure x Laminate	2	0.007544	0.003772	4.19	0.0375 *
Bot_Temp x Laminate	2	0.005177	0.002589	2.87	0.0900
Top_Temp x Laminate	2	0.000327	0.000163	0.18	0.83

* Indicating factor is significant at the 0.05 probability level.

Table 5.8 ANOVA of the Percent Change in Adsorption Capacity for Calendered Laminates.

Dependent Variable: Percent Change in Adsorption Capacity (%)					
Source	DF	Sum of Squares	Mean Square	F Value	Pr > F
Model	21	0.265221	0.012630	2.52	0.0396 *
Error	14	0.070044	0.005003		
Corrected Total	35	0.335265			

R^2	C.V.	Root MSE	Mean Percent Change in Adsorption Capacity
0.791078	13.21038	0.07073291	0.53543446

Source	DF	Type III SS	Mean Square	F value	Pr > F
Speed	2	0.037658	0.018829	3.76	0.0492 *
Pressure	2	0.052009	0.026004	5.20	0.0205 *
Bot_Temp	2	0.005030	0.002515	0.50	0.6154
Top_Temp	2	0.003290	0.001645	0.33	0.7252
Core Fiber	1	0.022009	0.022009	4.40	0.0446 *
Core_wt (laminate)	4	0.079208	0.019802	3.96	0.0236 *
Speed x Laminate	2	0.024798	0.012399	2.48	0.1198
Pressure x Laminate	2	0.045059	0.022530	4.50	0.0309 *
Bot_Temp x Laminate	2	0.015585	0.007793	1.56	0.2450
Top_Temp x Laminate	2	0.002794	0.001397	0.28	0.7605

* Indicating factor is significant at the 0.05 probability level.

5.3.2.1 Effect of Calender Speed

The calender speed is statistically significant at the 0.05 probability level for all four responses, breakthrough time, percent change in breakthrough time, adsorption capacity and percent change in adsorption capacity (Tables 5.5 through 5.8).

The adjusted (least squared) means of for the four responses are reported in Appendix D.3 through D.6. 6 m/min calender speed has the longest breakthrough time, the highest adsorption capacity, the lowest percent change in breakthrough time, and the lowest percent change in adsorption capacity. The 8 m/min has the shortest breakthrough time, the lowest adsorption capacity, the highest percent change in breakthrough time, and the highest percent change in adsorption capacity. Obviously, the calender speed determines the time available for the laminate structure deformation as well as the time for the heat transfer. However, all 3 calender speeds were in the very low range compared with the 50 m/min normally for the nonwoven production. The laminates were very small compared with the huge calender roll. The laminates were fed by hand. Therefore, the calendering might have been well controlled as expected, which might contribute to the obtained statistical results.

Contrast statements were also used to compare calender speeds. The statistics of the contrasts are reported in

Appendix D.23 through D.26. The results of the contrasts show that of the three levels of calender speed, 6 m/min has significantly longer breakthrough time, higher adsorption capacity, lower percent change in breakthrough time, and lower percent change in adsorption capacity than 4 m/min and 8 m/min respectively.

The effect of the calender speeds on the four responses are illustrated in Figures 5.3 through 5.6.

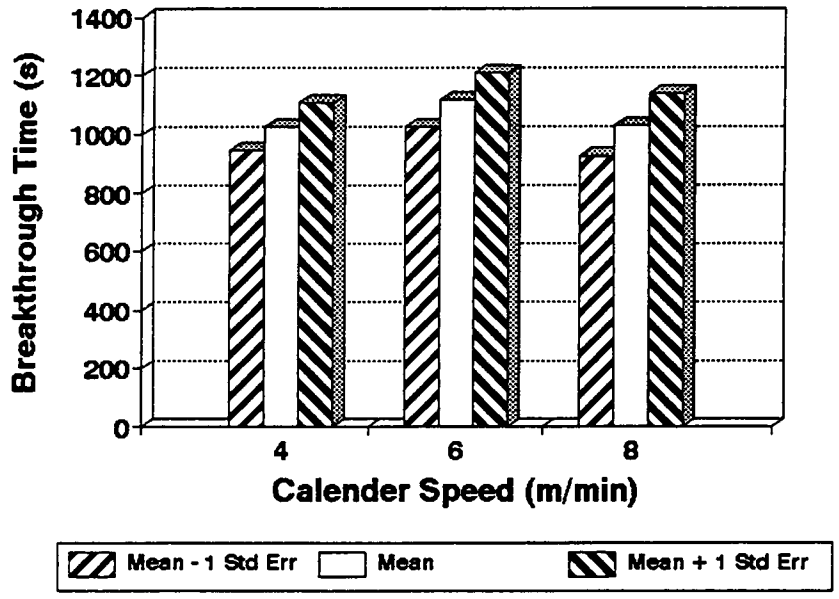

(a)

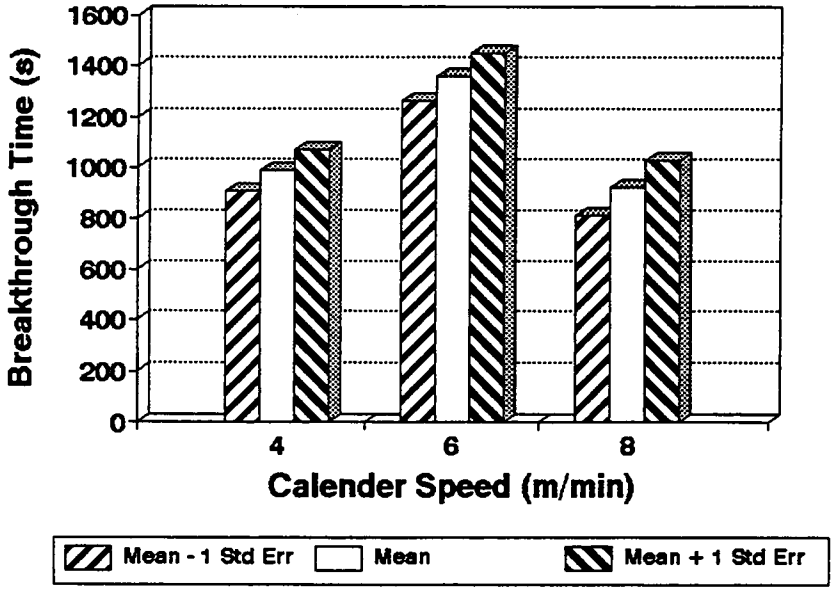

(b)

Figure 5.3 Effect of calender speed on breakthrough time. (a) Value on Y-axis is the average breakthrough time of experimentally measured data. (b) Value on Y-axis is the statistically adjusted mean breakthrough time.

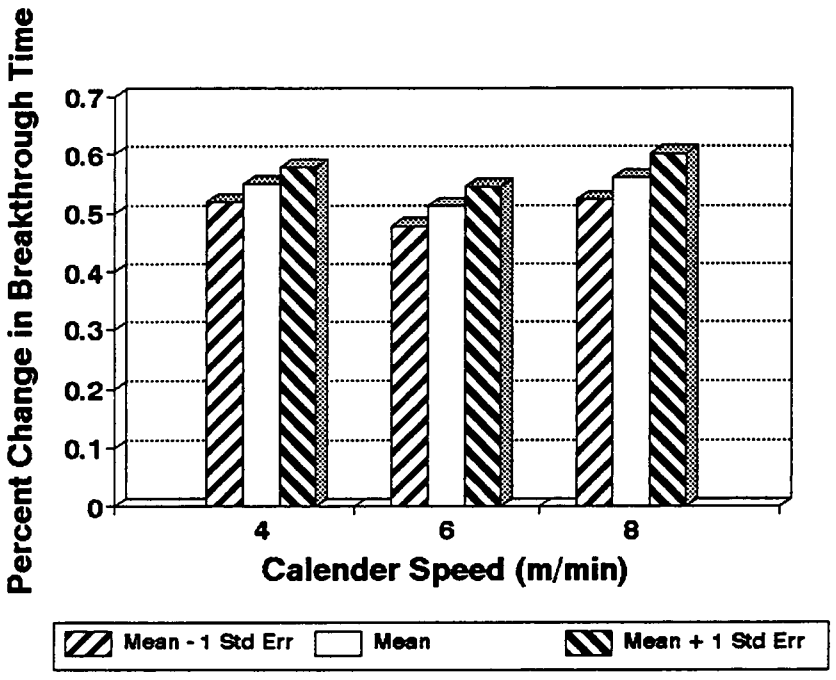

(a)

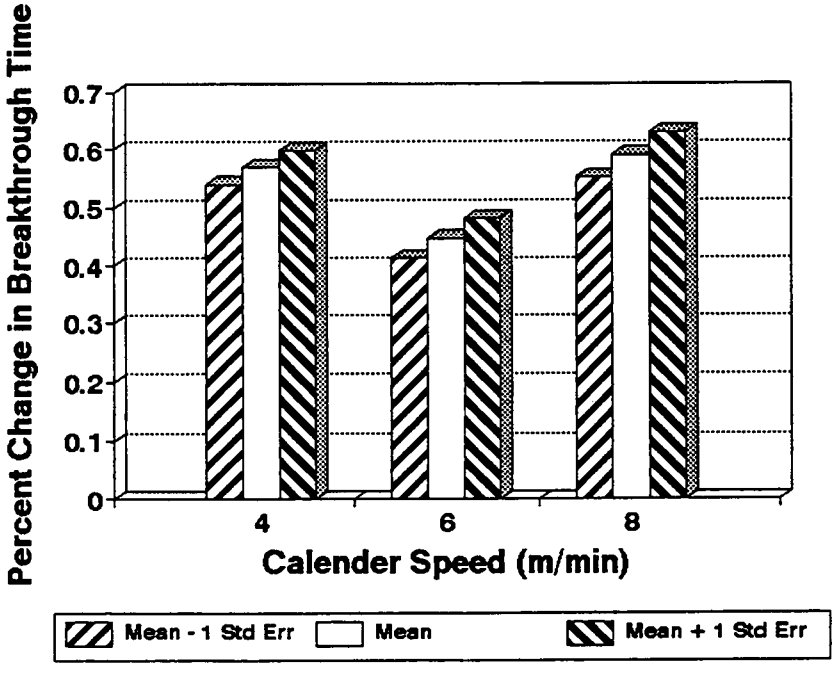

(b)

Figure 5.4 Effect of calender speed on percent change in breakthrough time.
(a) Value on Y-axis is the average percent change in breakthrough time of experimentally measured data.
(b) Value on Y-axis is the statistically adjusted mean percent change in breakthrough time.

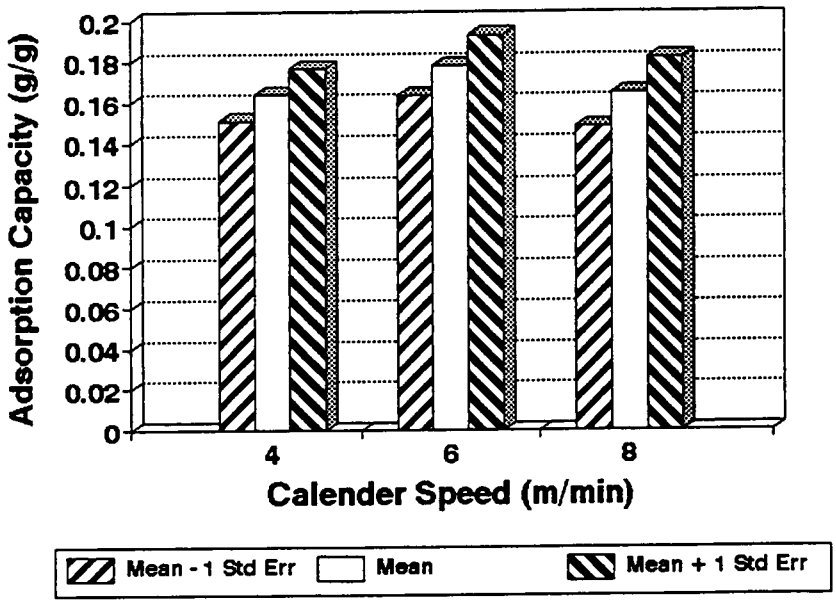

(a)

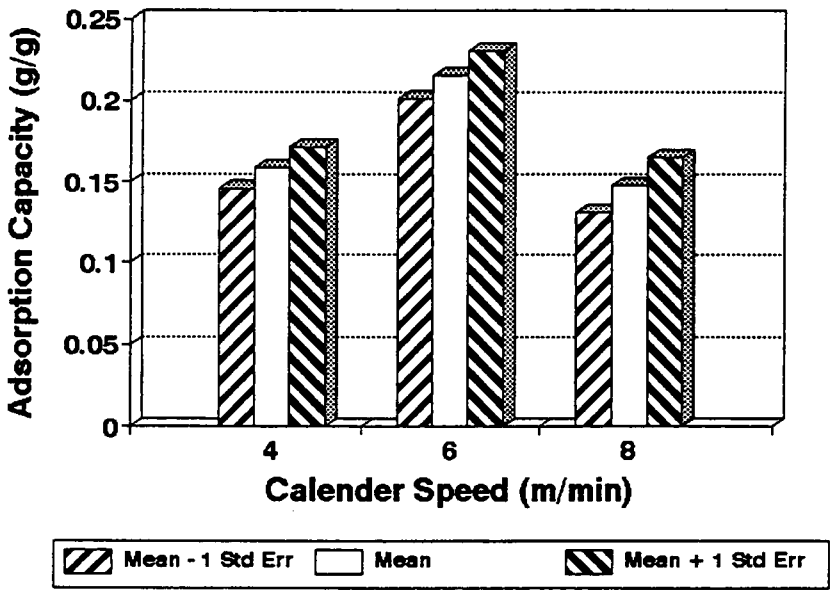

(b)

Figure 5.5 Effect of calender speed on adsorption capacity. (a) Value on Y-axis is the average adsorption capacity of experimentally measured data. (b) Value on Y-axis is the statistically adjusted mean adsorption capacity.

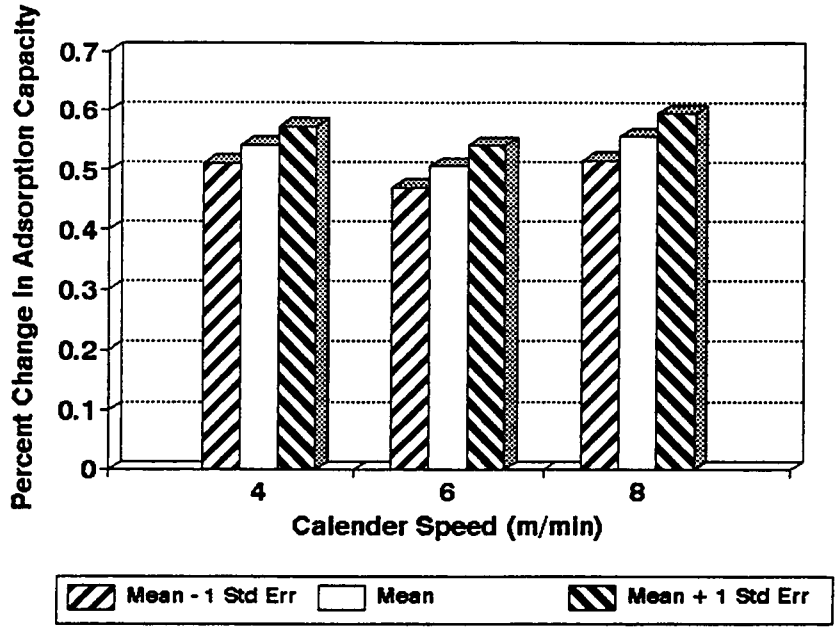

(a)

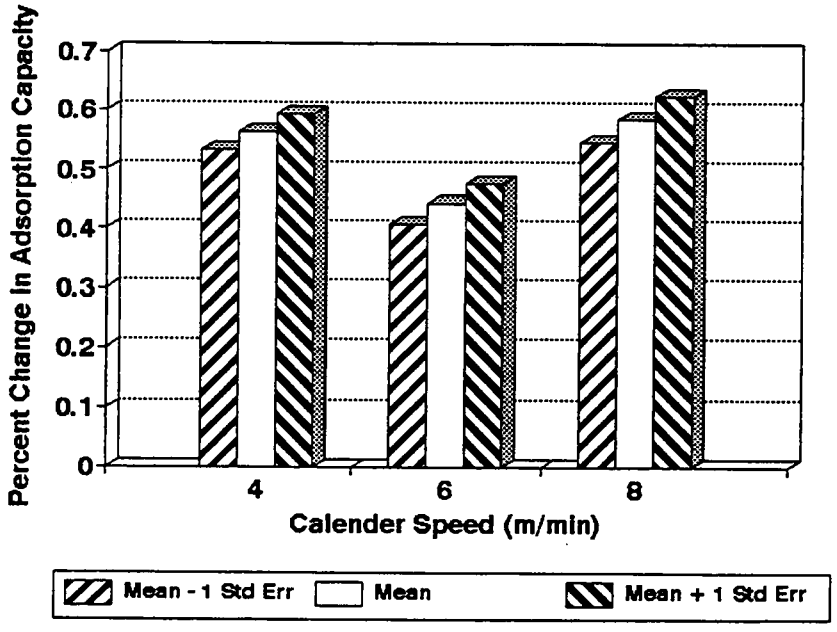

(b)

Figure 5.6 Effect of calender speed on percent change in adsorption capacity. (a) Value on Y-axis is the average percent change in adsorption capacity of experimentally measured data. (b) Value on Y-axis is the statistically adjusted mean percent change in adsorption capacity.

5.3.2.2 Effect of Calender Nip Pressure

The calender nip pressure has a statistically significant effect at the 0.05 probability level on all four responses (i.e, breakthrough time, adsorption capacity, percent change in breakthrough time, and percent change in adsorption capacity). (Tables 5.5 through 5.8).

The adjusted (least squared) means of the four responses are reported in Appendix D.7 through D.10. Of the three levels of calender nip pressure, 300 pli has the longest breakthrough time, the highest adsorption capacity, the lowest percent change in breakthrough time and the lowest percent change in adsorption capacity; 350 pli has the shortest breakthrough time, the lowest adsorption capacity, the highest percent change in breakthrough time and the highest percent change in adsorption capacity. Theoretically, the lower calender nip pressure, the less deformation of the laminate structure, therefore, the less change in breakthrough time and adsorption capacity. However, the fact that the calendering was not well controlled might have contributed to the obtained statistical results.

The contrast statements were also used to test the significance of the difference between the three levels of calender nip pressure. The statistics of the contrasts are reported in Appendix D.23 through D.26. The results of the contrasts show that of the three levels of calender nip

pressure, both 250 pli and 300 pli have significantly longer breakthrough time, higher adsorption capacity, lower percent change in breakthrough time and lower percent change in adsorption capacity than 350 pli.

The effect of the calender nip pressures on the four responses are illustrated in Figures 5.7 through 5.10.

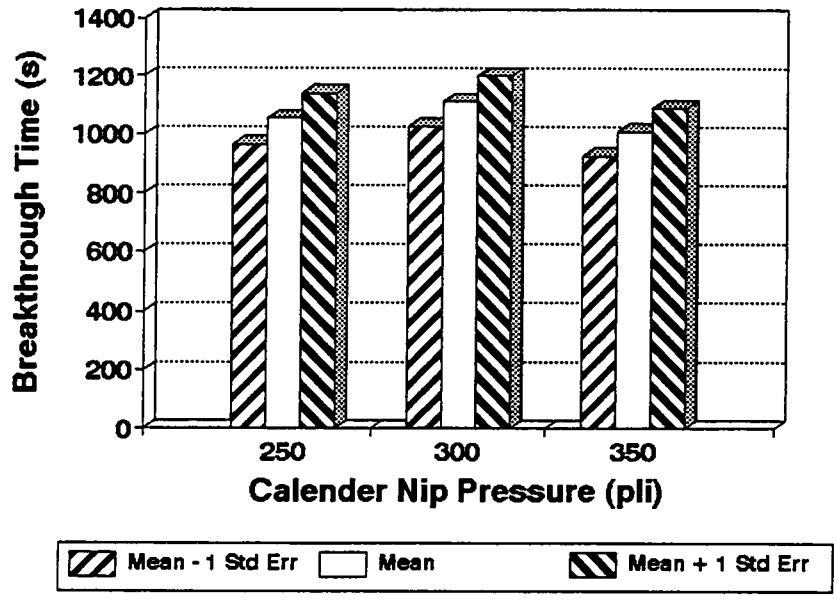

(a)

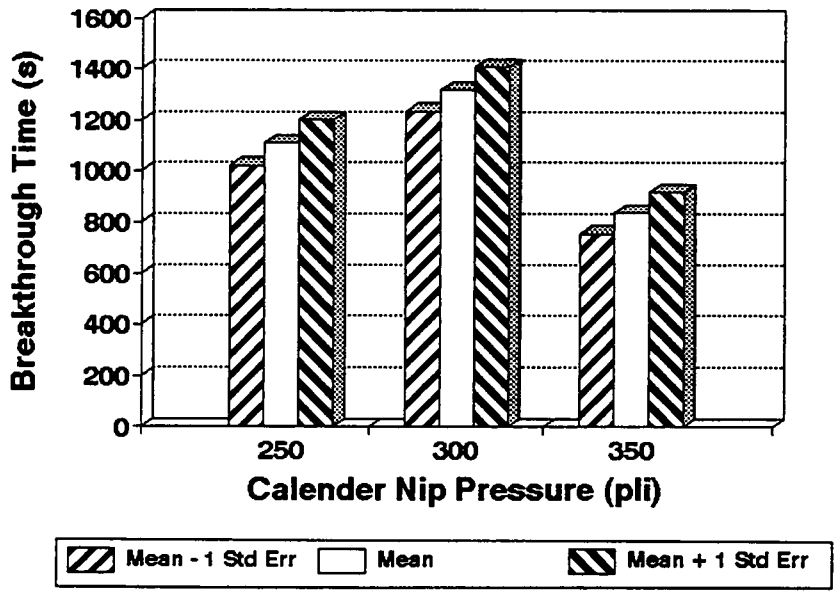

(b)

Figure 5.7 Effect of calender nip pressure on breakthrough time. (a) Value on Y-axis is the average breakthrough time of experimentally measured data. (b) Value on Y-axis is the statistically adjusted mean breakthrough time.

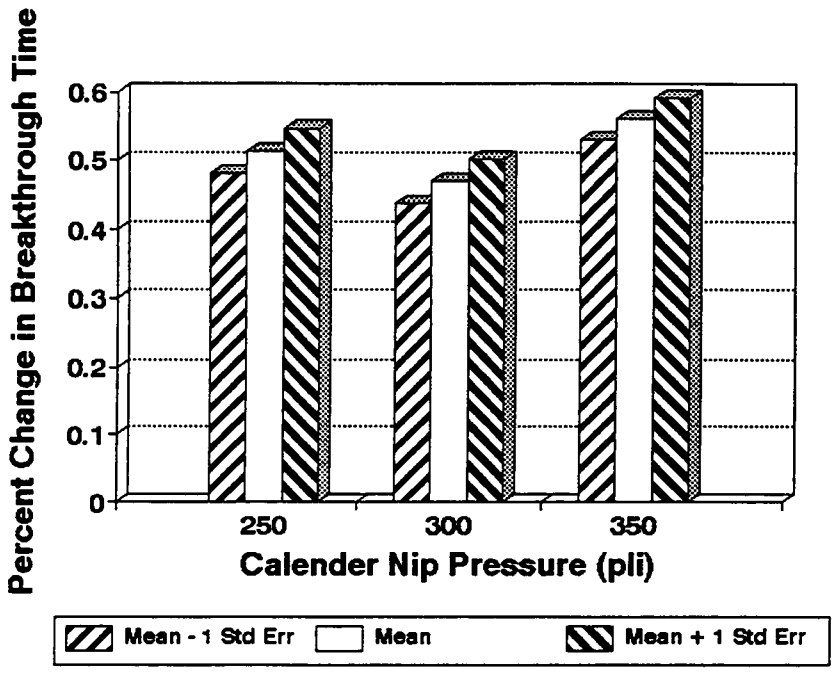

(a)

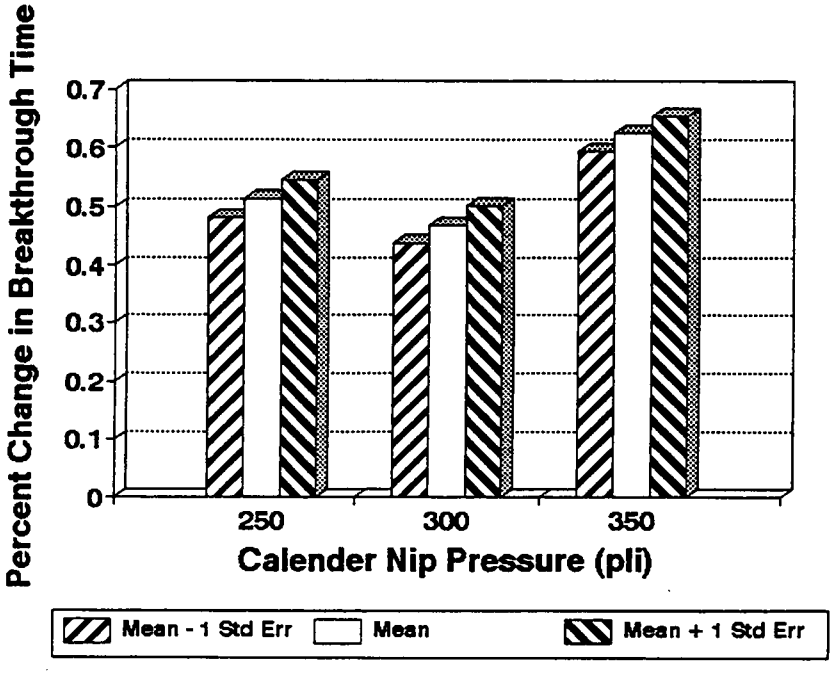

(b)

Figure 5.8 Effect of calender nip pressure on percent change in breakthrough time. (a) Value on Y-axis is the average percent change in breakthrough time of experimentally measured data. (b) Value on Y-axis is the statistically adjusted mean percent change in breakthrough time.

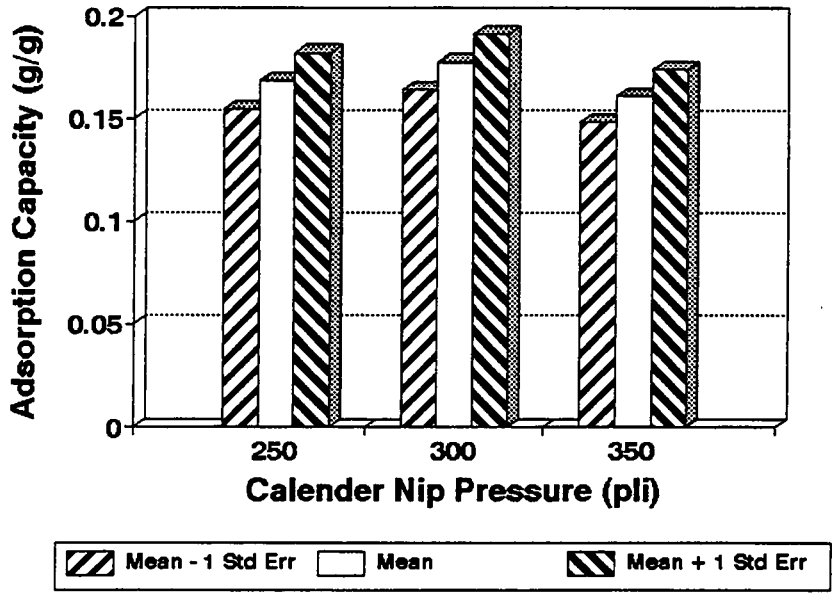

(a)

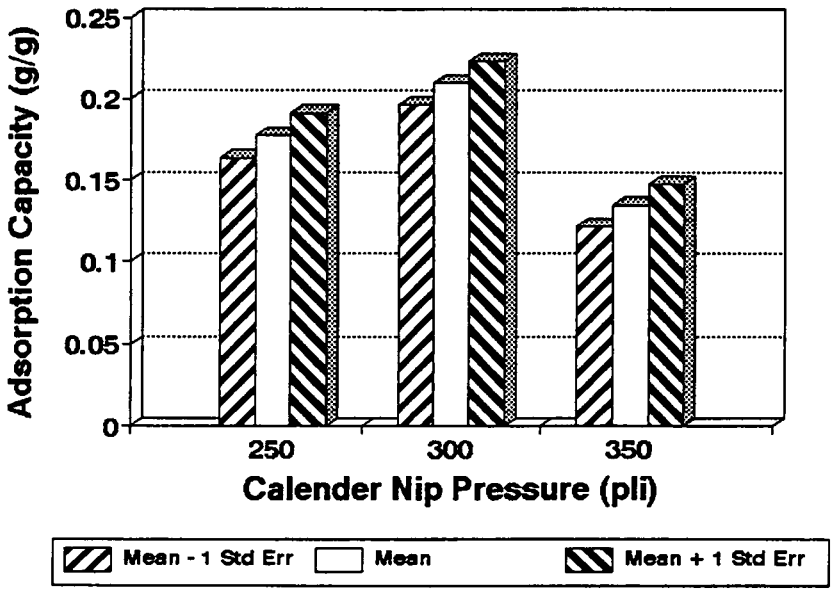

(b)

Figure 5.9 Effect of calender nip pressure on adsorption capacity. (a) Value on Y-axis is the average adsorption capacity of experimentally measured data. (b) Value on Y-axis is the statistically adjusted mean adsorption capacity.

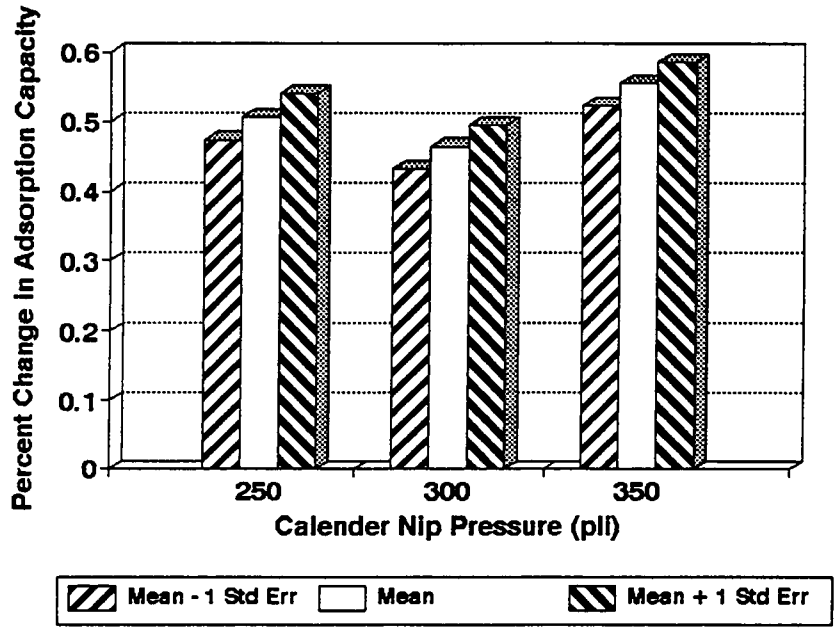

(a)

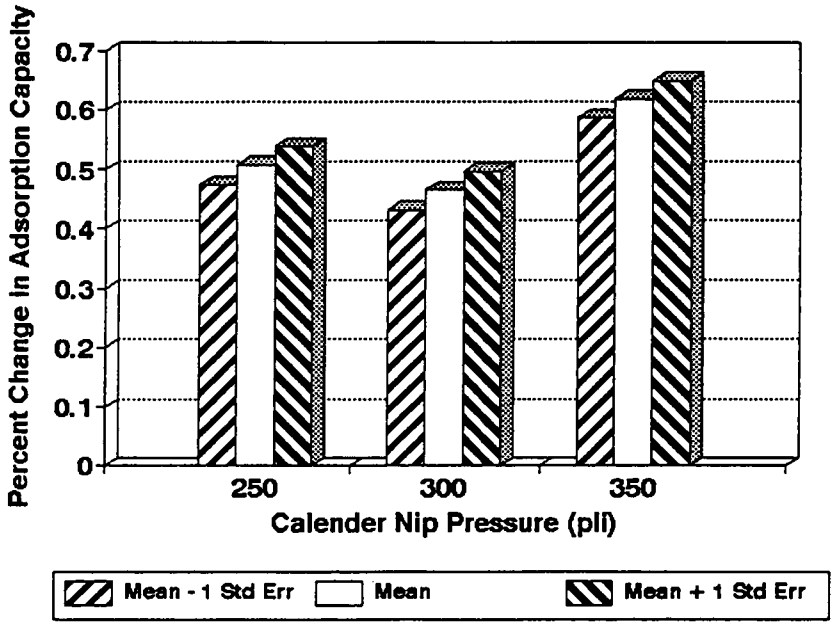

(b)

Figure 5.10 Effect of calender nip pressure on percent change in adsorption capacity. (a) Value on Y-axis is the average percent change in adsorption capacity of experimentally measured data. (b) Value on Y-axis is the statistically adjusted mean percent change in adsorption capacity.

5.3.2.3 Effect of Top and Bottom Calender Roll Temperatures

Both top and bottom calender roll temperatures have no statistically significant effect on the responses. This may be due to the limited number of design points and temperatures too similar to discriminate differences.

5.3.2.4 Effect of Laminate Core Fiber Type

The laminate core fiber type has a statistically significant effect on all responses (Tables 5.7 through 5.8)

The adjusted (least squared) means of four responses are reported in Appendix D.11 through D.14. Of the two fiber types, PP cores have longer breakthrough times, higher adsorption capacities, lower percent change in breakthrough times and lower percent change in adsorption capacities compared to the cotton cores.

The effect of the laminate core fiber type on the four responses are illustrated in Figures 5.11 through Figure 5.14.

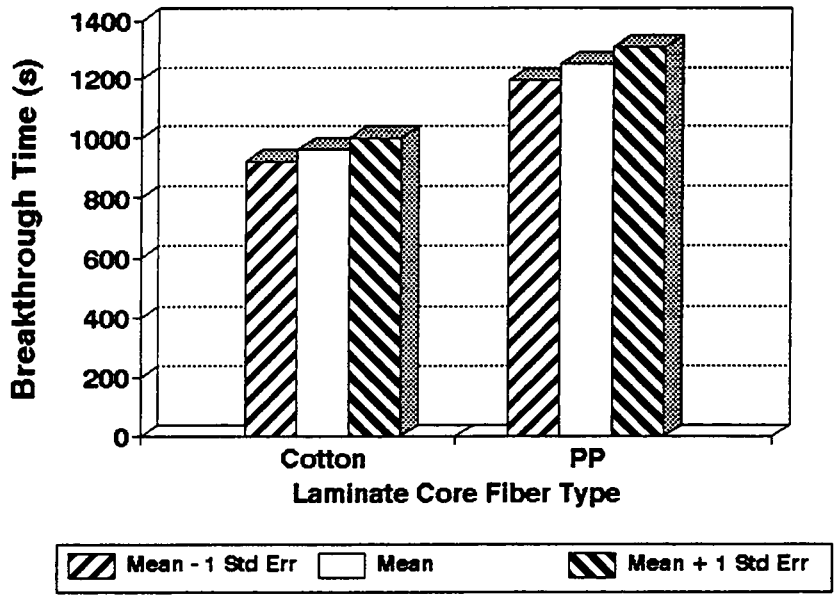

(a)

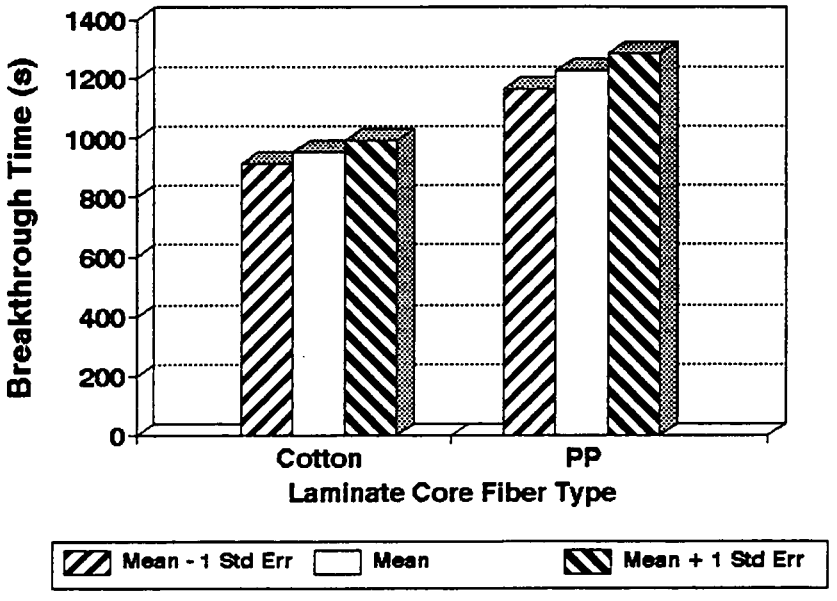

(b)

Figure 5.11 Effect of laminate core fiber type on breakthrough time. (a) Value on Y-axis is the average breakthrough time of experimentally measured data. (b) Value on Y-axis is the statistically adjusted mean breakthrough time.

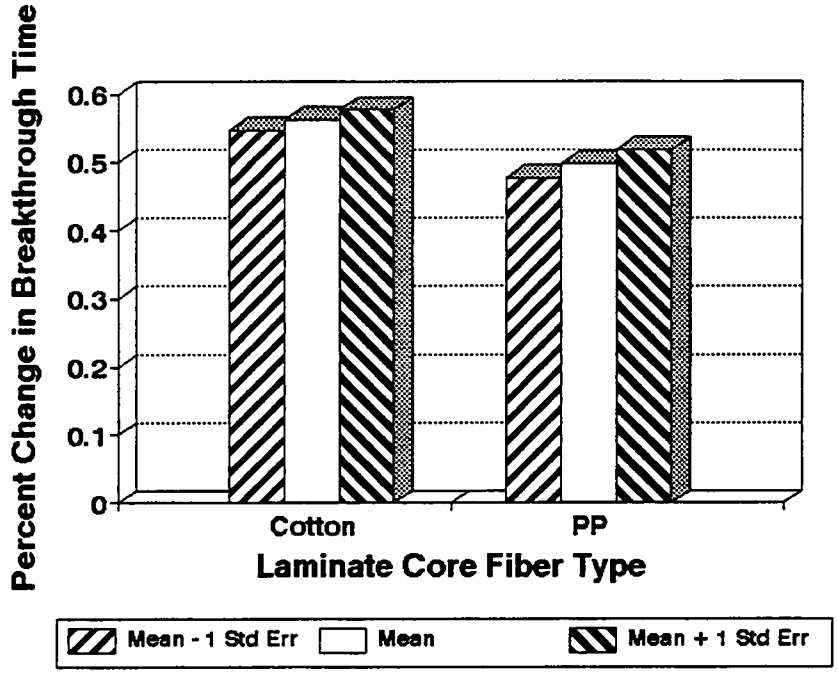

(a)

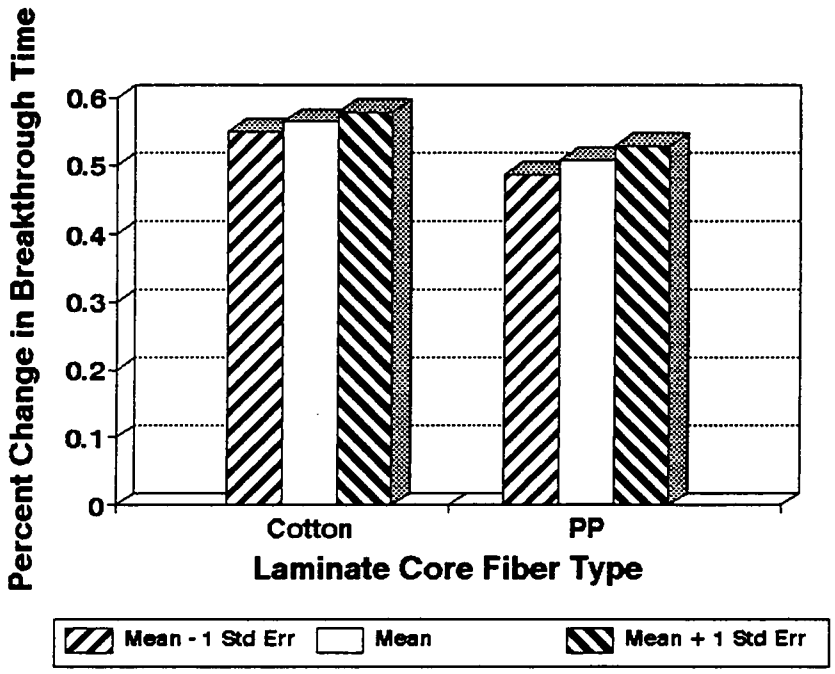

(b)

Figure 5.12 Effect of laminate core fiber type on percent change in breakthrough time. (a) Value on Y-axis is the average percent change in breakthrough time of experimentally measured data. (b) Value on Y-axis is the statistically adjusted mean percent change in breakthrough time.

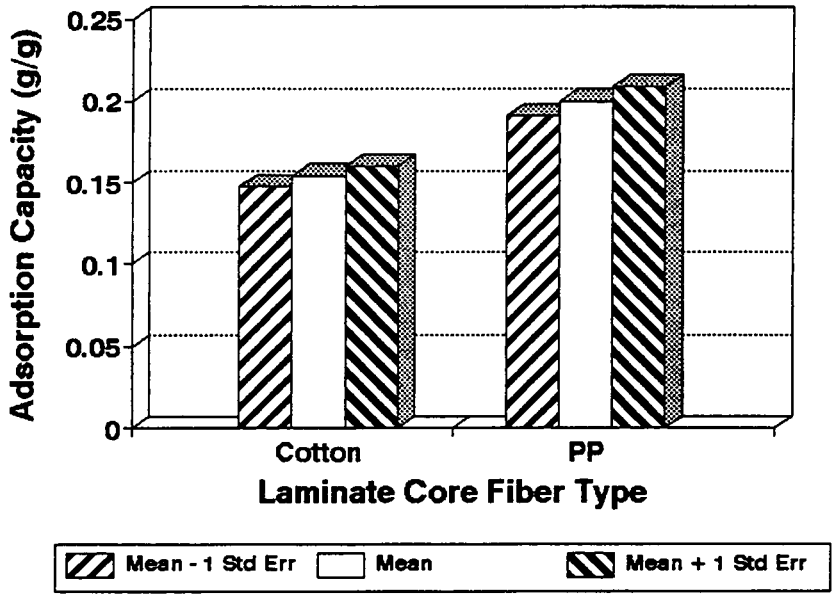

(a)

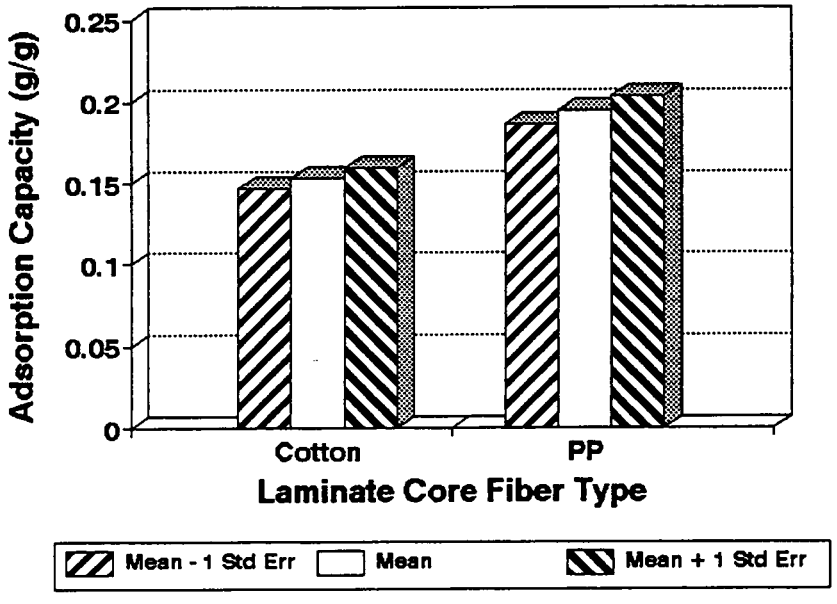

(b)

Figure 5.13 Effect of laminate core fiber type on adsorption capacity. (a) Value on Y-axis is the average adsorption capacity of experimentally measured data. (b) Value on Y-axis is the statistically adjusted mean adsorption capacity.

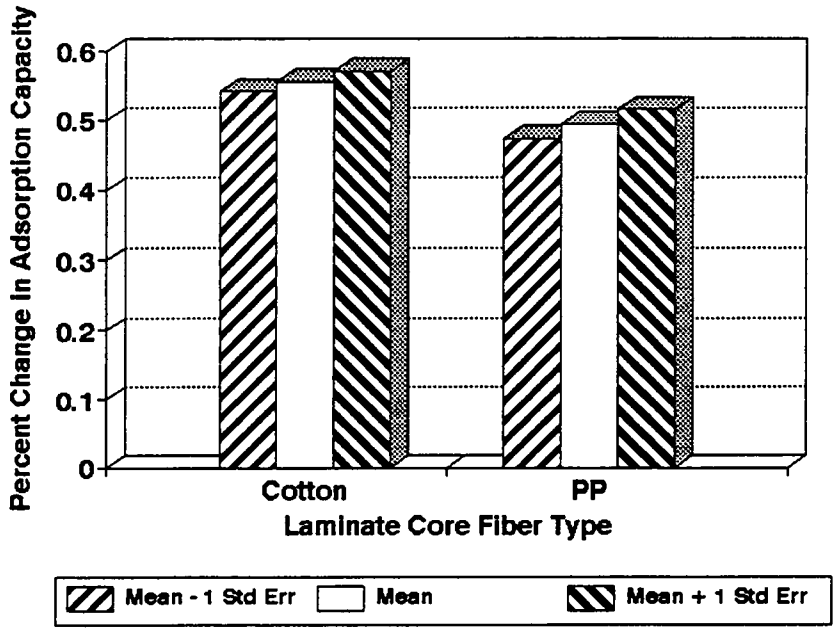

(a)

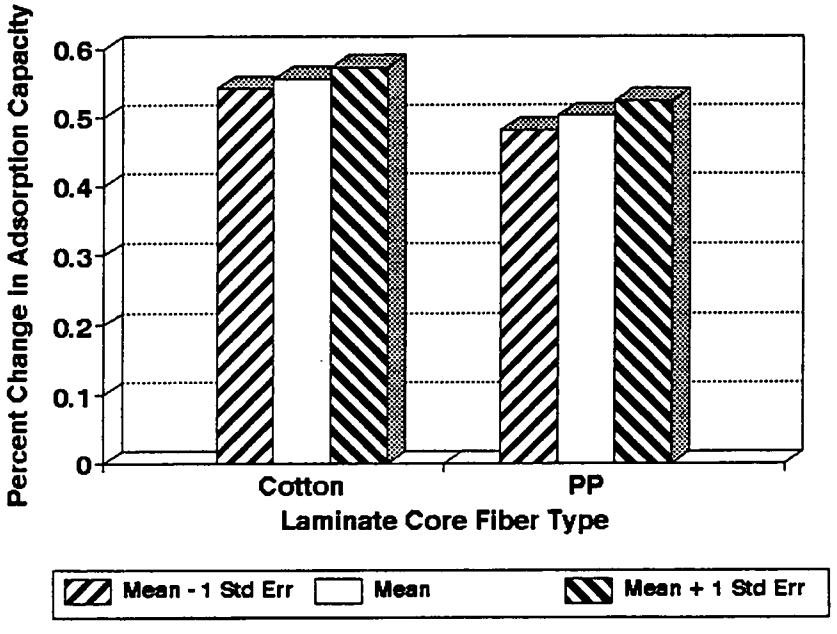

(b)

Figure 5.14 Effect of laminate core fiber type on percent change in adsorption capacity. (a) Value on Y-axis is the average percent change in adsorption capacity of experimentally measured data. (b) Value on Y-axis is the statistically adjusted mean percent change in adsorption capacity.

5.3.2.5 Effect of Core Weight

The core weight has a statistically significant effect on the percent change in breakthrough times and the percent change in adsorption capacities at the 0.05 significance level. It has no effect on the breakthrough times and adsorption capacities (Tables 5.7 through 5.10)

The adjusted (least squared) means of percent change in breakthrough time and percent change in adsorption capacity are reported in Appendix D Tables D.15 through D.16.

The effect of core weight on percent change in breakthrough times and percent change in adsorption capacities are illustrated in Figures 5.15 and 5.16. It is clear that both 2 and 3 oz/yd^2 cotton cores have significantly higher percent change in breakthrough times and higher percent change in adsorption capacities than the other core weights.

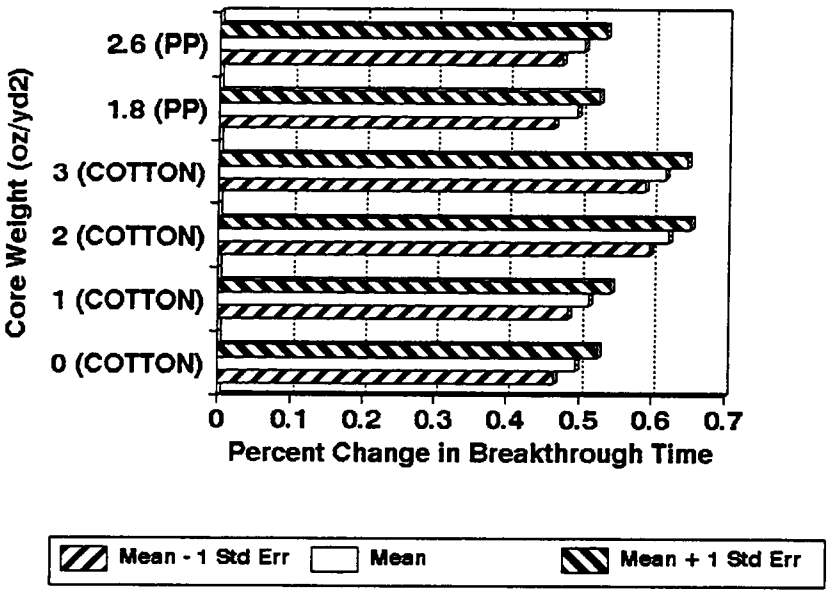

(a)

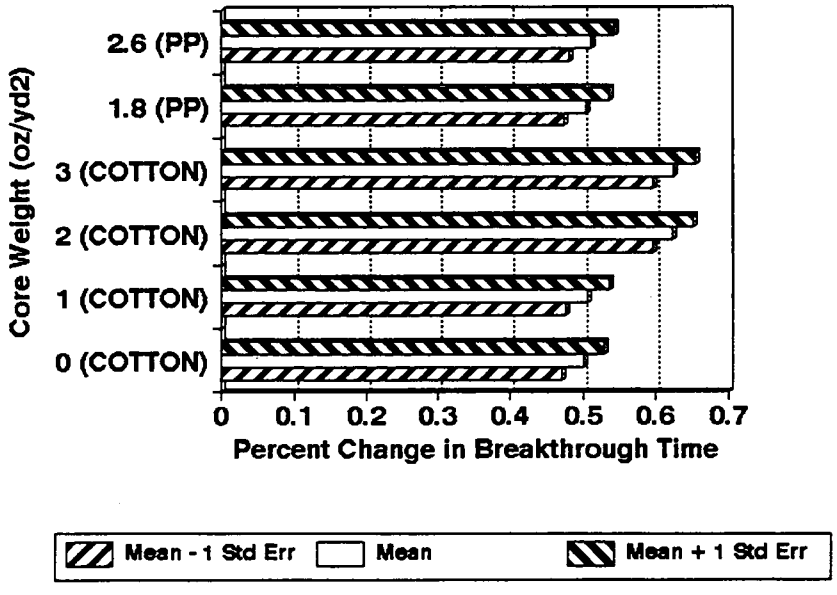

(b)

Figure 5.15 Effect of core weight on percent change in breakthrough time. (a) Value on X-axis is the average percent change in breakthrough time of experimentally measured data. (b) Value on X-axis is the statistically adjusted mean percent change in breakthrough time.

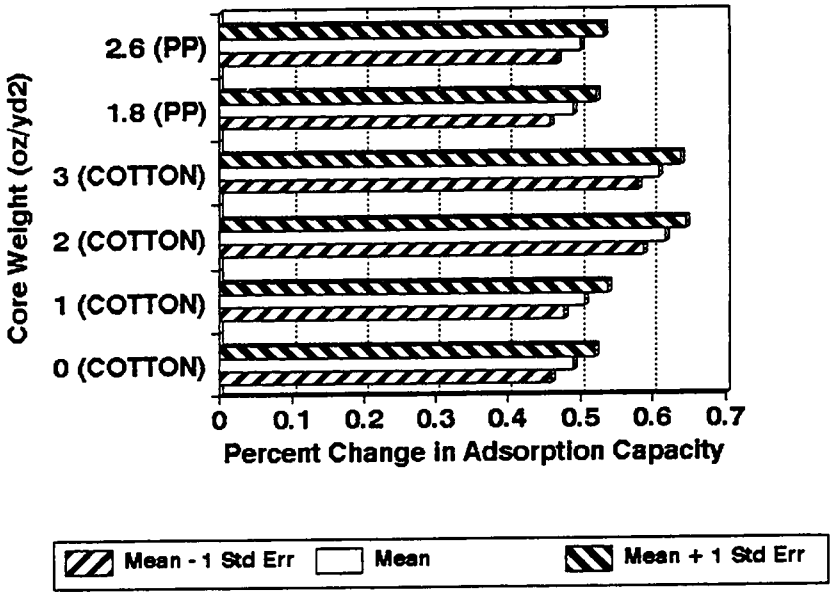

(a)

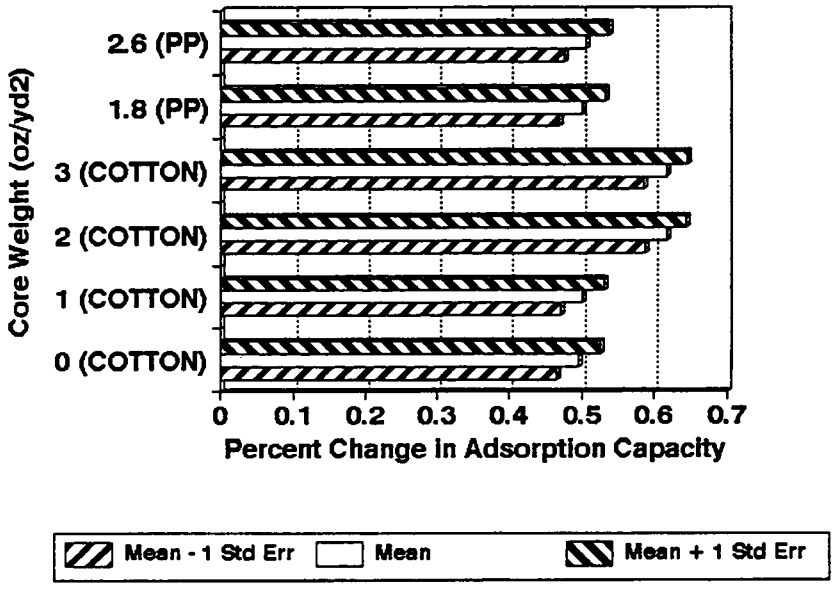

(b)

Figure 5.16 Effect of core weight on percent change in adsorption capacity. (a) Value on X-axis is the average percent change in adsorption capacity of experimentally measured data. (b) Value on X-axis is the statistically adjusted mean percent change in adsorption capacity.

5.3.2.6 Interaction Effect of Calender Speed with Laminate Core Fiber Type

The interaction effect of 'speed x core fiber' is statistically significant on responses breakthrough time and adsorption capacity, but not significant on responses percent change in breakthrough time and percent change in adsorption capacity at 0.05 significance level. The corresponding p-values of factor 'speed x core fiber' for the four responses are listed in Tables 5.5 through 5.8.

The adjusted (least squared) means of breakthrough time and adsorption capacity are reported in Appendix D Tables D.17 and D.18. Of the six interaction combinations, the calender speed of 6 m/min with the PP laminate core produces the longest breakthrough time and the highest adsorption capacity; the calender speed of 8 m/min with the PP laminate core yields the shortest breakthrough time and the lowest adsorption capacity.

The interaction effect of the calender speed with the laminate core fiber type on breakthrough time and adsorption capacity are illustrated in Figures 5.17 and 5.18.

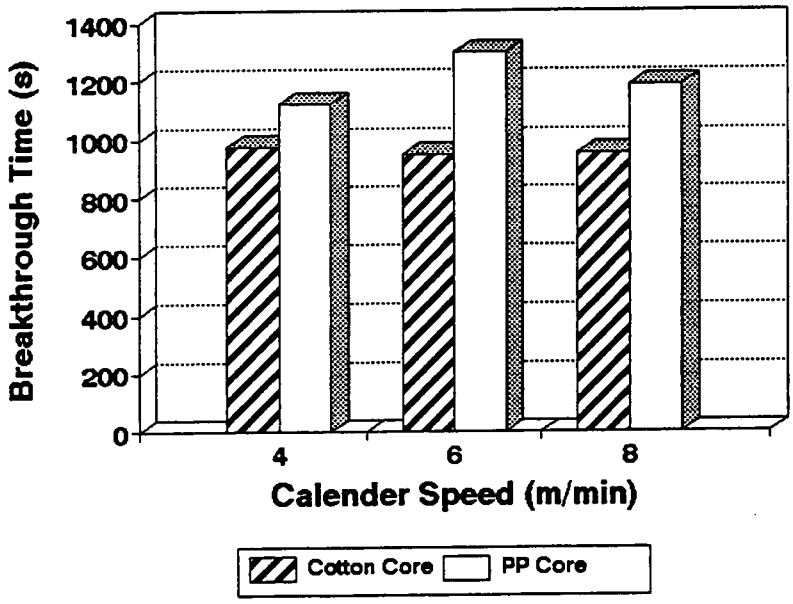

(a)

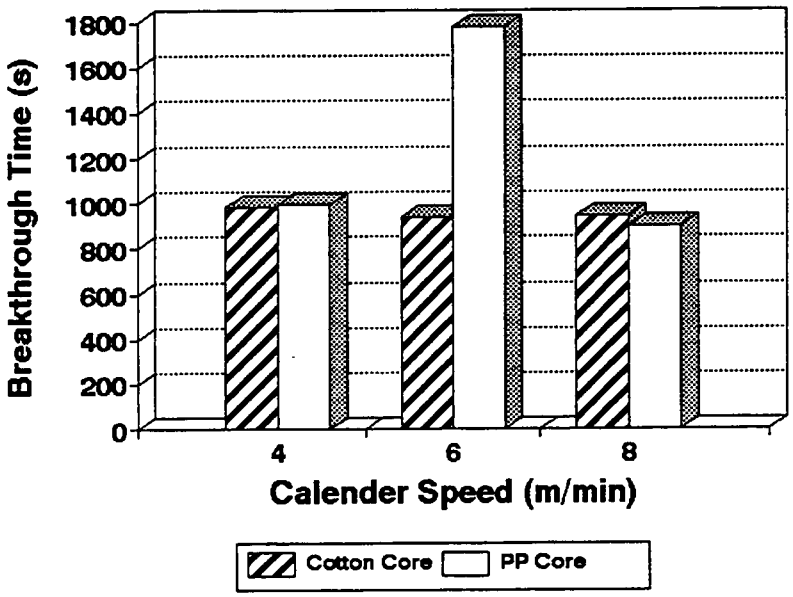

(b)

Figure 5.17 Interaction effect of calender speed with laminate core fiber type on breakthrough time. (a) Value on Y-axis is the average breakthrough time of experimentally measured data. (b) Value on Y-axis is the statistically adjusted mean breakthrough time.

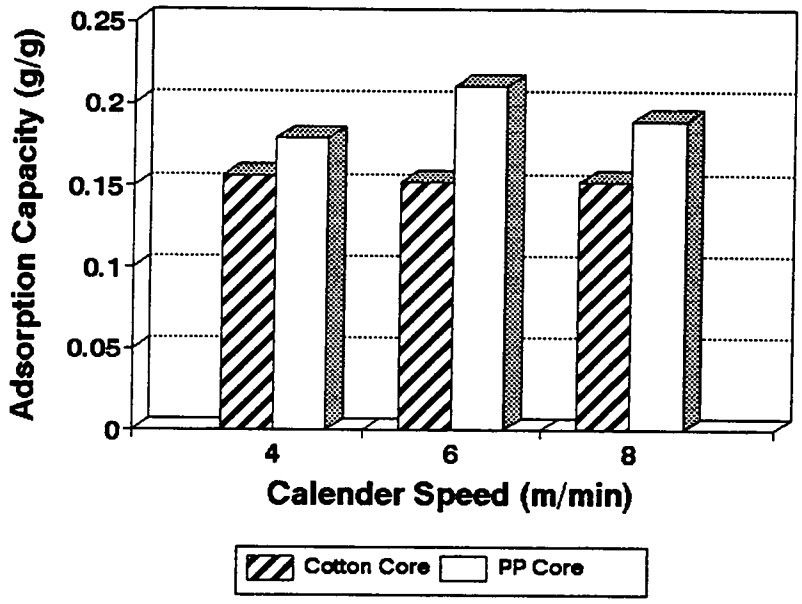

(a)

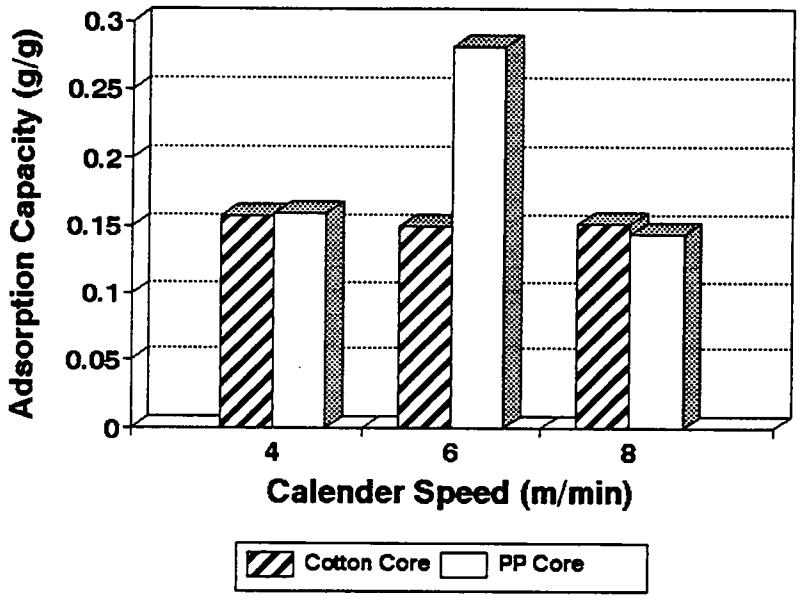

(b)

Figure 5.18 Interaction effect of calender speed with laminate core fiber type on adsorption capacity. (a) Value on Y-axis is the average adsorption capacity of experimentally measured data. (b) Value on Y-axis is the statistically adjusted mean adsorption capacity.

5.3.2.7 Interaction Effect of Calender Nip Pressure with Laminate Core Fiber Type

The interaction effect of 'pressure x core fiber' is significant at the 0.05 probability level on all four responses (Tables 5.5 through 5.8)

The adjusted (least squared) means of the four responses are reported in Appendix D.19 and D.22. Of the six interaction combinations, the calender nip pressure of 300 pli with the PP laminate core produces the longest breakthrough time, the highest adsorption capacity, the lowest percent change in breakthrough time, and the lowest percent change in adsorption capacity. The 350 pli calender nip pressure with the PP laminate core results in the shortest breakthrough time, the lowest adsorption capacity, the highest percent change in breakthrough time, and the highest percent change in adsorption capacity.

The interaction effect of calender nip pressure with laminate core fiber type on the four responses is illustrated in Figures 5.19 through 5.22.

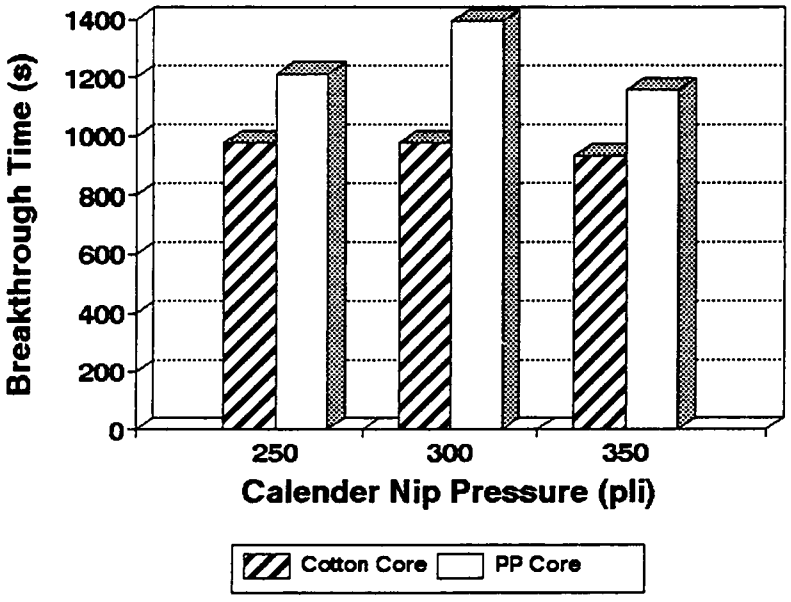

(a)

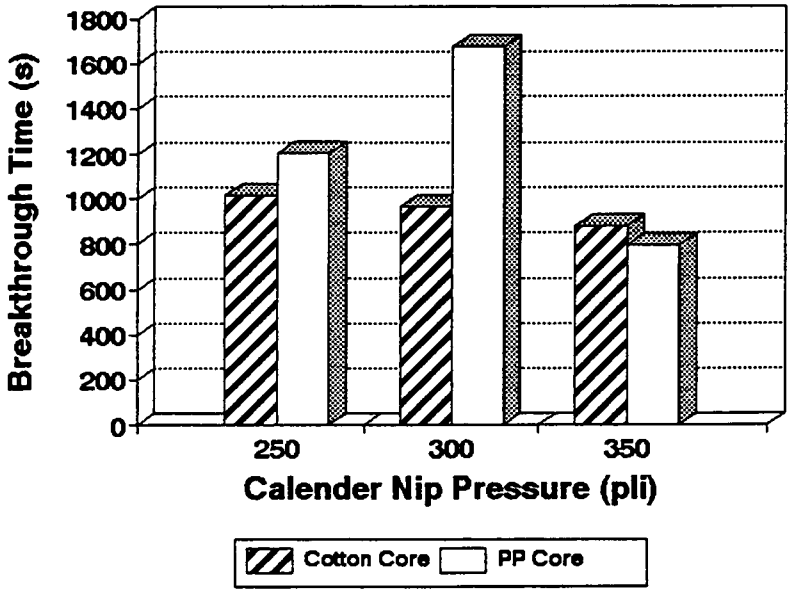

(b)

Figure 5.19 Interaction effect of calender nip pressure with laminate core fiber type on breakthrough time. (a) Value on Y-axis is the average breakthrough time of experimentally measured data. (b) Value on Y-axis is the statistically adjusted mean breakthrough time.

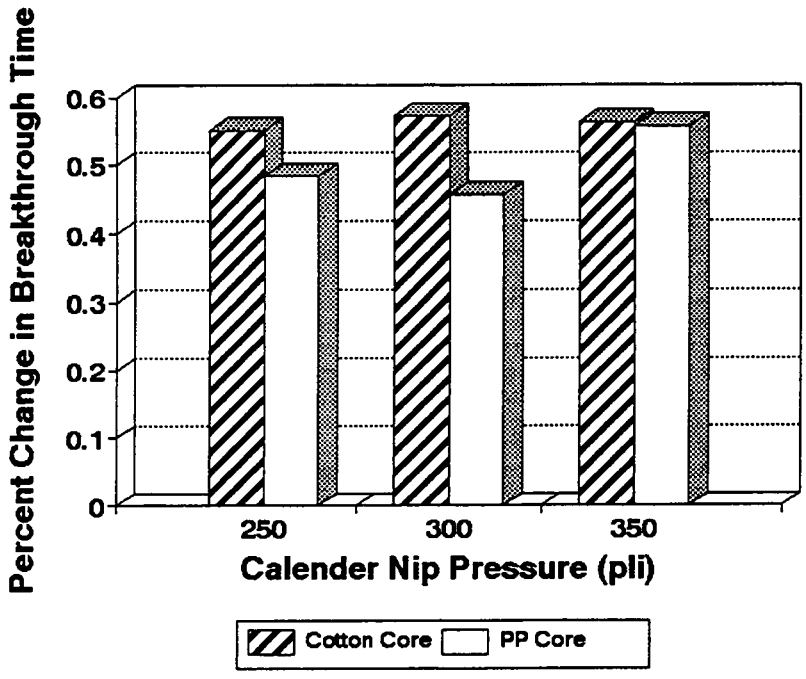

(a)

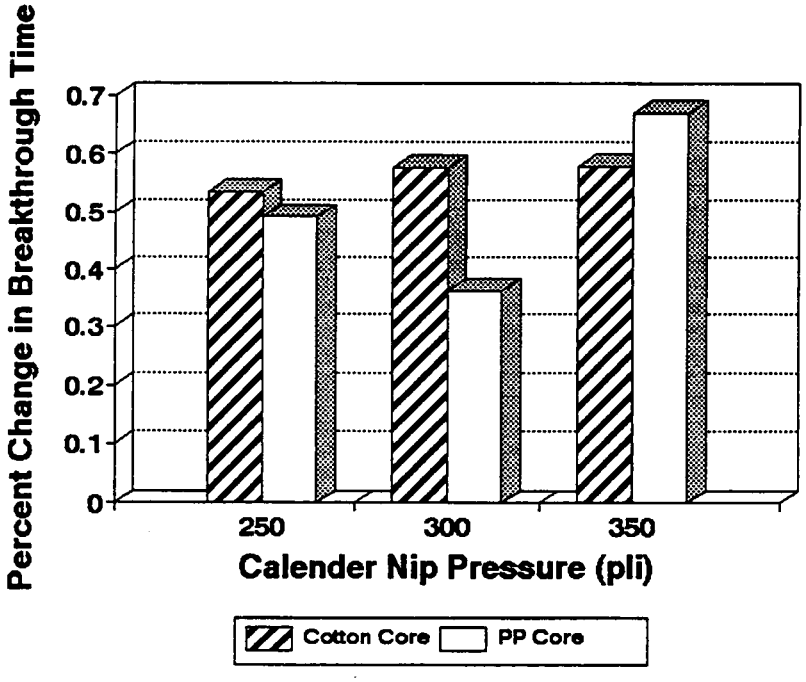

(b)

Figure 5.20 Interaction effect of calender nip pressure with laminate core fiber type on percent change in breakthrough time. (a) Value on Y-axis is the average percent change in breakthrough time of experimentally measured data. (b) Value on Y-axis is the statistically adjusted mean percent change in breakthrough time.

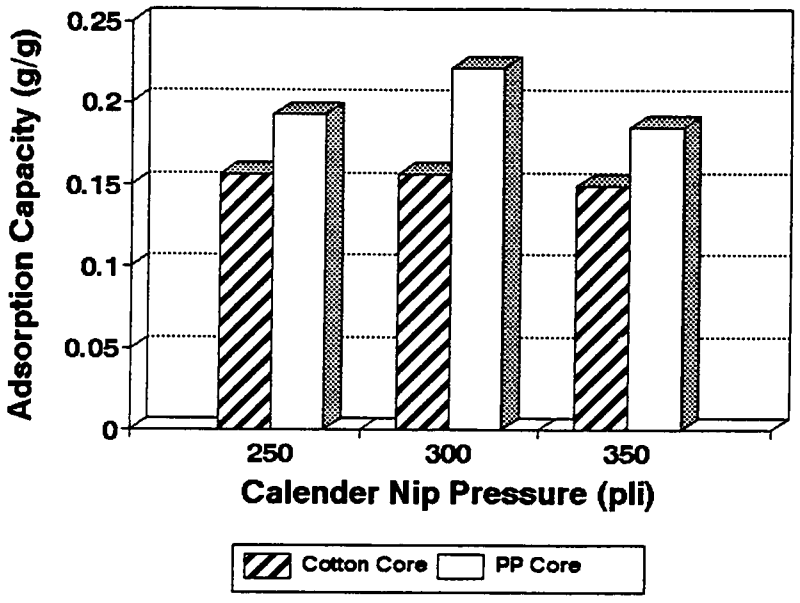

(a)

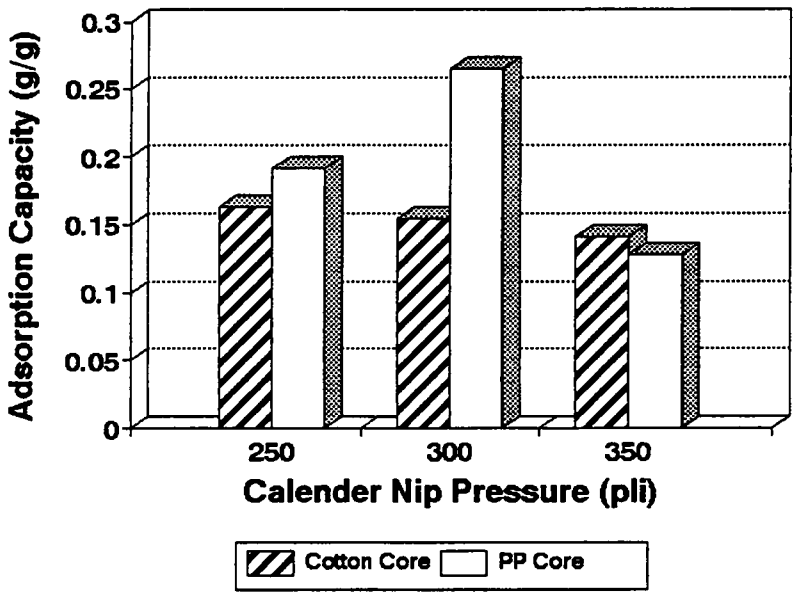

(b)

Figure 5.21 Interaction effect of calender nip pressure with laminate core fiber type on adsorption capacity. (a) Value on Y-axis is the average adsorption capacity of experimentally measured data. (b) Value on Y-axis is the statistically adjusted mean adsorption capacity.

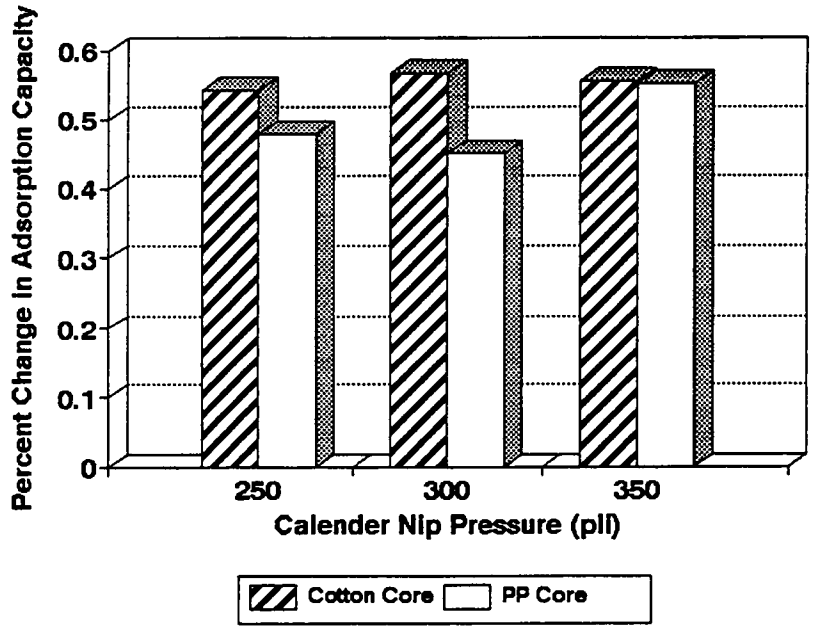

(a)

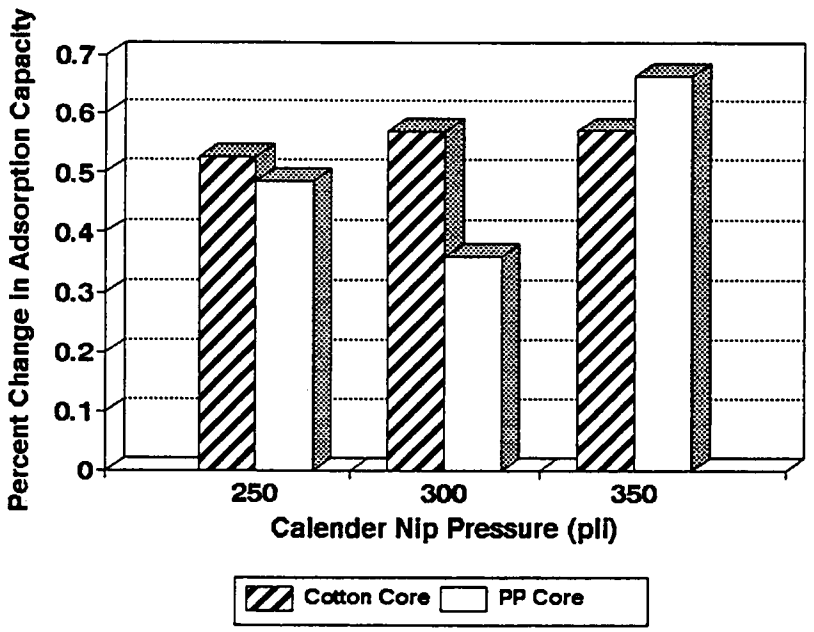

(b)

Figure 5.22 Interaction effect of calender nip pressure with laminate core fiber type on percent change in adsorption capacity. (a) Value on Y-axis is the average percent change in adsorption capacity of experimentally measured data. (b) Value on Y-axis is the statistically adjusted mean percent change in adsorption capacity.

5.3.2.8 Interaction Effect of Top Calender Roll Temperature with Laminate Core Type

The interaction effect of top calender roll temperature with laminate core fiber type is not statistically significant on any of the four responses. This may be due to the limited temperature range. The corresponding p-values of this interaction for the four responses are listed in Tables 5.5 through 5.8.

5.3.2.9 Interaction Effect of Bottom Calender Roll Temperature with Laminate Core Fiber Type

The interaction effect of the bottom calender roll temperature with the laminate core fiber type is not statistically significant on any of the four responses at the 0.05 probability level. However, the effect on the breakthrough times and adsorption capacities is found to be significant at the 0.10 probability level. The corresponding p-values of the interaction for the four responses are listed in Tables 5.5 through 5.8.

5.4 CONCLUSIONS

The statistical analysis of the study shows that the laminate core fiber type and thermal calendering parameters have statistically significant effects on the TCE adsorption performance by the HSA activated carbon loaded nonwoven laminates.

Calender speed has a significant effect on all four responses (i.e., breakthrough time, adsorption capacity, percent change in breakthrough time, and percent change in adsorption capacity). The calender speed of 6 m/min resulted in the best TCE adsorption performance, whereas speed of 8 m/min yields the worst.

Calender nip pressure also has a significant effect on all four responses. The calender nip pressures of both 250 and 300 pli (i.e., pounds per linear inch) generate better TCE adsorption performances than 350 pli does.

Both bottom and top calender roll temperatures are found not to be statistically significant on any of the four responses. This finding may be due to the limited observation numbers and the temperatures too similar to discriminate differences.

The PP cores have better TCE adsorption performance compared to cotton cores for all four response variables.

The core weight has a significant effect on the percent change in breakthrough time and percent change in adsorption

capacity. In terms of the average percent change in breakthrough time and the average percent change in adsorption capacity, the 2 and 3 oz/yd^2 cotton cores are not different from each other, but both are inferior to other core weights.

The interaction effects of calender speed with laminate core fiber type are significant on breakthrough time and adsorption capacity. The calender speed of 6 m/min with PP core produces the best TCE adsorption results, whereas 8 m/min with PP core has the worst adsorption results.

The interaction effects of calender nip pressure with laminate core fiber type are significant on all of the four responses. The nip pressure of 300 pli with PP core yields the best TCE adsorption results, whereas the nip pressure of 350 pli with PP core has the worst.

The optimum process conditions for the present study are listed in Table 5.9.

Table 5.9 Optimum Process Conditions.

Parameter	Value
Laminate core fiber type	PP
Laminate core weight	1.8 and 2.6 oz/yd^2
Calender speed	6 m/min
Calender nip pressure	250 - 300 pli*
Bottom calender roll temperature	80 - 90 °C
Top calender roll temperature	110 - 130 °C

* pli = pounds per liner inch.

Both the statistical results in this chapter and the adsorption isotherms described in Chapter 3 show that the thermal point bonding severely impaired the TCE adsorption performance by the high surface area activated carbon impregnated nonwoven laminates. On the average, breakthrough time for the calendered samples was reduced by over 50% compared with that for non-calendered samples. Likewise, adsorption capacity at break (1% penetration of the inlet TCE gas concentration) for the calendered samples was also decreased by over 50% on the average compared with that for the non-calendered samples. Because of the huge pressure and intensive heat on the samples during the thermal calendering, the carbon bed structure inside the samples was totally changed. This carbon bed structure change may account for an average reduction of more than 50% in the available carbon surface area for adsorption. By now, it is very clear that the thermal calendering is not the way to go. In order to sustain the maximum of the original carbon surface area (i.e., the carbon bed structure) for gas adsorption, other bonding techniques should be investigated.

CHAPTER 6

FUTURE WORK

The results of the study reveal that the 15% surface area thermal point bonding processing critically impaired the TCE gas adsorption performance of the activated carbon loaded nonwoven laminates. The breakthrough times for the calendered samples were generally decreased by over 50% compared with the non-calendered samples. This is because the geometrical structure of the carbon bed inside the laminates was totally changed after the thermal calendering. To retain as much of the original carbon bed structure as possible, other bonding techniques should be investigated. Among the possible bonding candidates, ultrasonic bonding may be the appropriate process to improve the strength of the meltblown-carbon nonwovens while retaining the original adsorption capacity of the carbon bed.

Efforts should be made to simulate other climatic conditions that military personnel may encounter (i.e., desert, jungle etc.). This could be achieved in the laboratory by controlling the temperature and humidity to determine the adsorbent-adsorbate behavior at other conditions.

In order to keep cost down and run a comparatively large experimental design, other inexpensive challenge gases should be studied and attempted.

Because the uniformity of the carbon bed is extremely

important to the adsorption behavior of the laminates, efforts must be also made to develop a technique of loading the carbon powder much more uniformly, preferably incorporating the carbon powder into the nonwoven materials when the laminates are being made.

LIST OF REFERENCES

LIST OF REFERENCES

[1] Dever, Maureen, Davis, Wayne T. and Hood, Christopher C., "Development of an Activated Carbon Loaded Melt Blown - Spunbonded Laminates", TAPPI Journal, Vol. 77, No. 2., February, 1994.

[2] Hood, Christopher C., "Characterization of Activated Carbon Adsorption Applied to A Thin Bed System", M.S. Thesis, the University of Tennessee, Knoxville, Dec. 1993.

[3] United States Department of the Army, Military Specification, Sept. 17, 1987, 22p, MIL-C-43858B (GL).

[4] Davis, W. T., Hood, C. C. and Dever, Maureen, "Adsorption of an Organic Vapor in an Activated Carbon Loaded Melt Blown Laminate, TAPPI Journal, Vol. 77, 1993.

[5] Davis, Wayne T. and Dever, Maureen, "Analysis of A Thin Activated Carbon Loaded Adsorption Medium". Presented at the 8th Symposium on Separation Science and Technology for Energy Applications, Oct. 24 - 28, 1993, Gatinburg, Tennessee.

[6] Wark, K. and Warner, C. F., Air Pollution: Its Origin and Control, Second Edition. Harper Collins, 1981.

[7] Sanders, W. L. and Schneider, John F., E4, Evolutionary Software, Inc., 1991.

[8] Xu, Ming, Wang, Jusheng and Gao, Fang, "FR Finish of Charcoal-Containing Cotton Flannel: Application of Caliban F/R P44 and Its Modification", Journal of Coated Fabrics, Vol. 20, July 1990, pp.43-47.

[9] Gournay, J. F. and Tetart, "Specific Garments for Soldiers' Protection Against Aggressive Products or Conditions", Lenzinger Berichte, Vol. 68, Dec. 1989, pp. 25-28.

[10] Anonymous, "Clothing for Chemical and Biological Protection", High Performance Textiles, Jan. 1993, pp.5-6.

[11] Jones, David William, "Vapour Sorption by Latex Bonded Carbon Particles", Ph.D. Dissertation, Trent Polytechnic, Clifton Lane, Nottingham, U.K., March 1986.

[12] Jones, D. W. and Watts, P., "Kinetics of Vapor Sorption by Latex Bonded Carbon Particles", Performance of Protective Clothing: Second Symposium, ASTM STP 989, American Society for Testing and Materials, Philadelphia, 1988, pp.832-846.

[13] Innes, R. W., Fryer, J. R. and Stoeckli, H. F., "On the Correlation Between Micropore Distribution Obtained from Molecular Probes and from High Resolution Electron Microscopy. Carbon, Vol. 27, No. 1, 1989, pp. 71-76.

[14] Jonas, L. A., Tewari, Y. B. and Sansone, E. B., "Prediction of Adsorption Rate Constants of Activated Carbon for Various Vapor", Carbon, Vol. 17, 1979, pp. 345-349.

[15] Dever, Maureen and Sanders, William, "A Fractional Factorial Design Model", The International Nonwovens Technical Conference, INDA Book of Papers, April 9-12 1991, Stouffer Orlando Hotel, Orlando, Florida, pp. 215-236.

APPENDICES

APPENDIX A

Experimental Results Before and After Calendering

Experimental Results Before and After Calendering.

SAMPLE NUMBER	ADSORPTION CAPACITY (G TCE/G CARBON)		ADSORPTION CAPACITY LOSS PERCENTAGE	BREAKTHROUGH TIME (SECONDS)		BREAKTHROUGH TIME LOSS PERCENTAGE
	BEFORE CALENDERING	AFTER CALENDERING		BEFORE CALENDERING	AFTER CALENDERING	
0-1	0.3637	0.2022	0.4440	2304	1272	0.4479
0-2	0.3449	0.1611	0.5462	2184	1008	0.5385
0-3	0.3299	0.1607	0.5128	2088	1008	0.5172
0-4	0.2961	0.1423	0.5194	1872	888	0.5256
0-5	0.3524	0.1874	0.4682	2232	1176	0.4731
0-6	0.3492	0.1874	0.4633	2208	1176	0.4674
1-1	0.3375	0.1497	0.5564	2136	936	0.5618
1-2	0.4123	0.1948	0.5275	2616	1224	0.5321
1-3	0.3224	0.1614	0.4994	2040	1008	0.5059
1-4	0.3040	0.1464	0.5184	1920	912	0.5250
1-5	0.3192	0.1609	0.4960	2016	1008	0.5000
1-6	0.3865	0.2139	0.4466	2448	1344	0.4510
2-1	0.4198	0.1506	0.6413	2664	936	0.6486
2-2	0.3187	0.1086	0.6592	2016	672	0.6667
2-3	0.3188	0.1311	0.5888	2016	816	0.5952
2-4	0.3341	0.1689	0.4945	2112	1056	0.5000
2-5	0.3150	0.0899	0.6987	1992	552	0.7229
2-6	0.3002	0.1198	0.6009	1896	744	0.6076

Experimental Results Before and After Calendering (continued)

SAMPLE NUMBER	ADSORPTION CAPACITY (G TCE/G CARBON)		ADSORPTION CAPACITY LOSS PERCENTAGE	BREAKTHROUGH TIME (SECONDS)		BREAKTHROUGH TIME LOSS PERCENTAGE
	BEFORE CALENDERING	AFTER CALENDERING		BEFORE CALENDERING	AFTER CALENDERING	
3-1	0.3280	0.1836	0.4402	2136	1152	0.4607
3-2	0.2811	0.1611	0.5870	1776	720	0.5946
3-3	0.3749	0.1086	0.7103	2376	672	0.7171
3-4	0.4725	0.1761	0.6273	3000	1104	0.6320
3-5	0.4462	0.1649	0.6304	2832	1032	0.6356
3-6	0.3075	0.1049	0.6589	1944	648	0.6667
PP18-1	0.4087	0.2848	0.3032	2592	1800	0.3056
PP18-2	0.3822	0.2286	0.4019	2424	1440	0.4059
PP18-3	0.4274	0.1910	0.5531	2712	1200	0.5575
PP18-4	0.4425	0.2473	0.4411	2808	1560	0.4444
PP18-5	0.3898	0.1011	0.7406	2472	624	0.7475
PP18-6	0.3598	0.1798	0.5003	2280	1128	0.5053
PP26-1	0.4386	0.2098	0.5217	2784	1320	0.5259
PP26-2	0.3373	0.1236	0.6336	2136	768	0.6404
PP26-3	0.3491	0.1801	0.4841	2208	1128	0.4891
PP26-4	0.4425	0.2285	0.4836	2808	1440	0.4872
PP26-5	0.3524	0.1835	0.4793	2232	1152	0.4839
PP26-6	0.3899	0.2360	0.3947	2472	1488	0.3981

APPENDIX B

E4 Fractional Factorial Experimental Design

E4 Fractional Factorial Experimental Design

E4

Version 91.1

The number of factors in the design is.....5
The number of levels of SPEED is..... 3
The number of levels of PRESSURE is..... 3
The number of levels of BOT-TEMP is..... 3
The number of levels of TOP-TEMP is..... 3
The number of levels of CORE is..... 6

The number of observations in the design is.....36

Here is a layout of your design:
(A randomization of the runs has already been made)

Obs.	SPEED	PRESSURE	BOT-TEMP	TOP-TEMP	CORE
1	1	1	3	3	6
2	3	2	2	1	1
3	3	1	3	2	1
4	1	3	2	1	3
5	1	1	3	2	3
6	2	2	1	2	3
7	2	3	3	1	1
8	3	2	1	3	6
9	3	3	1	1	2
10	1	3	2	2	1
11	1	2	3	3	2
12	2	2	3	1	2
13	2	1	2	3	4
14	3	3	1	3	3
15	3	1	2	1	3
16	3	3	1	3	5
17	2	1	2	3	4
18	1	3	2	3	2
19	2	3	2	2	6
20	3	2	2	3	5
21	3	1	3	2	4
22	1	1	1	1	6
23	1	2	2	2	5
24	2	1	1	3	1
25	1	2	1	1	4
26	2	3	1	2	6
27	1	1	1	2	5

28	2	2	3	3	3
29	2	2	1	2	2
30	2	1	2	1	5
31	3	1	2	2	2
32	3	3	3	2	4
33	1	2	1	1	4
34	3	2	3	1	6
35	1	3	3	3	1
36	2	3	3	1	5

The efficiency of SPEED is.....1.0000
The efficiency of PRESSURE is.....0.9300
The efficiency of BOT-TEMP is.....0.9441
The efficiency of TOP-TEMP is.....0.9849
The efficiency of CORE is.....0.9658

APPENDIX C

Actual Calendering Run Sheet

Actual Calendering Runsheet

SAMPLE_#	OBS	SPEED (m/min)	PRESSURE (pli)	BOT_TEMP (°C)	TOP_TEMP (°C)	FIBER	CORE_WT (oz/yd^2)
PP26-5	1	4	250	80	110	PP	2.6
3-6	2	4	300	80	110	COTTON	3.0
3-4	3	4	300	80	110	COTTON	3.0
1-5	4	8	350	80	110	COTTON	1.0
PP18-6	5	4	250	80	120	PP	1.8
2-5	6	6	300	80	120	COTTON	2.0
1-4	7	6	300	80	120	COTTON	1.0
PP26-6	8	6	350	80	120	PP	2.6
0-2	9	6	250	80	130	COTTON	0.0
PP26-4	10	8	300	80	130	PP	2.6
2-3	11	8	350	80	130	COTTON	2.0
PP18-5	12	8	350	80	130	PP	1.8
2-2	13	4	350	90	110	COTTON	2.0
PP18-1	14	6	250	90	110	PP	1.8
2-1	15	8	250	90	110	COTTON	2.0
0-1	16	8	300	90	110	COTTON	0.0
PP18-2	17	4	300	90	120	PP	1.8
0-5	18	4	350	90	120	COTTON	0.0
PP26-1	19	6	350	90	120	PP	2.6
1-3	20	8	250	90	120	COTTON	1.0
1-1	21	4	350	90	130	COTTON	1.0
3-1	22	6	250	90	130	COTTON	3.0
3-2	23	6	250	90	130	COTTON	3.0
PP18-4	24	8	300	90	130	PP	1.8
1-6	25	6	300	100	110	COTTON	1.0
0-6	26	6	350	100	110	COTTON	0.0
PP18-3	27	6	350	100	110	PP	1.8
PP26-3	28	8	300	100	110	PP	2.6
2-4	29	4	250	100	120	COTTON	2.0
0-4	30	8	250	100	120	COTTON	0.0
3-5	31	8	250	100	120	COTTON	3.0
3-3	32	8	350	100	120	COTTON	3.0
PP26-2	33	4	250	100	130	PP	2.6
1-2	34	4	300	100	130	COTTON	1.0
0-3	35	4	350	100	130	COTTON	0.0
2-6	36	6	300	100	130	COTTON	2.0

APPENDIX D

Statistics Tables

D.1. Least Square Means of Breakthrough Time for Non-calendered Samples for the Independent Variable Laminate Core Fiber Type

Laminate Core Fiber Type	Breakthrough Time (s) (LSMEAN)	Standard Error (s) (LSMEAN)	Pr > |T| H_0: LSMEAN=0
Cotton	2201.0	61.3	0.0001
PP	2494.0	86.7	0.0001

D.2 Least Square Means of Adsorption Capacity for Non-calendered Samples for the Independent Variable Laminate Core Fiber Type.

Laminate Core Fiber Type	Adsorption Capacity (g TCE/g carbon) (LSMEAN)	Standard Error (g TCE/g carbon) (LSMEAN)	Pr > |T| H_0: LSMEAN=0
Cotton	0.3473	0.0096	0.0001
PP	0.3934	0.0136	0.0001

D.3 Least Square Means of Breakthrough Time for Calendered Samples for the Independent Variable Calender Speed.

Calender Speed (m/min)	Breakthrough Time (s) (LSMEAN)	Standard Error (s) (LSMEAN)	Pr > |T| H_0: LSMEAN=0
4	991.2	82.0	0.0001
6	1356.7	93.3	0.0001
8	922.0	107.5	0.0001

D.4 Least Square Means of Percent Change in Breakthrough Time for Calendered Samples for the Independent Variable Calender Speed.

Calender Speed (m/min)	Percent Change in Breakthrough Time (LSMEAN)	Standard Error (LSMEAN)	Pr > |T| H_0: LSMEAN=0
4	0.5692	0.0298	0.0001
6	0.4470	0.0339	0.0001
8	0.5909	0.0391	0.0001

D.5 Least Square Means of Adsorption Capacity for Calendered Samples for the Independent Variable Calender Speed.

Calender Speed (m/min)	Adsorption Capacity (g TCE/g carbon) (LSMEAN)	Standard Error (g TCE/g carbon) (LSMEAN)	Pr > |T| H_0: LSMEAN=0
4	0.1584	0.0128	0.0001
6	0.2156	0.0146	0.0001
8	0.1478	0.0168	0.0001

D.6 Least Square Means of Percent Change in Adsorption Capacity for Calendered Sample for the Independent Variable Calender Speed.

Calender Speed (m/min)	Percent Change in Adsorption Capacity (LSMEAN)	Standard Error (LSMEAN)	Pr > |T| H_0: LSMEAN=0
4	0.5635	0.0302	0.0001
6	0.4419	0.0344	0.0001
8	0.5850	0.0397	0.0001

D.7 Least Square Means of Breakthrough Time for Calendered Samples for the Independent Variable Calender Nip Pressure.

Calender Nip Pressure (pli)	Breakthrough Time (s) (LSMEAN)	Standard Error (s) (LSMEAN)	Pr > |T| H_0: LSMEAN=0
250	1112.5	88.7	0.0001
300	1320.0	86.8	0.0001
350	837.4	83.1	0.0001

D.8 Least Square Means of Percent Change in Breakthrough Time for Calendered Samples for the Independent Variable Calender Nip Pressure.

Calender Nip Pressure (pli)	Percent Change in Breakthrough Time (LSMEAN)	Standard Error (LSMEAN)	Pr > |T| H_0: LSMEAN=0
250	0.5135	0.0323	0.0001
300	0.4691	0.0316	0.0001
350	0.6245	0.0302	0.0001

D.9 Least Square Means of Adsorption Capacity for Calendered Samples for the Independent Variable Calender Nip Pressure.

Calender Nip Pressure (pli)	Adsorption Capacity (g TCE/g carbon) (LSMEAN)	Standard Error (g TCE/g carbon) (LSMEAN)	Pr > |T| H_0: LSMEAN=0
250	0.1775	0.0139	0.0001
300	0.2098	0.0136	0.0001
350	0.1344	0.0130	0.0001

D.10 Least Square Means of Percent Change in Adsorption Capacity for Calendered Samples for the Independent variable Calender Nip Pressure.

Calender Nip Pressure (pli)	Percent Change in Adsorption Capacity (LSMEAN)	Standard Error (LSMEAN)	Pr > |T| H_0: LSMEAN=0
250	0.5075	0.0327	0.0001
300	0.4647	0.0320	0.0001
350	0.6182	0.0306	0.0001

D.11 Least Square Means of Breakthrough Time for Calendered Samples for the Independent Variable Laminate Core Fiber Type.

Laminate Core Fiber Type	Breakthrough Time (s) (LSMEAN)	Standard Error (s) (LSMEAN)	Pr > |T| H_0: LSMEAN=0
Cotton	955.1	39.4	0.0001
PP	1224.8	57.3	0.0001

D.12 Least Square Means of Percent Change in Breakthrough Time for Calendered Samples for the Independent Variable Laminate Core Fiber Type.

Laminate Core Fiber Type	Percent Change in Breakthrough Time (LSMEAN)	Standard Error (LSMEAN)	Pr > |T| H_0: LSMEAN=0
Cotton	0.5635	0.0143	0.0001
PP	0.5079	0.0209	0.0001

D.13 Least Square Means of Adsorption Capacity for Calendered Samples for the Independent Variable Laminate Core Fiber Type.

Laminate Core Fiber Type	Adsorption Capacity (g TCE/g carbon) (LSMEAN)	Standard Error (g TCE/g carbon) (LSMEAN)	Pr > |T| H_0: LSMEAN=0
Cotton	0.1529	0.0062	0.0001
PP	0.1950	0.0090	0.0001

D.14 Least Square Means of Percent Change in Adsorption Capacity for Calendered Samples for the Independent variable Laminate Core Fiber Type.

Laminate Core Fiber Type	Percent Change in Adsorption Capacity (LSMEAN)	Standard Error (LSMEAN)	Pr > |T| H_0: LSMEAN=0
Cotton	0.5570	0.0145	0.0001
PP	0.5032	0.0211	0.0001

D.15 Least Square Means of Percent Change in Breakthrough Time for Calendered Samples for the Independent Variable Core Weight.

Laminate		Percent Change in Breakthrough Time (LSMEAN)	Standard Error (LSMEAN)	Pr > |T| H_0: LSMEAN=0
Core_wt (oz/yd^2)	Core Fiber			
0	Cotton	0.4998	0.0298	0.0001
1	Cotton	0.5058	0.0295	0.0001
2	Cotton	0.6235	0.0285	0.0001
3	Cotton	0.6250	0.0293	0.0001
1.8	PP	0.5043	0.0310	0.0001
2.6	PP	0.5114	0.0307	0.0001

D.16 Least Square Means of Percent Change in Adsorption Capacity for Calendered Samples for the Independent Variable Core Weight.

Laminate		Percent Change in Adsorption Capacity (LSMEAN)	Standard Error (LSMEAN)	Pr > |T| H_0: LSMEAN=0
Core_wt (oz/yd^2)	Core Fiber			
0	Cotton	0.4950	0.0302	0.0001
1	Cotton	0.5004	0.0299	0.0001
2	Cotton	0.6165	0.0289	0.0001
3	Cotton	0.6164	0.0297	0.0001
1.8	PP	0.4998	0.0315	0.0001
2.6	PP	0.5067	0.0311	0.0001

D.17 Least Square Means of Breakthrough Time for Calendered Samples for the Independent Variables Calender Speed with Laminate Core Fiber Type.

Calender Speed (m/min)	Core Fiber	Breakthrough Time (s) (LSMEAN)	Standard Error (s) (LSMEAN)	Pr > |T| H_0: LSMEAN=0
4	Cotton	985.3	72.1	0.0001
4	PP	997.0	147.4	0.0001
6	Cotton	935.1	73.6	0.0001
6	PP	1778.3	171.4	0.0001
8	Cotton	944.9	75.0	0.0001
8	PP	899.1	201.6	0.0001

D.18 Least Square Means of Adsorption Capacity for Calendered Samples for the Independent Variables Calender Speed with Laminate Core Fiber Type.

Calender Speed (m/min)	Core Fiber	Adsorption Capacity (g/g) (LSMEAN)	Standard Error (g/g) (LSMEAN)	Pr > |T| H_0: LSMEAN=0
4	Cotton	0.1576	0.0113	0.0001
4	PP	0.1593	0.0231	0.0001
6	Cotton	0.1498	0.0115	0.0001
6	PP	0.2813	0.0268	0.0001
8	Cotton	0.1513	0.0117	0.0001
8	PP	0.1443	0.0315	0.0001

D.19 Least Square Means of Breakthrough Time for Calendered Samples for the Independent Variables Calender Nip Pressure with Laminate Core Fiber Type.

Calender Nip Pressure (pli)	Core Fiber	Breakthrough Time (s) (LSMEAN)	Standard Error (s) (LSMEAN)	Pr > |T| H_0: LSMEAN=0
250	Cotton	1020.9	80.7	0.0001
250	PP	1204.0	157.9	0.0001
300	Cotton	965.7	79.6	0.0001
300	PP	1674.3	154.3	0.0001
350	Cotton	878.7	73.3	0.0001
350	PP	796.1	149.1	0.0001

D.20 Least Square Means of Percent Change in Breakthrough Time for Calendered Samples for the Independent Variables Calender Nip Pressure Laminate Core Fiber Type.

Calender Nip Pressure (pli)	Core Fiber	Percent Change in Breakthrough Time (LSMEAN)	Standard Error (LSMEAN)	Pr > |T| H_0: LSMEAN=0
250	Cotton	0.5354	0.0294	0.0001
250	PP	0.4915	0.0574	0.0001
300	Cotton	0.5764	0.0290	0.0001
300	PP	0.3618	0.0561	0.0001
350	Cotton	0.5787	0.0267	0.0001
350	PP	0.6703	0.0543	0.0001

D.21 Least Square Means of Adsorption Capacity for Calendered Samples for the Independent Variables Calender Nip Pressure with Laminate Core Fiber Type.

Calender Nip Pressure (pli)	Core Fiber	Adsorption Capacity (g/g) (LSMEAN)	Standard Error (g/g) (LSMEAN)	Pr > |T| H_0: LSMEAN=0
250	Cotton	0.1633	0.0126	0.0001
250	PP	0.1918	0.0247	0.0001
300	Cotton	0.1545	0.0124	0.0001
300	PP	0.2651	0.0241	0.0001
350	Cotton	0.1408	0.0115	0.0001
350	PP	0.1280	0.0233	0.0001

D.22 Least Square Means of Percent Change in Adsorption Capacity for Calendered Samples for the Independent Variables Calender Nip Pressure with Laminate Core Fiber Type.

Calender Nip Pressure (pli)	Core Fiber	Percent Change in Adsorption Capacity (LSMEAN)	Standard Error (LSMEAN)	Pr > |T| H_0: LSMEAN=0
250	Cotton	0.5284	0.0298	0.0001
250	PP	0.4867	0.0582	0.0001
300	Cotton	0.5704	0.0293	0.0001
300	PP	0.3591	0.0569	0.0001
350	Cotton	0.5723	0.0270	0.0001
350	PP	0.6640	0.0550	0.0001

D.23 Contrasts for Breakthrough Time for Calendered Samples.

Dependent Variable: Breakthrough Time (s)					
Contrast	DF	Contrast SS	Mean Square	F value	Pr > F
Speed (m/min) '4 vs 6'	1	280869.13	280869.13	7.63	0.0153 *
Speed (m/min) '4 vs 8'	1	7539.9725	7539.9725	0.20	0.6578
Speed (m/min) '6 vs 8'	1	237780.17	237780.17	6.46	0.0235 *
Pressure (pli) '250 vs 300'	1	78565.785	78565.785	2.13	0.1661
Pressure (pli) '250 vs 350'	1	163310.01	163310.01	4.44	0.0537
Pressure (pli) '300 vs 350'	1	456831.39	456831.39	12.41	0.0034 *

* indicating contrast is significant at the 0.05 probability level.

D.24 Contrasts for Percent Change in Breakthrough Time for Calendered Samples.

Dependent Variable: Percent Change in Breakthrough Time					
Contrast	DF	Contrast SS	Mean Square	F value	Pr > F
Speed (m/min) '4 vs 6'	1	0.0313557	0.0313557	6.43	0.0237 *
Speed (m/min) '4 vs 8'	1	0.0007410	0.0007410	0.15	0.7024
Speed (m/min) '6 vs 8'	1	0.0260268	0.0260268	5.34	0.0366 *
Pressure (pli) '250 vs 300'	1	0.0035860	0.0035860	0.74	0.4054
Pressure (pli) '250 vs 350'	1	0.0265925	0.0265925	5.46	0.0349 *
Pressure (pli) '300 vs 350'	1	0.0473257	0.0473257	9.71	0.0076 *

* indicating contrast is significant at the 0.05 probability level.

D.25 Contrasts for Adsorption Capacity for Calendered Samples.

Dependent Variable: Adsorption Capacity (g TCE/g carbon)					
Contrast	DF	Contrast SS	Mean Square	F value	Pr > F
Speed (m/min) '4 vs 6'	1	0.0068555	0.0068555	7.61	0.0154 *
Speed (m/min) '4 vs 8'	1	0.0001800	0.0001800	0.20	0.6617
Speed (m/min) '6 vs 8'	1	0.0057836	0.0057836	6.42	0.0238 *
Pressure (pli) '250 vs 300'	1	0.0018988	0.0018988	2.11	0.1686
Pressure (pli) '250 vs 350'	1	0.0040152	0.0040152	4.46	0.0532
Pressure (pli) '300 vs 350'	1	0.0111497	0.0111497	12.38	0.0034 *

* indicating contrast is significant at the 0.05 probability level.

D.26 Contrasts for Percent Change in Adsorption Capacity for Calendered Samples.

Dependent Variable: Percent Change in Adsorption Capacity					
Contrast	DF	Contrast SS	Mean Square	F value	Pr > F
Speed (m/min) '4 vs 6'	1	0.0311099	0.0311099	6.22	0.0258 *
Speed (m/min) '4 vs 8'	1	0.0007248	0.0007248	0.14	0.7092
Speed (m/min) '6 vs 8'	1	0.0257674	0.0257674	5.15	0.0396 *
Pressure (pli) '250 vs 300'	1	0.0033361	0.0033361	0.67	0.4278
Pressure (pli) '250 vs 350'	1	0.0264371	0.0264371	5.28	0.0374 *
Pressure (pli) '300 vs 350'	1	0.0461762	0.0461762	9.23	0.0089 *

* indicating contrast is significant at the 0.05 probability level.

APPENDIX E

Basic Computer Program Developed by Wayne T. Davis

for the Modeling of the Activated Carbon

Impregnated Nonwoven Adsorption Medium

Basic Computer Program Developed by Wayne T. Davis.

```
10  REM THIS PROGRAM DEVELOPED BY W.T.DAVIS-OCT 1993
20  REM PROGRAM PREDICTS THE CONCENTRATION VERSUS TIME PROFILE
    EXITING A BED OF DEPTH,L, GIVEN THE CARBON
    CHARACTERISTICES AND ADSORPTION ISOTHERM
30  REM EQUATIONS ARE FROM WARK,WARNER,DAVIS AND CRAWFORD (AIR
    POLLUTION THEORY)
70  INPUT "Velocity of the carrier gas, m/s";VA
80  INPUT "Density of the adsorbent, kg/m^3 ";RHOAD
90  INPUT "Alpha, kg/m^3";ALPHA
100 INPUT "Beta";BETA
110 INPUT "Inlet concentration, kg/m^3";CO
120 INPUT "K value, s^-1";K
130 INPUT "Length of the adsorption bed, m"; L
140 INPUT "Area of the filter, m^2"; AF
150 REM LPRINT "The Input bed conditions are:"
160 LPRINT "Velocity of the carrier gas, m/s";VA
170 LPRINT "Density of the adsorbent, kg/m^3 = ";RHOAD
180 LPRINT "Alpha, kg/m^3 = ";ALPHA
190 LPRINT "Beta = ";BETA
200 LPRINT "Inlet concentration, kg/m^3 = ";CO
210 LPRINT "K value, s^-1 = ";K
220 LPRINT "Length of the adsorption bed, m = "; L
230 LPRINT "Area of the filter, m^2"; AF
240 REM ADSORPTION WAVE VELOCITY IN M/S
280 VAD = (VA/RHOAD)*(ALPHA^(1/BETA))*(CO^((BETA-1)/BETA))
300 LPRINT "Adsorption wave velocity = "VAD" m/s"
320 B1 = BETA-1
330 B = 1/B1
340 REM DELTA FOR ADSORPTION WAVE, METERS, FOR C/CO = 0.01 TO
    0.99
350 DELTA =
    (VA/K)*(LOG(.99/.01)+B*LOG((1-.01^B1)/(1-(.99)^B1)))
363 LPRINT "DELTA = "DELTA" METERS"
420 REM DIM VARIABLES TO CALCULATE VALUES FOR C/CO = .02-.99
432 DIM C1(100):DIM T(100):DIM A(100):DIM SUMA(100):DIM
    TT(100)
434 C1(1)=.01: T(1)=DELTA/VAD: SUMA(1)=0
435 FOR I = 2 TO 99 STEP 1
440 C1(I)=.01 + C1(I-1)
450 REM CALCULATE AREA OVER C VS T CURVE FOR BREAKTHRU CURVE
470 T(I) =
    (VA/(K*VAD))*(LOG(.99/C1(I))+B*LOG((1-((C1(I))^B1))/
    (1-((.99)^B1))))
475 A(I)=(1-((C1(I-1)+C1(I))/2))*(T(I-1)-T(I))
480 SUMA(I)=SUMA(I-1)+A(I)
570 NEXT
575 X=(CO/ALPHA)^(1/BETA)
600 KG=X*RHOAD*AF*L
610 LPRINT "TOTAL MASS ADSORBED = "KG" KG"
```

```
625 M1=KG-SUMA(99)*AF*VA*CO
635 LPRINT"MASS ADSORBED AT BREAKTHRU = "M1" KG"
650 TB=M1/(CO*VA*AF)
675 LPRINT"TIME TO BREAKTHRU = "TB" SECS"
680 ST=TB+(DELTA/VAD)
690 LPRINT"TOTAL TIME TO CAPACITY = "ST" SECS"
700 REM CALCULATE TIME TO C/CO=.01....99
750 FOR I = 2 TO 99 STEP 1
800 TT(I) =
    ST-(VA/(K*VAD))*(LOG(.99/C1(I))+B*LOG((1-((C1(I))^B1))/
    (1-((.99)^B1))))
850 NEXT
900 PRINT"CREATE ASCII DATAFILE? TYPE 1, ELSE TYPE 2 AND GET
    PRINTOUT ONLY"
925 INPUT "ENTER 1 OR 2:";Q
950 IF Q=2 GOTO 960
955 OPEN "ADSORB3.DAT" FOR OUTPUT AS #1
960 FOR I = 2 TO 99 STEP 1
970 LPRINT "C/CO = ";C1(I),"TIME = "TT(I) "SECS"
980 IF Q=2 GOTO 990
985 WRITE #1, I, C1(I), TT(I)
990 NEXT
1000 IF Q=2 GOTO 1010
1005 CLOSE #1
1010 END
```

APPENDIX F

Chemical Properties and Toxicity of Trichloroethylene

Chemical Properties and Toxicity of Trichloroethylene

CHARACTERISTICS	TRICHLOROETHYLENE
Chemical Formula	C2Cl3H3
Molecular Weight (g/mole)	133.39
Gas Density (kg/m^3)	4.450
Liquid Density (kg/m^3)	1465.0
Boiling Temperature at Atmospheric Pressure (°C)	86.7
Latent Heat of Vaporization (kJ/kg)	240
Vapor Pressure of Pure Compound (kPa at 20°C)	7.61
CAS Number	79-01-6
OSHA-PEL (8 hours)	100 ppm

VITA

Derong Tu was born on August 14, 1965 in Shanghai, China. He received his Bachelor of Engineering Degree in Textile Technology from China Textile University in July 1986. He worked for two international companies in Shanghai from August 1986 to July 1992 in charge of textiles/garments and general merchandise exports from China to the U.S.A., Canada, and Europe. He came to U.S.A. in August 1992, and became a M.S. degree candidate in Textiles Science Program in the Department of Textiles, Retailing and Interior Design at the University of Tennessee, Knoxville.